



EQ-1601-10984: Ardent Oil - Snowdon Prospect Summary PowerPoint Report

Phase 0: Data Loading

Phase 1a: Petrophysical Analysis

Phase 1b: Rock Physics Analysis

15/07/2016

The Present And Future
Of GeoPrediction

Contents

1. Project structure	3
2. Facies assumptions	4
3. Phase 0: Data Loading	5
4. Phase 1a: Petrophysical Analysis	34
5. Phase 1b: Rock Physics Analysis & Modelling	35
6. Summary and Conclusions	108
7. Recommendations and Next Steps	110



Project Structure

- Phase 0: Data Loading
- Phase 1a: Petrophysical Analysis
- Phase 1b: Rock Physics Analysis & Modelling
- Phase 1c: 2D Seismic Modelling
- Phase 2: Well to Seismic Ties
- Phase 3: Seismic Data Conditioning and Inversion Testing
- Phase 4: Pre-stack Seismic Inversion
- Phase 5: Reservoir Characterisation



Facies Logs

- Facies logs were define using the following petrophysical cut-offs:

- Shale: VSh ≥ 0.8 ; VLime = 0; VTuff = 0
- Sand: VSh ≤ 0.2 ; VLime = 0; VTuff =
- Limestone: VLime ≥ 0
- Tuffaceous Shale: VTuff ≥ 0
- Non-endmember Silt = VSh ≥ 0.2 ; VSh ≤ 0.8

- The first four facies represent end-member lithologies, for which trends will be derived.



Phase 0: Data Loading

1. Log Data Review, inc. well log panels, single well QC cross-plots (Vp/RhoB).
2. Multi-well cross-plots
3. Mineral Properties
4. Fluid Properties
5. Pressure and Temperature Profiles



1. Log Data Review



1. Log Data Review

Workflow

The study contains 3 wells, which were selected based on their location, data quality and data availability.

The elastic logs (Vp, Vs and density) were reviewed to identify intervals of poor and unreliable data. This review was performed in two stages:

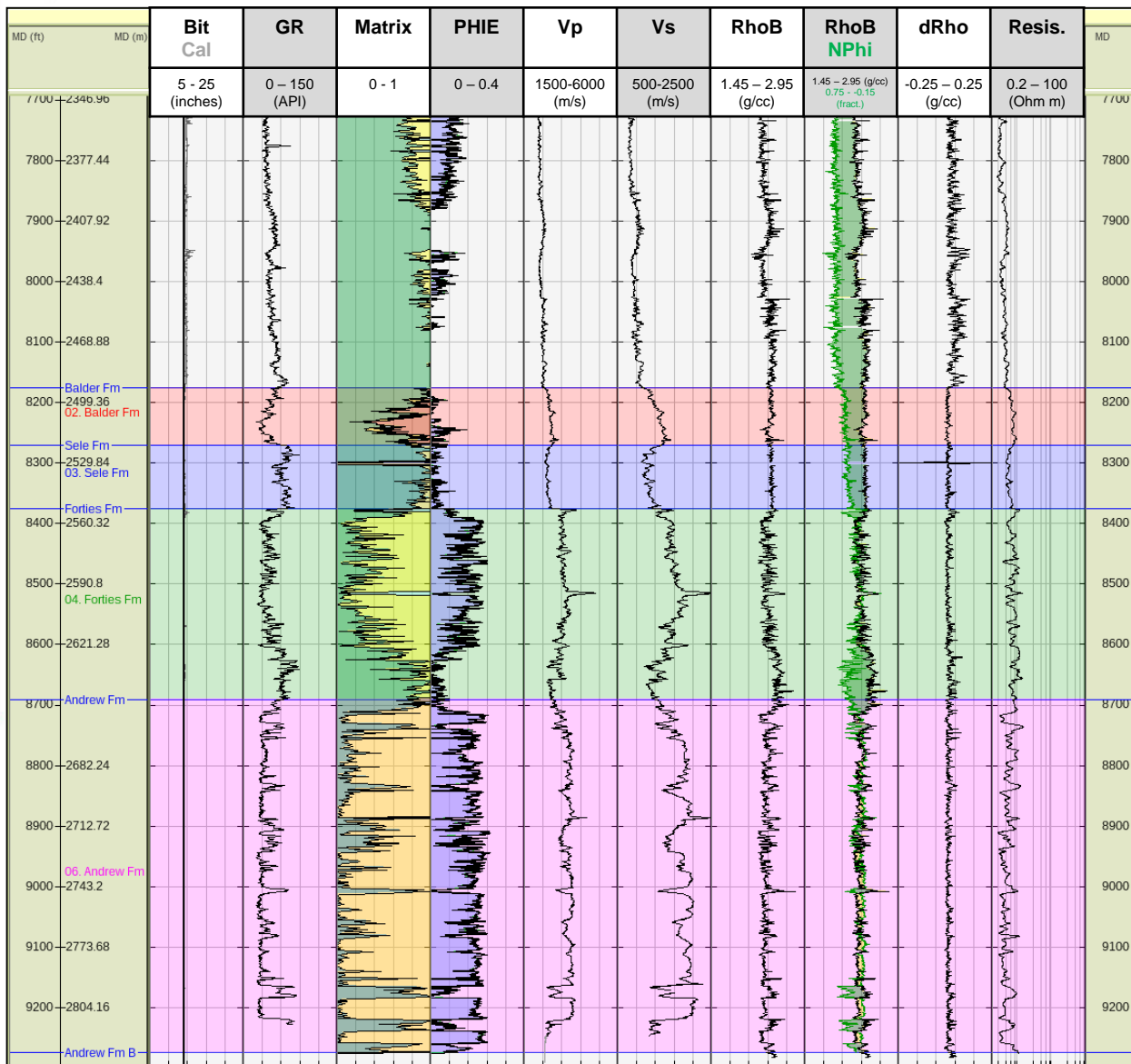
- **Log plot QC** involves plotting the log data against depth and analysing dRho, PR (where available) and dCal for any signs of poor data or poor hole conditions.
- **Cross-plot QC** involves plotting Vp/RhoB and Vp/Vs cross-plots and looking for any obviously anomalous data. All rock physics models shown are uncalibrated. Cross-plots are shown for the interval of interest only.

Well Name	Log Data						Well Data			Petrophysics				Fluid Data									
	Cal	GR	Vp	Vs	Rhob	NPhi	dRho	R	Deviation	Check-shot	Markers	Phi	Vsh	Sw	SXO	Salinity (kppm)	Instiu Fluids	API	GOR	GG (air= 1)	Mud Type	Pressure	Temp
22/3A-3	✓	✓	✓	✓	✓	✓	✓	✓	Vertical	✓	from EOWR	✓	✓	✓	✗	80-144	Brine	-	-	-	OBM	✓	✓
22/7-4	✓	✓	✓	✗	✓	✓	✓	✓	✓	?	from EOWR	✓	✓	✓	✗	48-127	Brine	-	-	-	OBM	?	✓
22/8A-2	✓	✓	✓	✓	✓	✓	✓	✓	Vertical	✓	from EOWR	✓	✓	✓	✓	40-88	Oil stain - no sample	-	-	-	WBM	✗	✓

- There doesn't appear to be any pressure data for 22/7-4 – is this expected? No pressure data is expected for 22/8A-2, based on Ikon's previous experience.
- No check-shot data for 22/8A-2.
- No Forties or Andrew markers in 22/8A-2.
- Need some information on expected fluid properties and on insitu oil properties in 22/8A-2.

1. Log Data Review: 22/3a-3

QC Log Plot



Visual QC

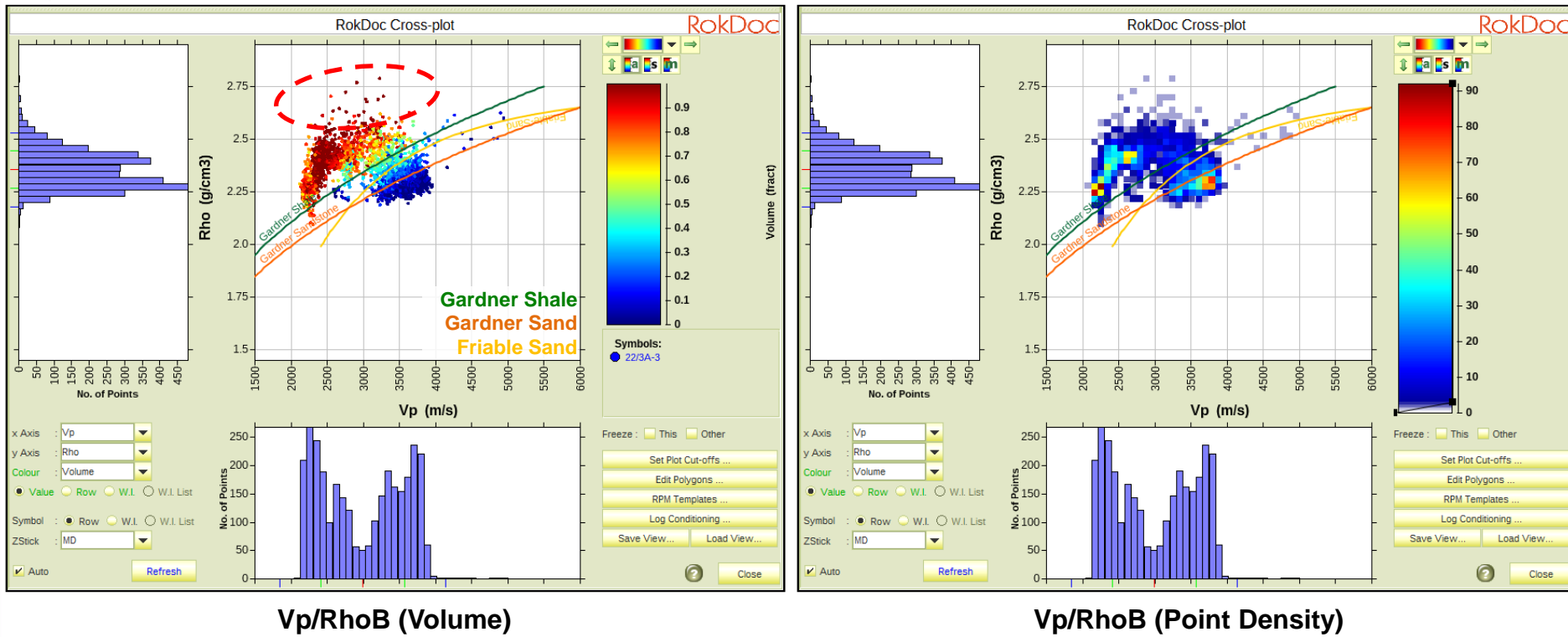
The caliper log stays close to the bit size log and the dRho log is generally low, which indicates that the hole conditions were good. One area of concern for the RhoB log is in the Eocene above the Balder Fm, where the dCal is >0.1g/cc and behaves erratically.

There is measured Vs for this well and it is present throughout this interval of interest.

The well is vertical.

1. Log Data Review: 22/3a-3

QC Cross-plot



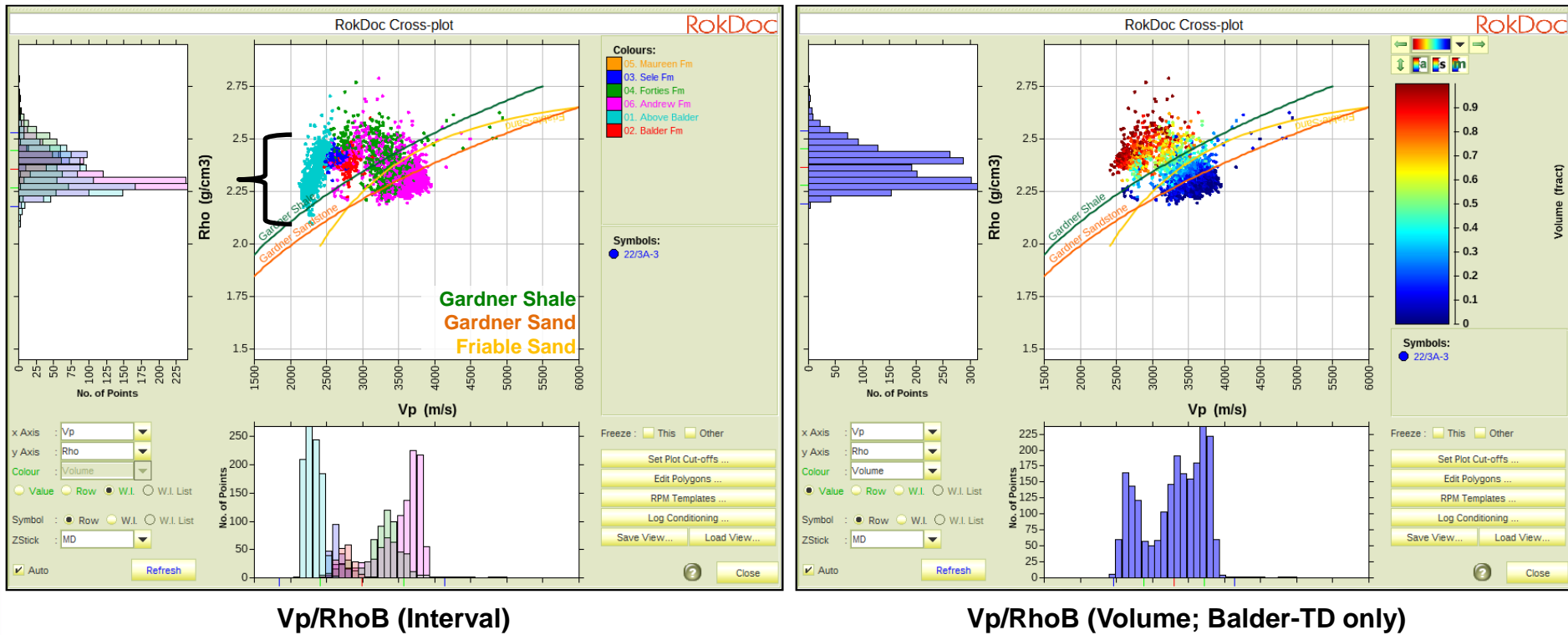
The data quality appears to be generally good, based on the Vp/RhoB data plotting close to established rock physics trends and (uncalibrated) models.

The shale data above the Balder Fm show a rapid increase in RhoB relative to the expected increase in Vp, which flattens out to become parallel to the Gardner shale within the Balder Fm and deeper. This may be linked to the erratic dRho log.

There are several high RhoB points (circled in red) that appear to have a much slower Vp than expected. These are most likely thin calcite stringers, where the RhoB log has resolved them but the Vp log has not. A calcite flag will be added here.

1. Log Data Review: 22/3a-3

QC Cross-plot

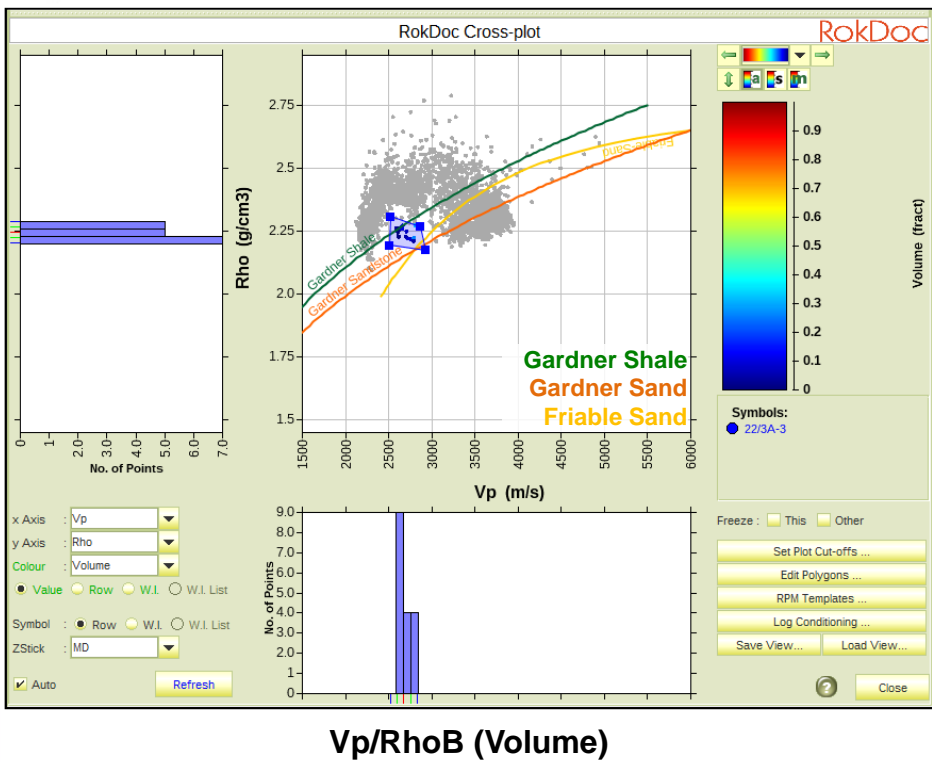


The shale data above the Balder Fm show a rapid increase in RhoB relative to the expected increase in Vp, which flattens out to become parallel to the Gardner shale within the Balder Fm and deeper.

Removing the erratic at points with erratic results in the data above the Balder Fm showing the same trend, so the data will not be removed.

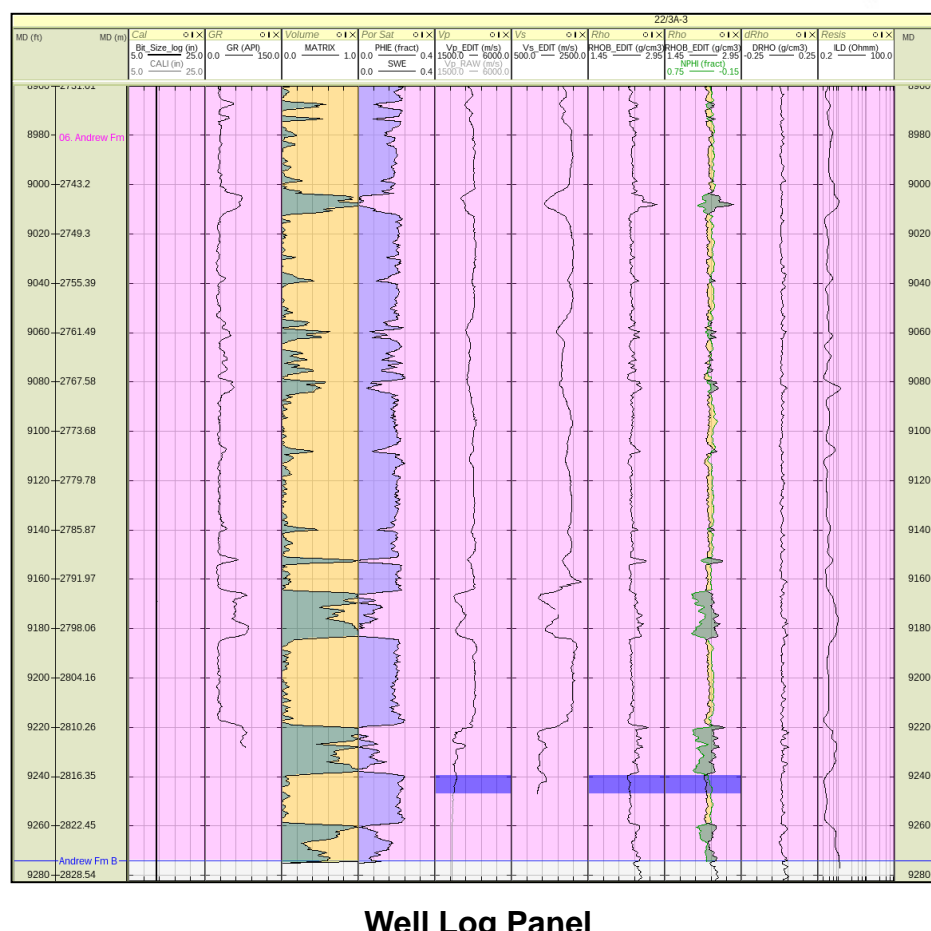
1. Log Data Review: 22/3a-3

QC Cross-plot



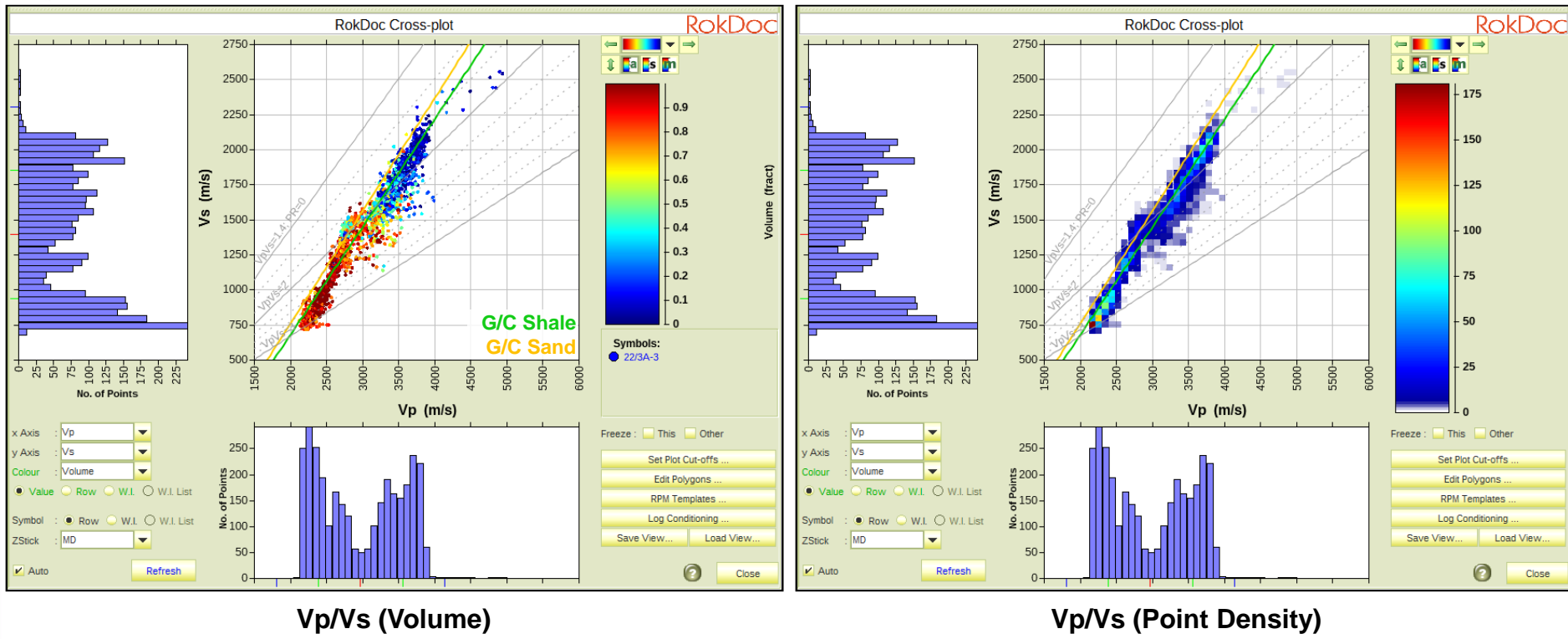
In addition to the calcite stringers, there also appears to be an end-of-log artefact in the Vp that needs removing (highlighted in blue on the cross-plot and well log panel).

This Vp log has already been edited in the petrophysics, but needs a small additional section removing, based on the slow Vp compared to the overlying sands.



1. Log Data Review: 22/3a-3

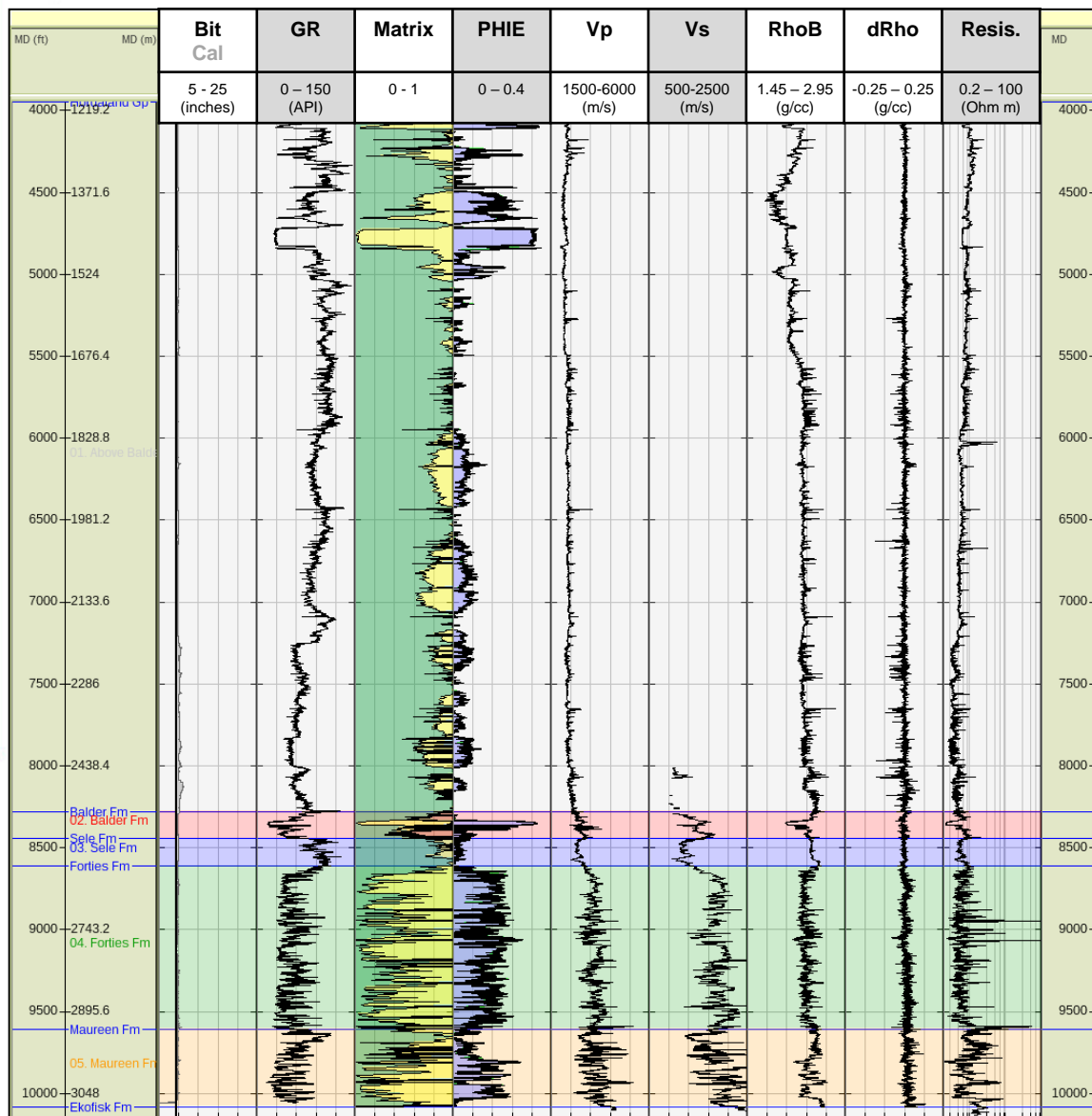
QC Cross-plot



The Vp/Vs data is of good quality, showing distinct trends for sand and shale.

1. Log Data Review: 22/7-4

QC Log Plot



Visual QC

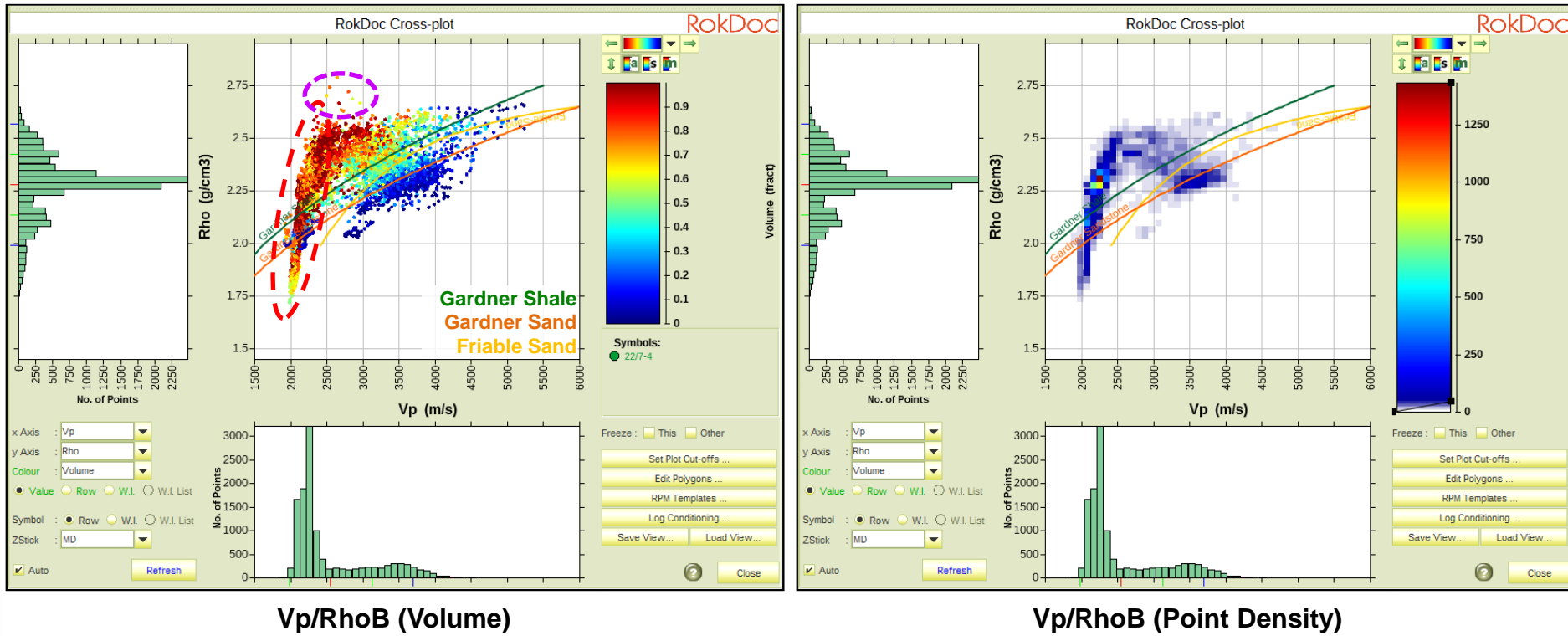
The caliper log indicates that the hole conditions were good, based on the caliper log plotting close to the bit size log.

The dRho log is generally low and within acceptable limits.

There is measured Vs through the interval of interest, but none in the section above the Balder Fm.

1. Log Data Review: 22/7-4

QC Cross-plot



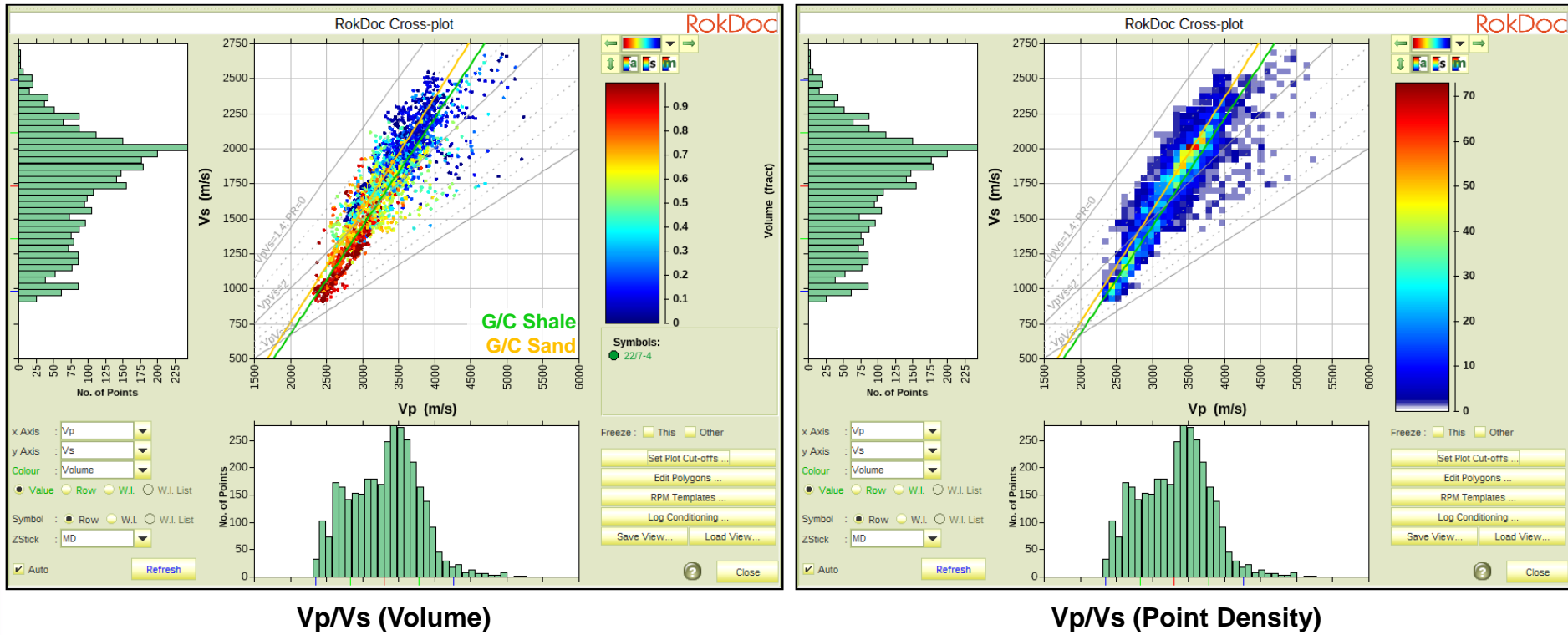
The data quality appears to be generally good, based on the Vp/RhoB data plotting close to established rock physics trends and (uncalibrated) models. However, there are a number of mis-ties between the Vp and RhoB logs, indicated by the cross-plot behaviour.

As in 22/3A-3, the shale data above the Balder Fm show a rapid increase in RhoB relative to the expected increase in Vp (circled in red), which flattens out to become parallel to the Gardner shale within the Balder Fm and deeper. This is indicative of friable shale behaviour.

There are several high RhoB points (circled in purple) that appear to have a much slower Vp than expected. These are most likely thin calcite stringers, where the RhoB log has resolved them but the Vp log has not. A calcite flag will be added here.

1. Log Data Review: 22/7-4

QC Cross-plot

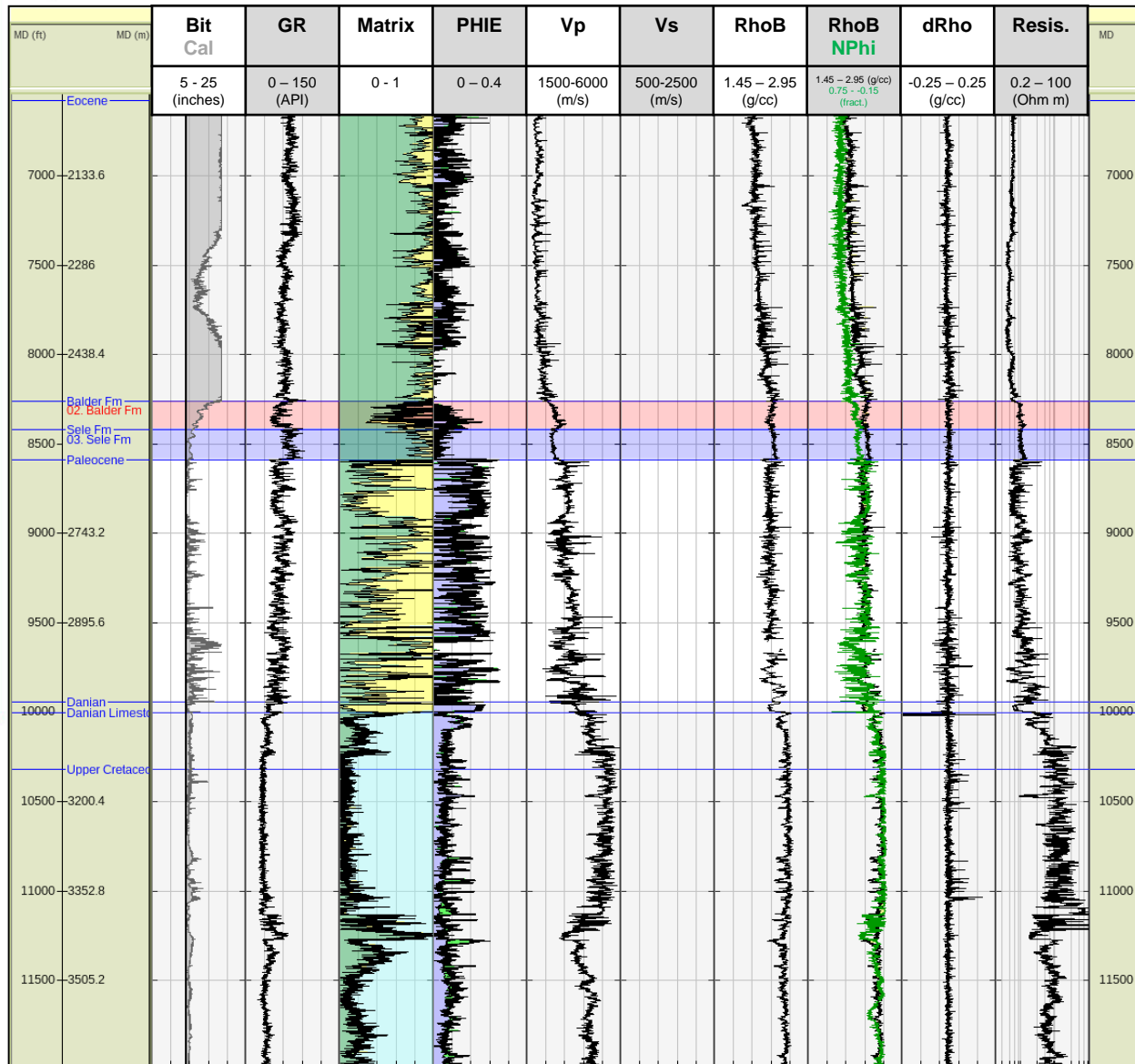


The V_p/V_s data quality is average and there are no sections of significantly poor data, based on the V_p/V_s data generally plotting close to established rock physics trends.

However, there are a reasonable number of data points that plot away from the trend, which appears to be due to some sections having poor quality V_s .

1. Log Data Review: 22/8A-2

QC Log Plot



Visual QC

The large difference between the bit size and caliper logs in the Eocene (above the Balder) indicates that the hole conditions were poor and the log data quality may also be poor.

However, the dRho log is generally low and within acceptable limits.

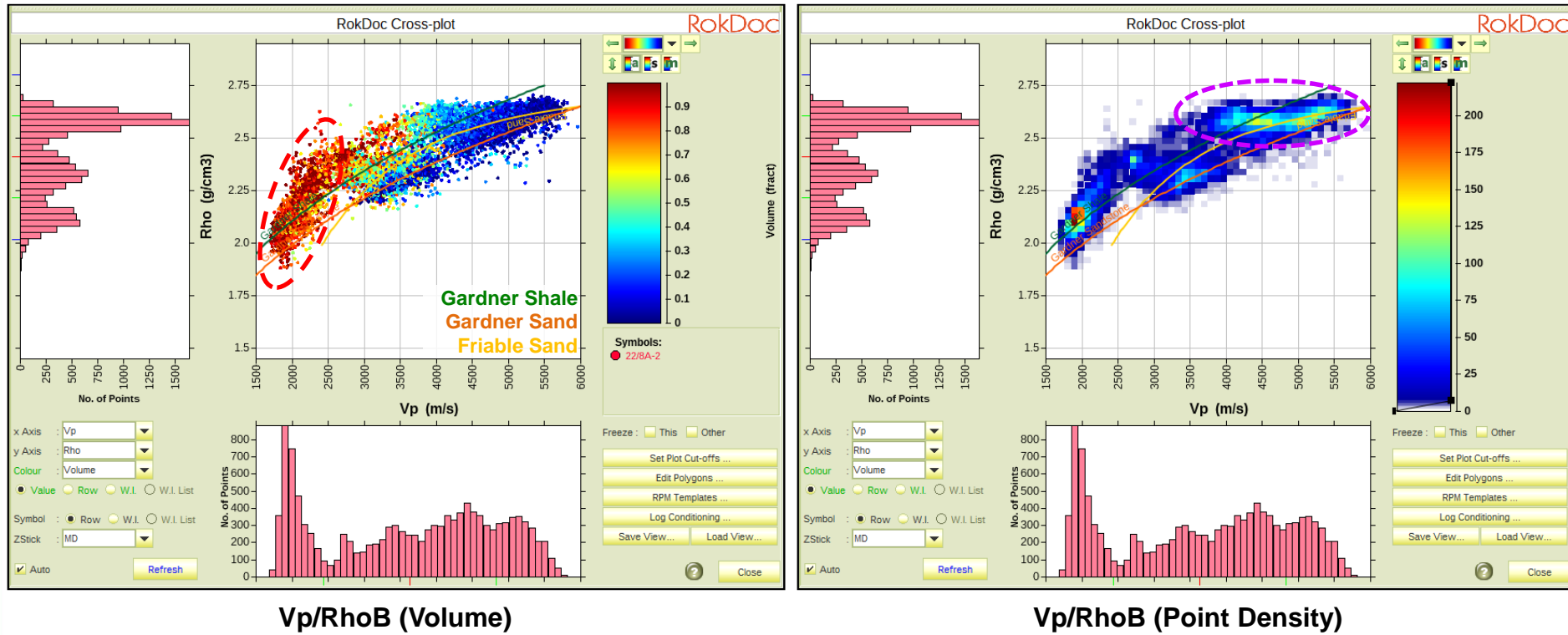
There is no measured Vs, so that will need modelling during rock physics analysis.

Vertical well.

Lack of intra-paleocene markers.

1. Log Data Review: 22/8A-2

QC Cross-plot



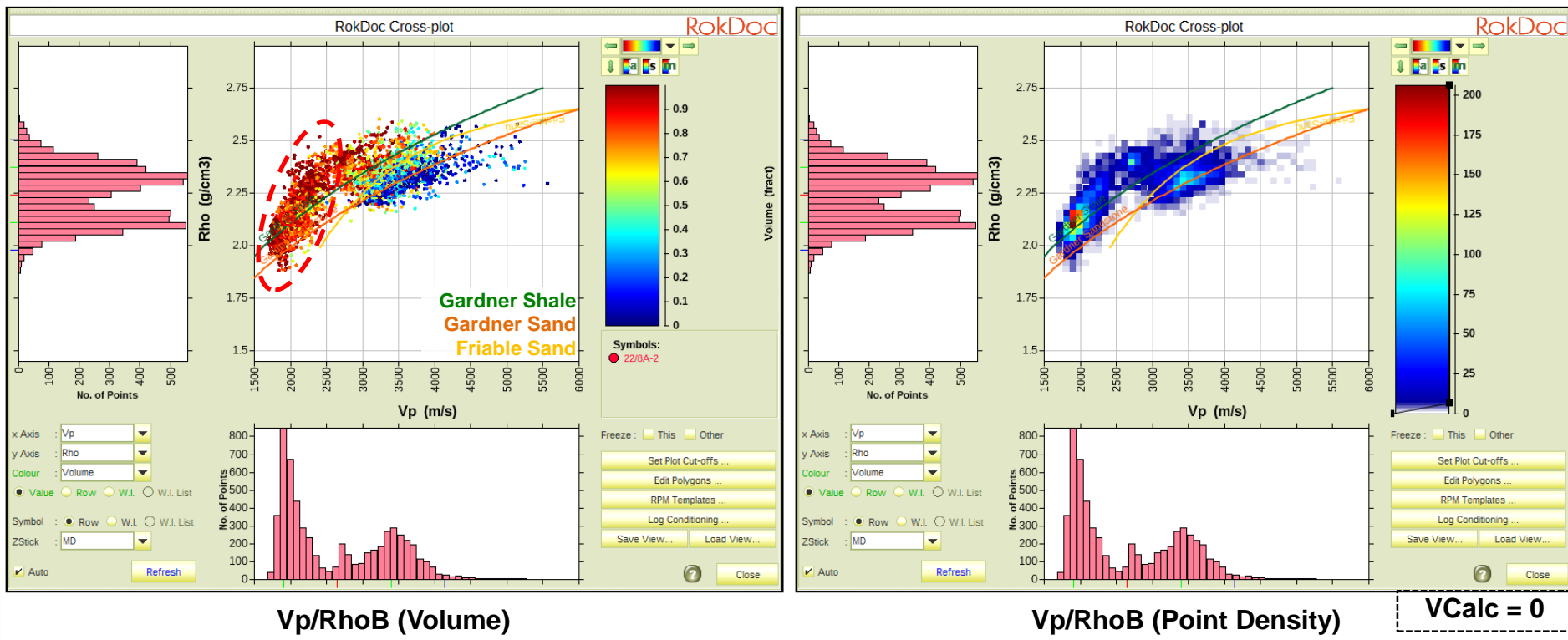
The data quality appears to be generally good, based on the Vp/RhoB data plotting close to established rock physics trends and (uncalibrated) models. There don't appear to be any significant mis-ties between the Vp and RhoB logs.

The shale data above the Balder Fm (circled in red) plots on a different shale trend to the shale data below the Balder Fm.

A large amount of data in the cross-plot is from the Danian limestone (circled in purple). The following cross-plot is shown without this data.

1. Log Data Review: 22/8A-2

QC Cross-plot



The data quality appears to be generally good, based on the Vp/RhoB data plotting close to established rock physics trends and (uncalibrated) models. There don't appear to be any significant mis-ties between the Vp and RhoB logs.

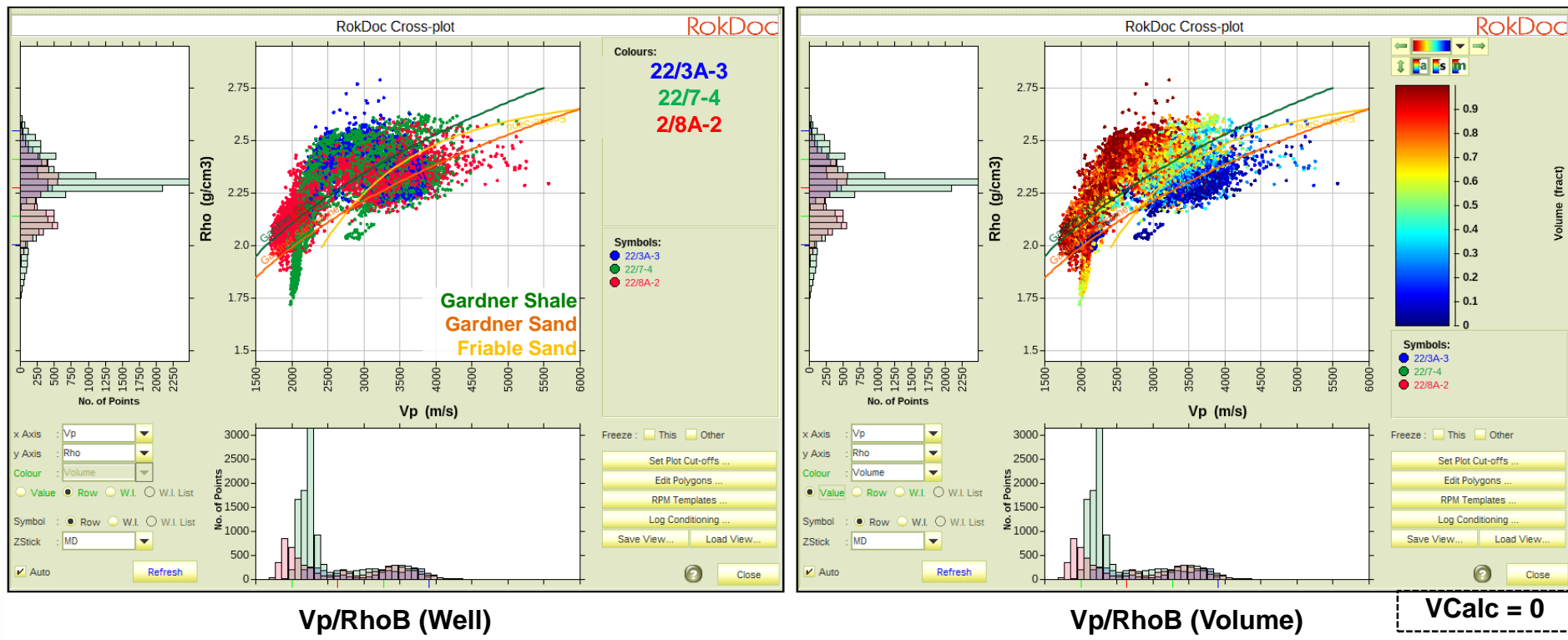
The shale data above the Balder Fm (circled in red) plots on a different shale trend to the shale data below the Balder Fm.

2. Multi-well Cross-plots



2. Multi-well QC Cross-plots

All Wells

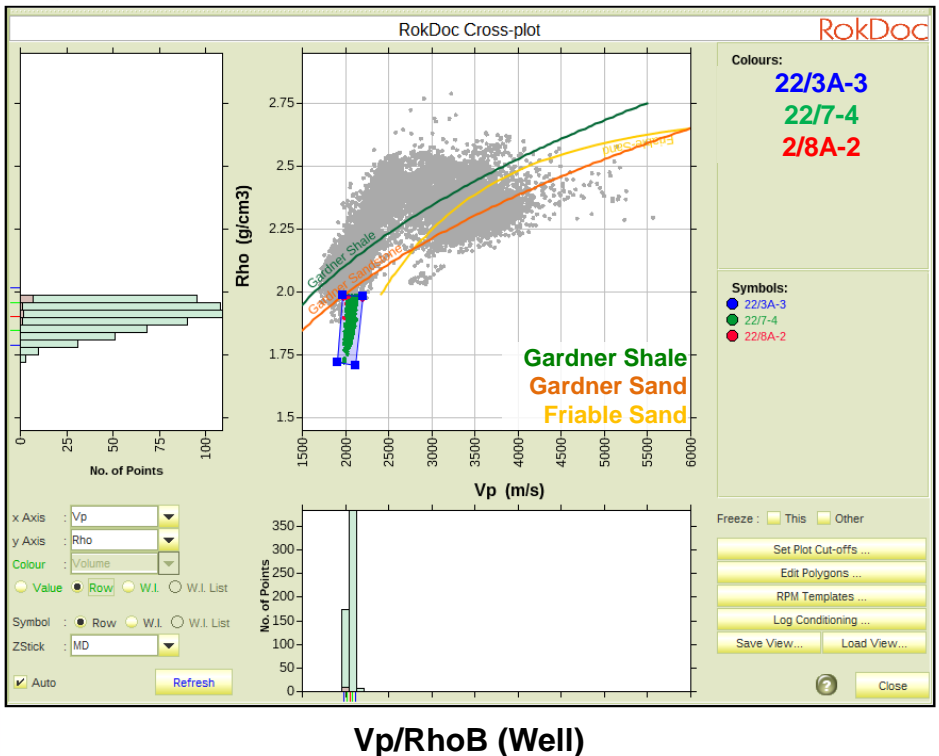


The data appears to correlate well. The data in 22/7-4 is obviously more scattered than the data in 22/3A-3, which was observed in the single-well plots.

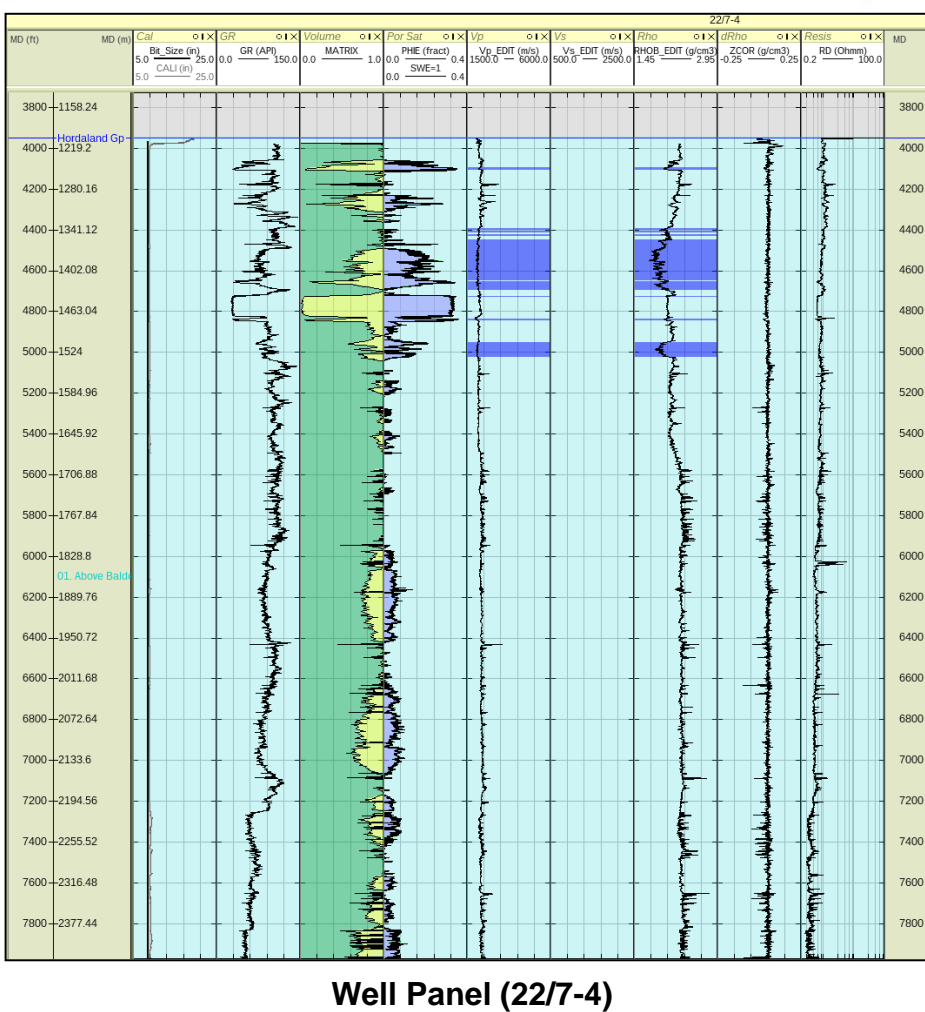
There are also some low Vp/RhoB data in 22/7-4 that look suspicious because they plot away from the data in 22/8A-2

2. Multi-well QC Cross-plots

All Wells

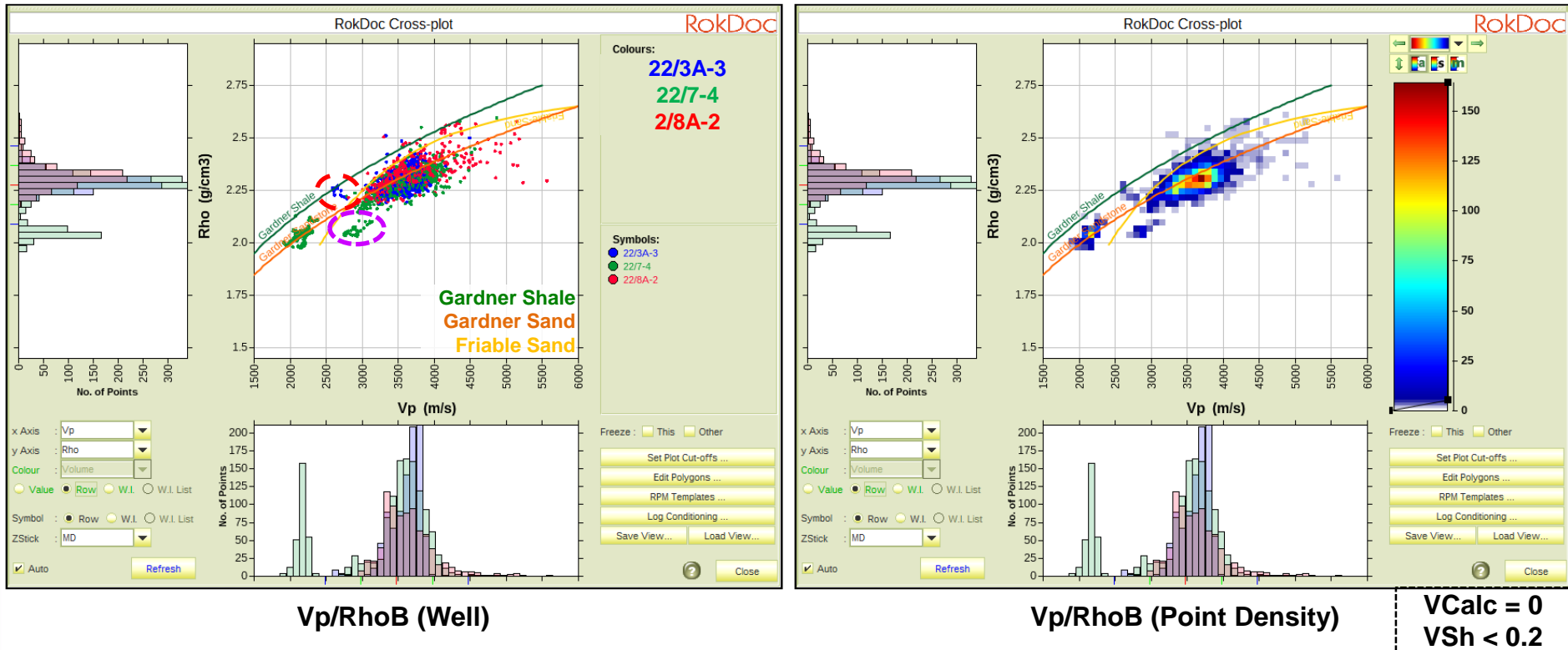


Some of the density data in 22/7-4 looks suspicious, although the caliper and dRho logs indicate that the hole quality is good.



2. Multi-well QC Cross-plots

All Wells – Sand

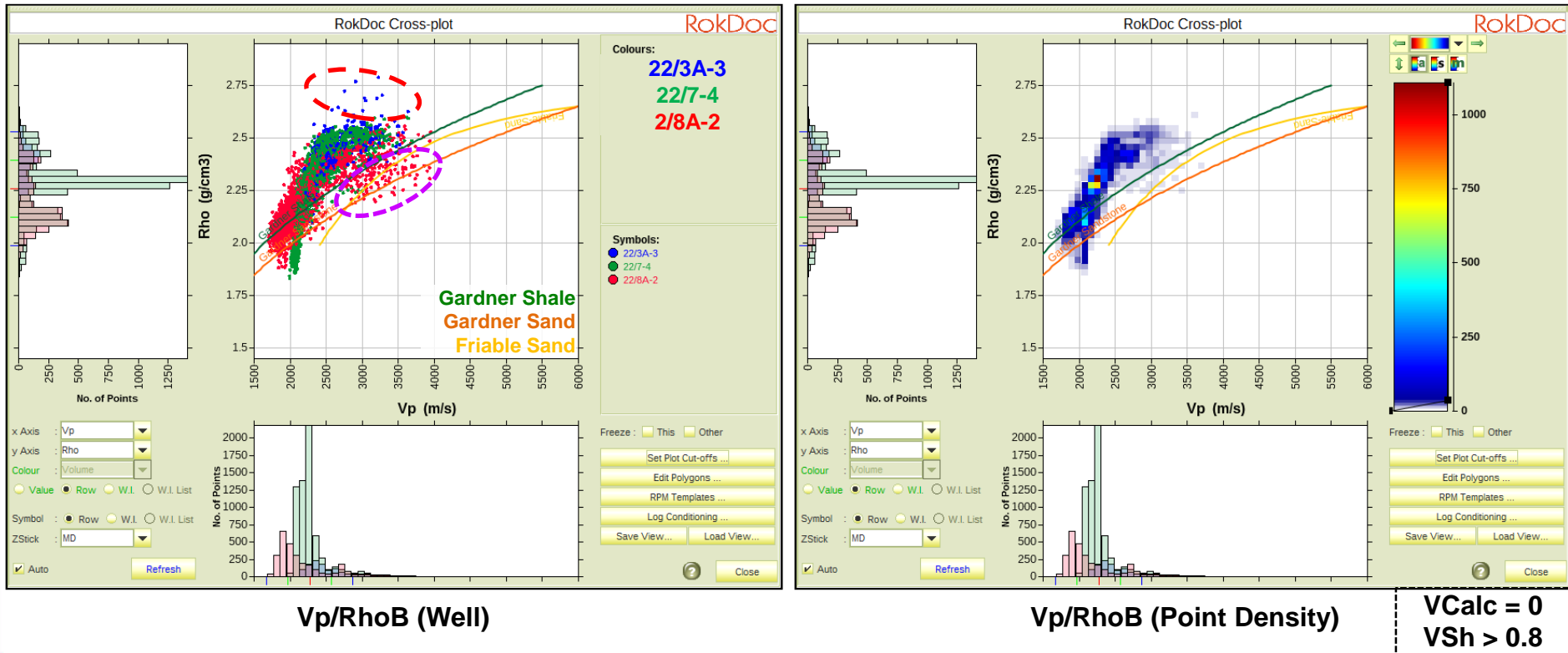


The sand Vp/RhoB data plot in a similar location on the cross-plot for all wells.

There are several suspicious intervals – the end-of-log artefact in 22/3A-3 highlighted on a previous slide (circled in red), and the Balder Fm sand in 22/7-4 (circled in purple).

2. Multi-well QC Cross-plots

All Wells – Shale



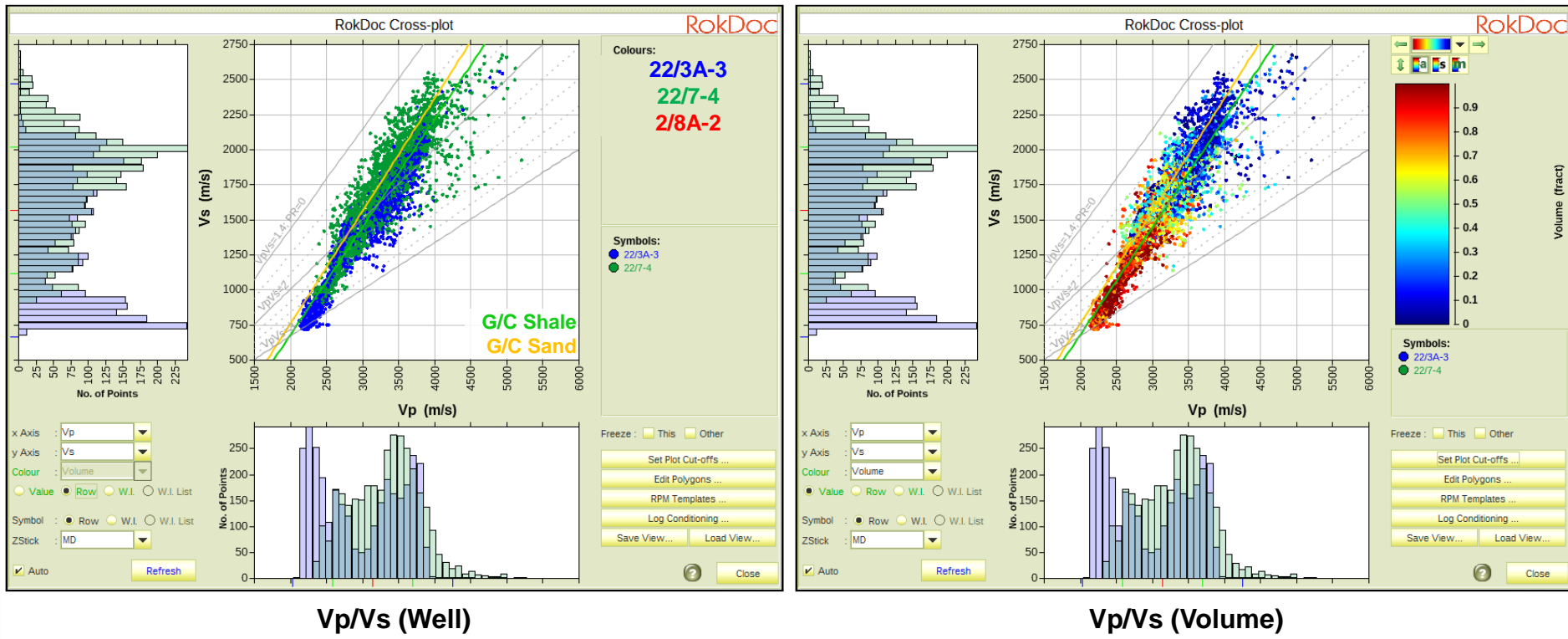
The shale Vp/RhoB data generally show consistent behaviour. There is a distinct compaction trends across the three wells, although it is not clear whether the different trends in the shallower section of 2/8A-2 and 22/7-4 is geological or a data quality issue at this stage.

Limestone stringers, unresolved by the Vp log, are circled in red.

There appears to be some issue with thing interbedded sands and shales in 2/8A-2, where the Vp log is measured a mix of sand and shale (circled in purple).

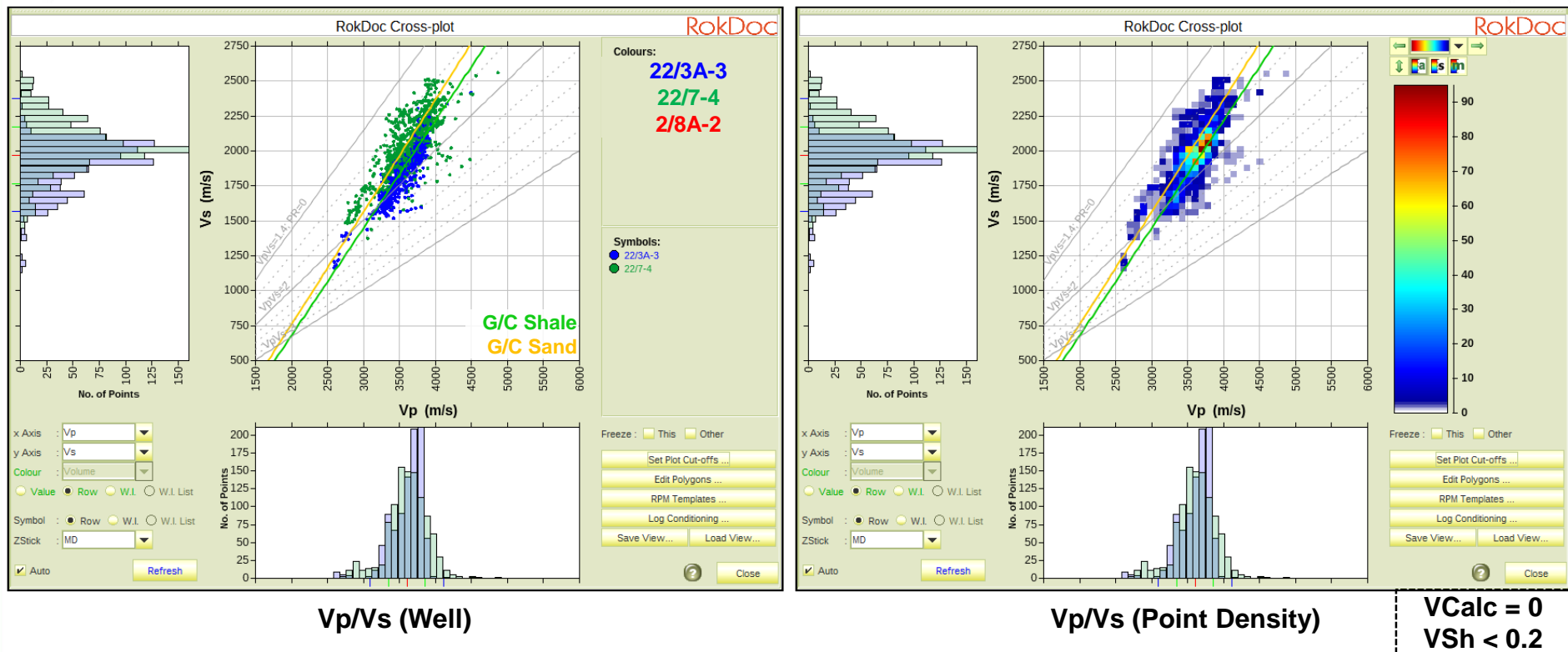
2. Multi-well QC Cross-plots

All Wells



2. Multi-well QC Cross-plots

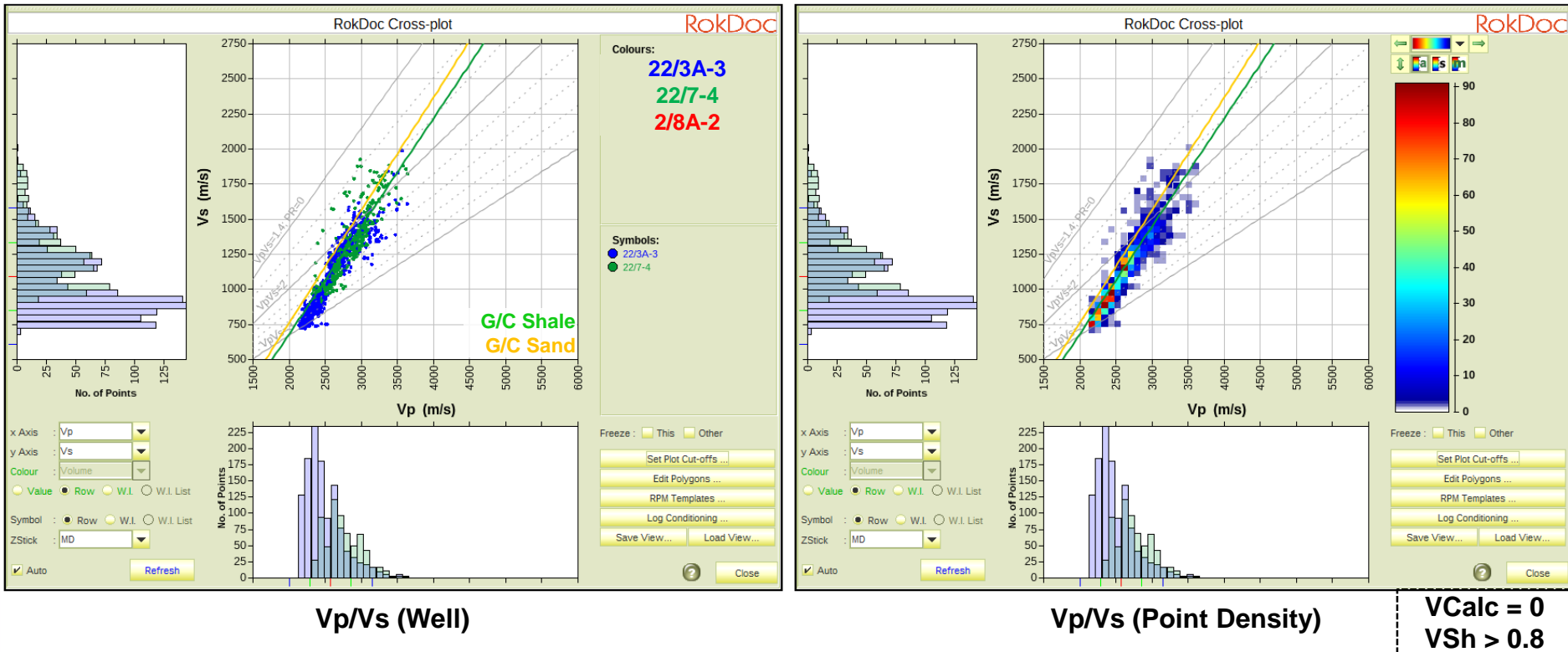
All Wells – Sand



V_s faster for a given V_p in 22/7-4 compared to 22/3A-3.

2. Multi-well QC Cross-plots

All Wells – Shale



Shale data looks similar between the wells.

3. Mineral Properties



3. Mineral Properties

Minerals



Mineral sets will now be defined, containing the elastic properties of the minerals for each Working Interval in the study.

Quartz, Calcite and Dolomite

These minerals can be considered to have constant elastic properties over the study area and each mineral set will be given a standard value, detailed in the table below.

The quartz density will be adjusted to match the matrix density used in the petrophysics (2.65gcm^{-3} throughout this study)

Shale

The elastic properties of shale are expected to be much more variable and will not be considered to be constant over the study area. These values will need to be derived directly from the log data because the project is working in effective porosity.

Mineral	Well	Interval	Ko (GPa)	Mu (GPa)	Rho (gcm^{-3})	Vp (ms^{-1})	Vs (ms^{-1})
Quartz	All	All	36.6	45	2.65	6038	4121
Calcite	All	All	76.8	32	2.71	6640	3436
Tuff	All	All					
Shale	22/3A-3	04. Forties Fm					
		06. Andrew Fm					
	22/7-4	01. Hordaland Gp					
		02. Balder Fm					
		04. Forties Fm					
		05. Maureen Fm					
	22/8A-2	04. Forties Fm ??					
		06. Andrew Fm ??					

4. Fluid Properties



4. Fluid Properties

Fluid logs define the acoustic properties of the fluids, using the FLAG (FLuid Acoustics for Geophysics, Batzle, CSM, 2011) calculator within RokDoc. The fluid logs are used for Gassmann fluid substitution to brine conditions and a corresponding fluid substitution to hydrocarbon conditions. The two sets of fluid logs don't necessarily have to be the same.

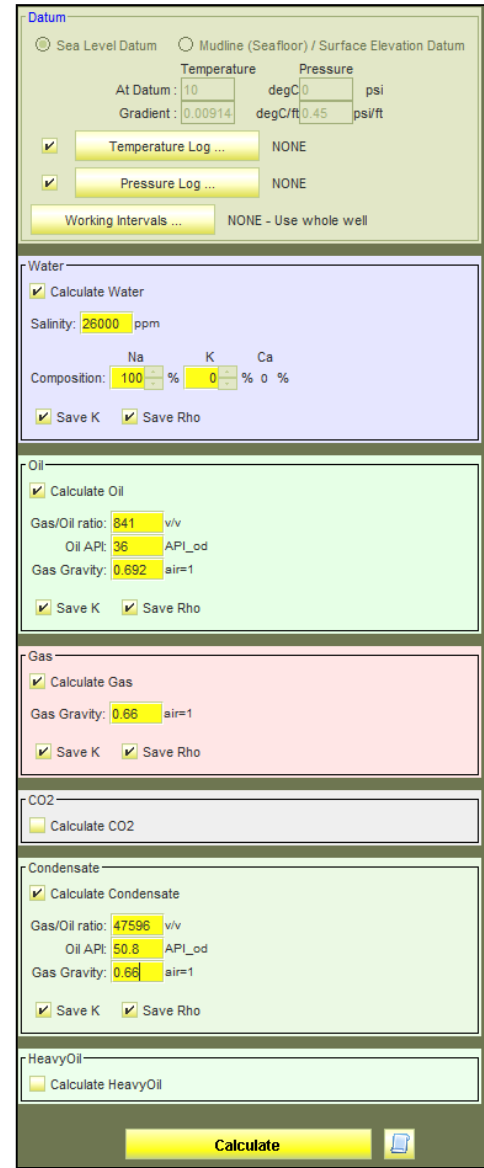
The fluid property parameters that are needed as input to the FLAG calculator are:

- Temperature profile
- Pressure profile
- Salinity (ppm)
- Gas Gravity
- Gas Oil Ratio (v/v)
- Oil API (API_{od})

Temperature and pressure profiles will be discussed in the next section and salinity logs are generated from the petrophysics.

The following fluid properties were used in this study:

Well	Oil			Gas	Brine
	API	GOR (scf/stb)	Gas Gravity (GG)	GG	Salinity (kppm)
22/3a-3	X	X	X	X	X
22/7-4	X	X	X	X	X
22/8A-2	X	X	X	X	X



Datum

Sea Level Datum (radio button selected) Mudline (Seafloor) / Surface Elevation Datum

At Datum: 10 degC 0 psi
Gradient: 0.00914 degC/ft 0.45 psi/ft

Temperature Log ... NONE
Pressure Log ... NONE
Working Intervals ... NONE - Use whole well

Water

Calculate Water (checkbox checked)
Salinity: 26000 ppm
Composition: Na 100 % K 0 % Ca 0 %
Save K (checkbox checked) Save Rho (checkbox checked)

Oil

Calculate Oil (checkbox checked)
Gas/Oil ratio: 841 v/v
Oil API: 36 API_{od}
Gas Gravity: 0.692 air=1
Save K (checkbox checked) Save Rho (checkbox checked)

Gas

Calculate Gas (checkbox checked)
Gas Gravity: 0.66 air=1
Save K (checkbox checked) Save Rho (checkbox checked)

CO₂

Calculate CO₂

Condensate

Calculate Condensate (checkbox checked)
Gas/Oil ratio: 47596 v/v
Oil API: 50.8 API_{od}
Gas Gravity: 0.66 air=1
Save K (checkbox checked) Save Rho (checkbox checked)

HeavyOil

Calculate HeavyOil

Calculate (yellow button) Print (blue icon)

5. Pressure and Temperature Profiles



5. Pressure & Temperature Profiles

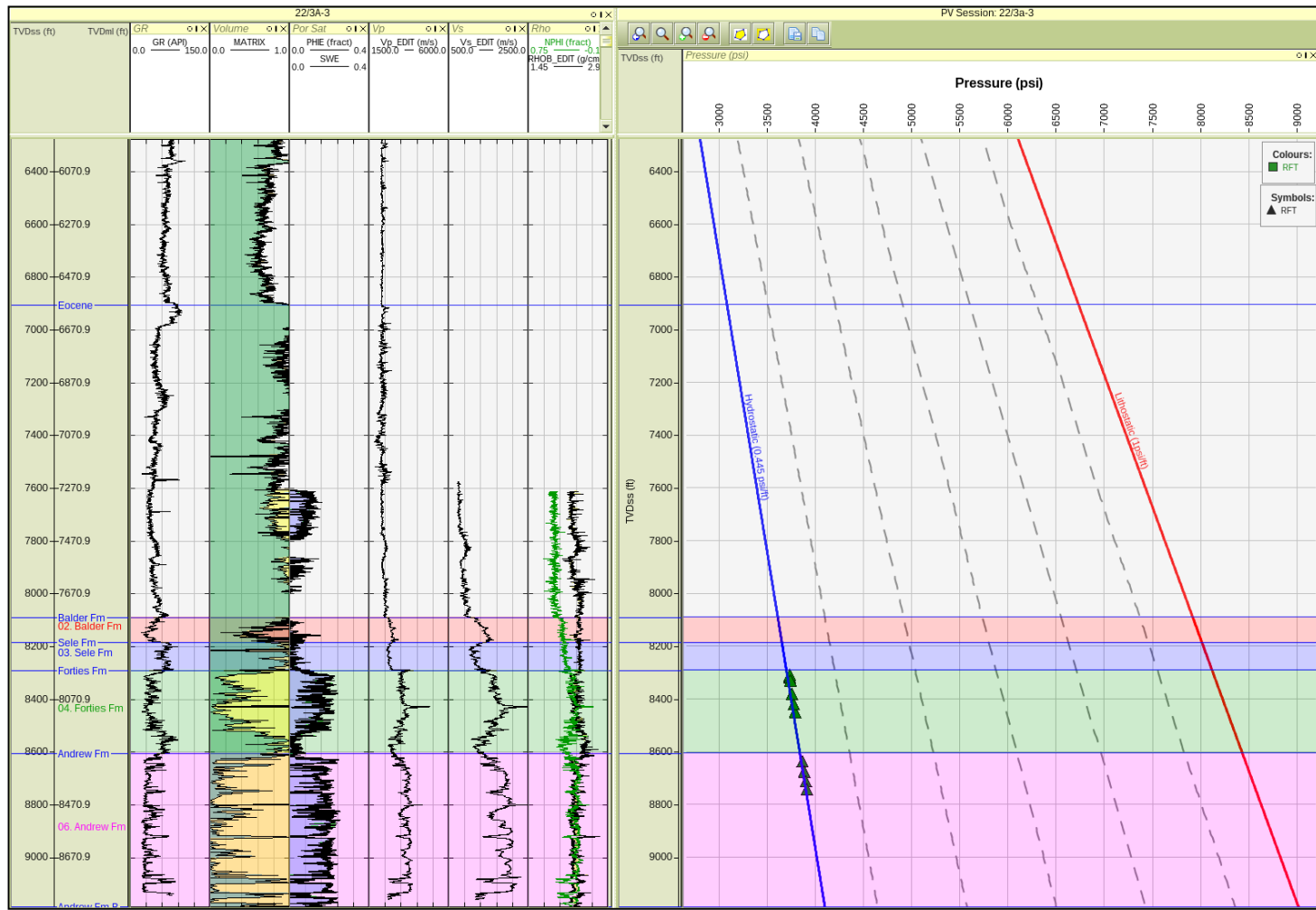
Pressure

The only pressure data available were a run of RFTs in 22/3a-3, which are displayed in the pressure-depth plot to the right.

Also shown are a 0.445 psi/ft hydrostatic gradient in blue and a 1 psi/ft overburden in red.

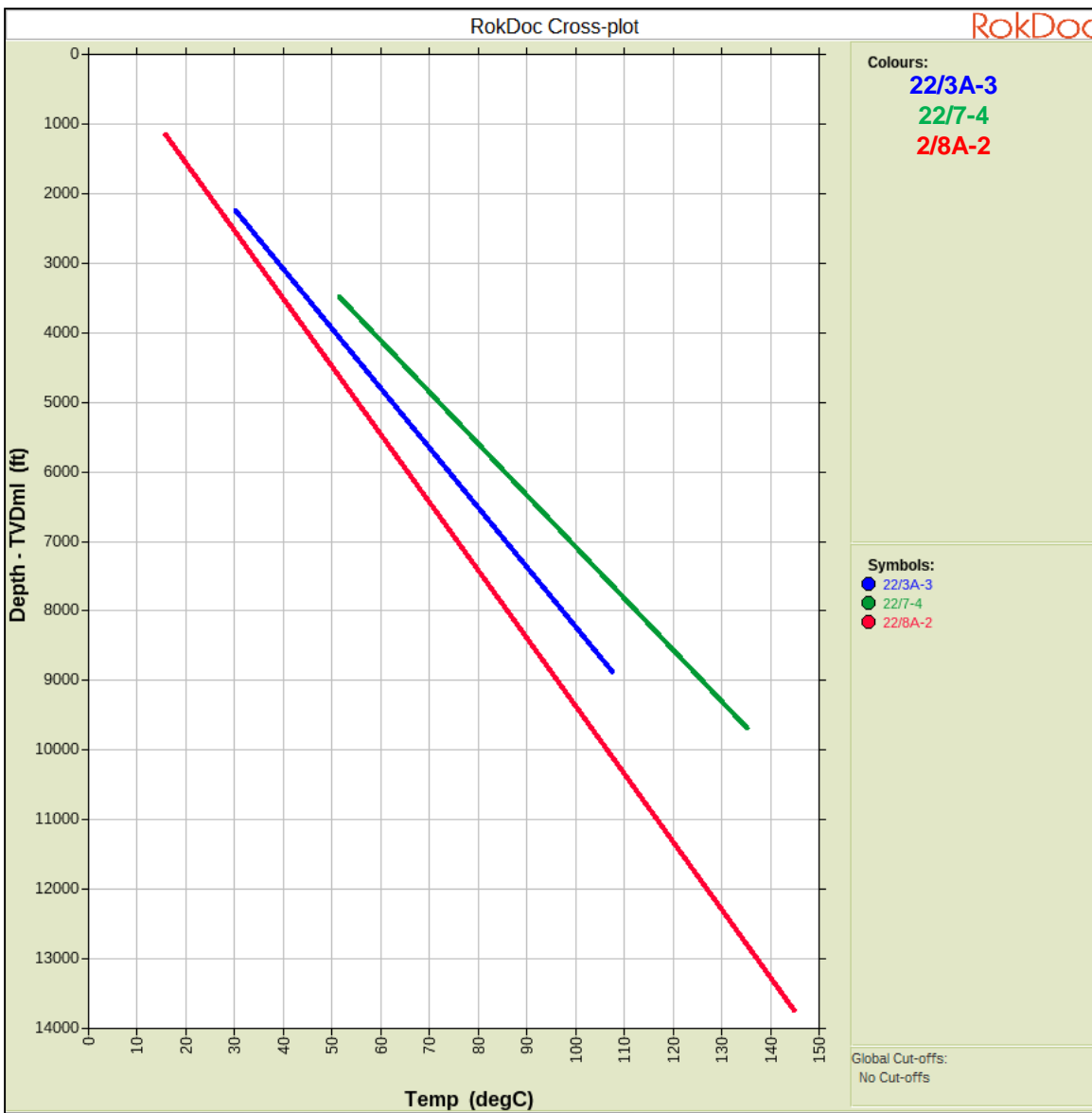
The Forties and Andrew sandstones in 22/3a-3 are observed to have almost no overpressure, with the pressure data plotting on the hydrostatic pressure trend.

Hydrostatic pressure will be used reservoir pressure profiles in all wells.



5. Pressure & Temperature Profiles

Temperature



Measured temperature data were corrected using *time since circulation* during the petrophysics analysis.

Temperature profiles were then supplied for use in the rock physics analysis.

Phase 1a: Petrophysical Analysis

See .las files, CPI reports and petrophysical reports for:

- 22/3a – 3
- 22/7 – 4
- 22/8a – 2



Phase 1b: Rock Physics Analysis & Modelling

1. Invasion Correction
2. Cross-plot Analysis
3. Vs Modelling
4. Log Modelling and Gap Filling
5. Gassmann Fluid Substitution to Brine and Hydrocarbon Cases
6. Synthetic Gathers
7. Inversion Feasibility



1. Invasion Correction

1.1 Introduction

1.2 Invasion Correction

1.1 Invasion Correction

Introduction

Before starting the rock physics analysis, the density logs must be corrected for the effects of the drilling mud invading the formation.

It is only required when the drilling mud has different properties to the reservoir *in situ* fluid (e.g. water-based mud invading a gas-filled reservoir, or oil-based mud invading a brine-bearing reservoir), which is the case in all three wells.

The density log needs correcting because it reads only a short distance into the borehole wall, whereas it is assumed that the sonic log reads much deeper into the formation and is therefore not affected by invasion.

The correction usually takes the form of a RokDoc User Programmer script and works by comparing the measured bulk density with the combined expected matrix and fluid densities, given the saturation and porosity. Where the bulk density is too high (in the case of water-based mud), drilling mud is inferred to have invaded the formation and this will need correcting.

Well	Drilling Mud	In situ reservoir fluid	Invasion correction needed?
22/3A-3	Oil-based mud	Brine	Yes
22/7-4	Oil-based mud	Brine	Yes
22/8A-2	Water-based mud	Brine, Oil	Yes

1.1 Invasion Correction

Mass-balancing Script

A correction is applied to the measured RhoB log to account for the effect of invasion (the measurement being a combination of matrix and mud filtrate) using the following method. The method relies on the porosities being core calibrated, which is the case here.

- Calculate the density of the insitu fluids. The fluid densities are calculated using FLAG, and the density of the fluid portion of the rock calculated at each point throughout the reservoir section based on the saturation curves.

$$\rho_{insitu} = (S_{we} \rho_{water}) + (S_o \rho_{oil})$$

- Calculate the apparent fluid density as measured by the bulk density log. This is calculated by using a modified porosity equation where the measured bulk density, grain density and porosity are known.

$$\rho_{fl} = \rho_{ma} - \left(\frac{\rho_{ma} - \rho_B}{\varphi} \right)$$

- The correction applied to the bulk density log is determined by the difference between the insitu fluid density and the apparent fluid density.

$$\rho_{corr} = \rho_B - (\varphi \rho_{fl} - \varphi \rho_{insitu})$$

- An estimate of the invaded zone saturation can also be made based on this difference.

1.2 Invasion Correction

22/3A-3

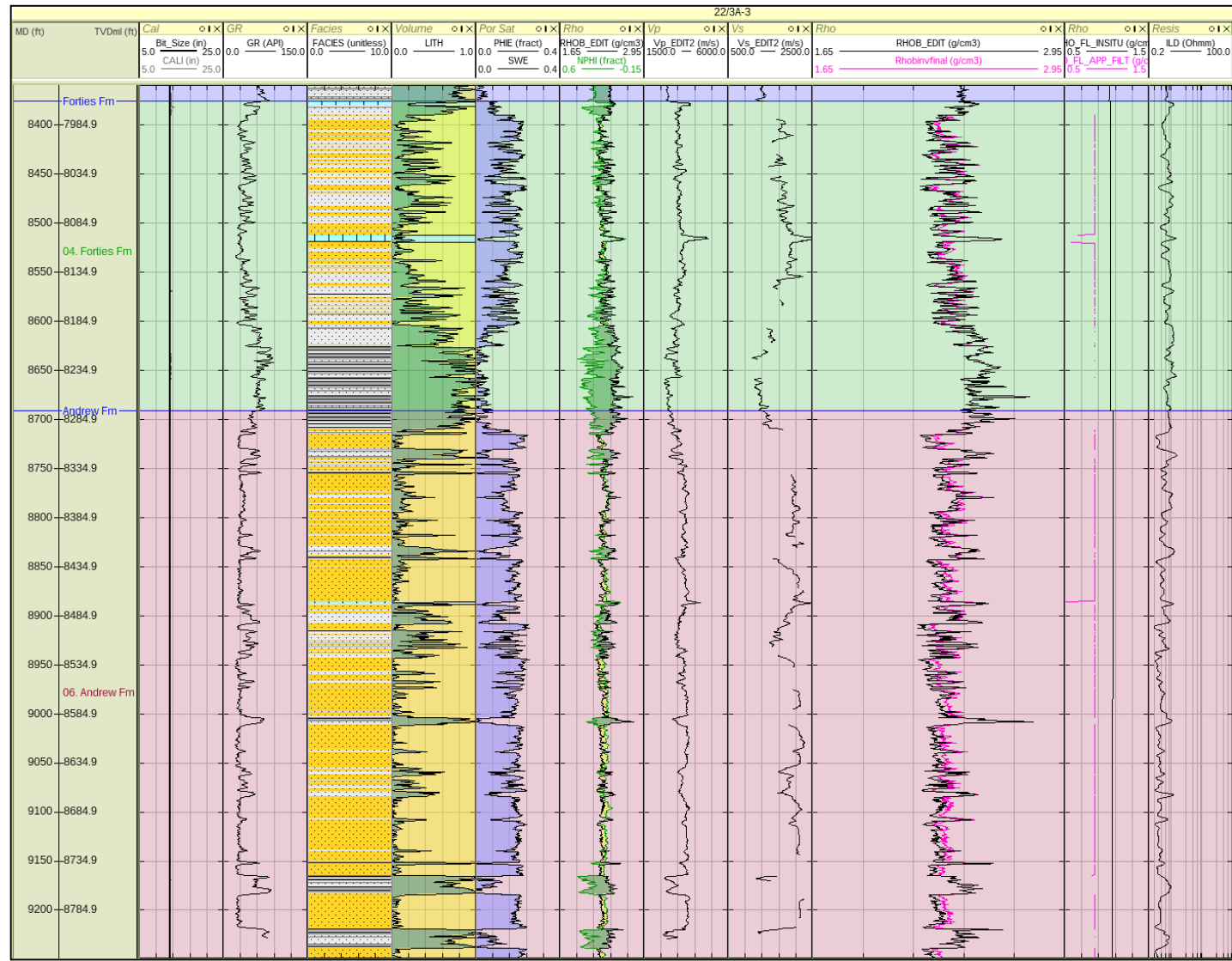
The image to the right shows the density log invasion correction applied to 22/3A-3.

The **black** log in the third last track is the measured density and the **pink** log underlying it is the invasion-corrected density – Rhobinvfinal.

Invasion correction using the mass-balancing script determined that the brine sands had been invaded by less dense oil-based mud.

The script applies a correction to remove the drilling mud from the sands and replace it with brine in the brine sands, increasing the density log.

The second to last track shows the insitu fluid density (**black**) and the apparent fluid density (as calculated by the script, **pink**).



1.2 Invasion Correction

22/7-4

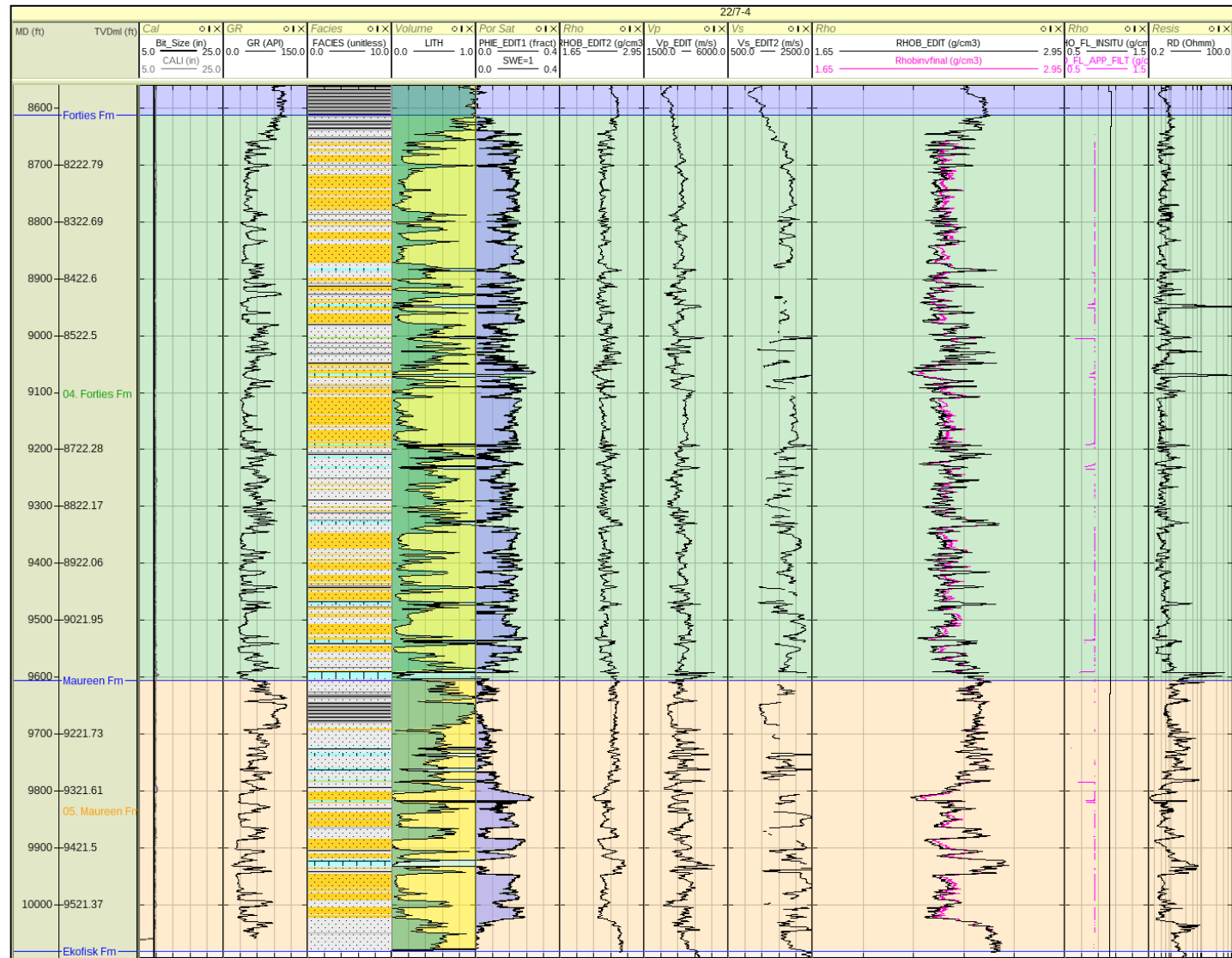
The image to the right shows the density log invasion correction applied to 22/7-4.

The **black** log in the third last track is the measured density and the **pink** log underlying it is the invasion-corrected density – Rhobinvfinal.

Invasion correction using the mass-balancing script determined that the brine sands had been invaded by less dense oil-based mud.

The script applies a correction to remove the drilling mud from the sands and replace it with brine in the brine sands, increasing the density log.

The second to last track shows the insitu fluid density (**black**) and the apparent fluid density (as calculated by the script, **pink**).



1.2 Invasion Correction

22/8A-2

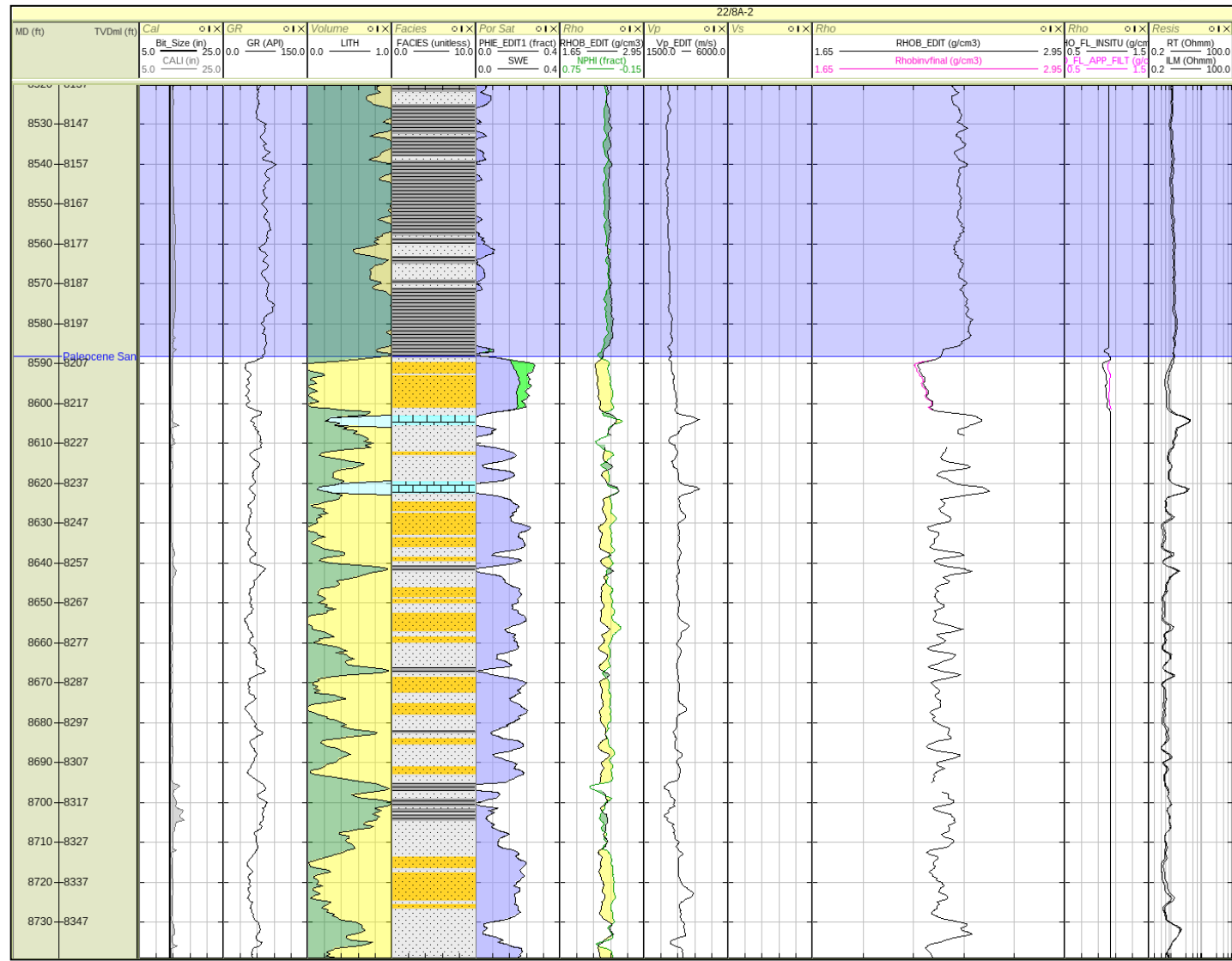
The image to the right shows the density log invasion correction applied to 22/8A-2.

The **black** log in the third last track is the measured density and the **pink** log underlying it is the invasion-corrected density – Rhobinvfinal.

Invasion correction using the mass-balancing script determined that the oil-bearing sand had been invaded by more dense water-based mud.

The script applies a correction to remove the drilling mud from the sands and replace it with oil, decreasing the density log.

The second to last track shows the insitu fluid density (**black**) and the apparent fluid density (as calculated by the script, **pink**).



2. Cross-plot Analysis

- 2.1 Introduction
- 2.2 Vp/Vs Cross-plots for Sand and Shale
- 2.3 Vp/RhoB Cross-plots for Sand and Shale
- 2.4 Summary

2.1 Rock Physics Cross-plot Analysis

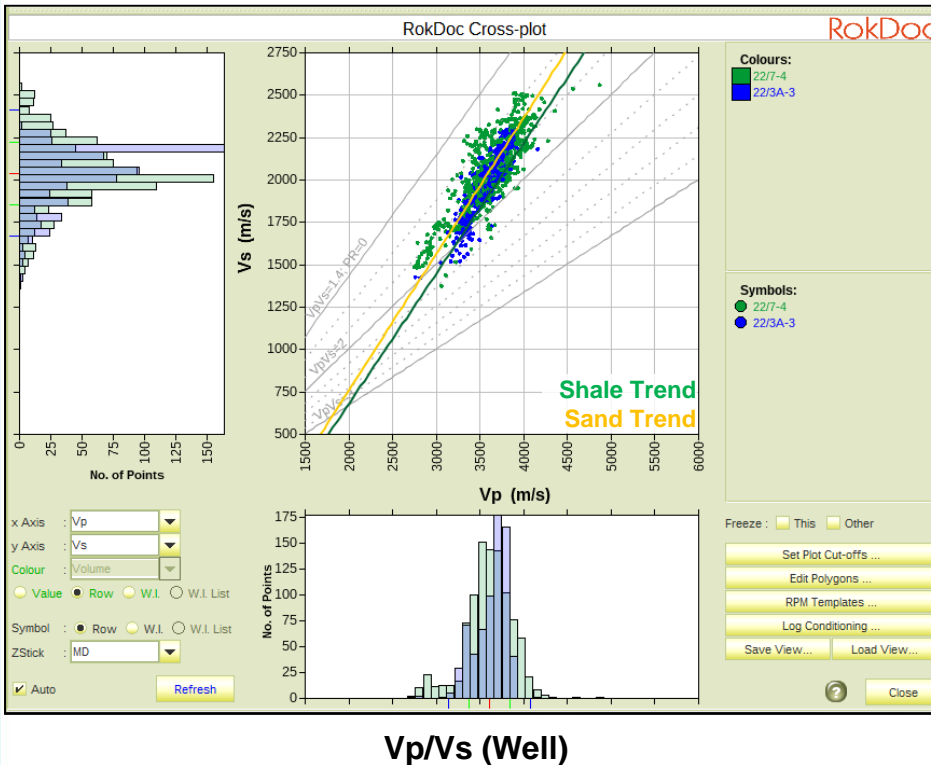
Introduction



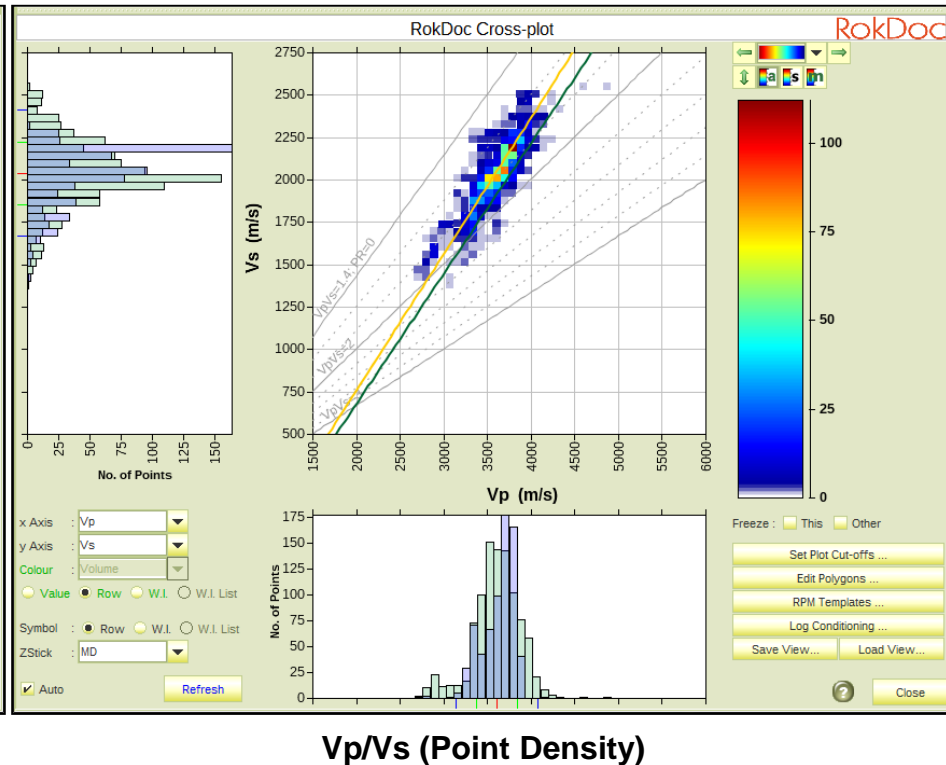
- Vp/Vs and Vp/RhoB trends are derived in this section, which are then used to model missing logs and fill larger gaps in the log data. Smaller gaps will be filled with spline interpolations.
- Trends are derived for the sand and shale end-members in the interval of interest: Eocene – Base Paleocene.
- Trends are derived for the end-member facies:
 - Sand
 - Shale
 - Limestone
 - Tuff (~Tuffaceous shale due to the lack of clean Tuff)

2.2 Vp/Vs Cross-plot

Sands



Vp/Vs (Well)



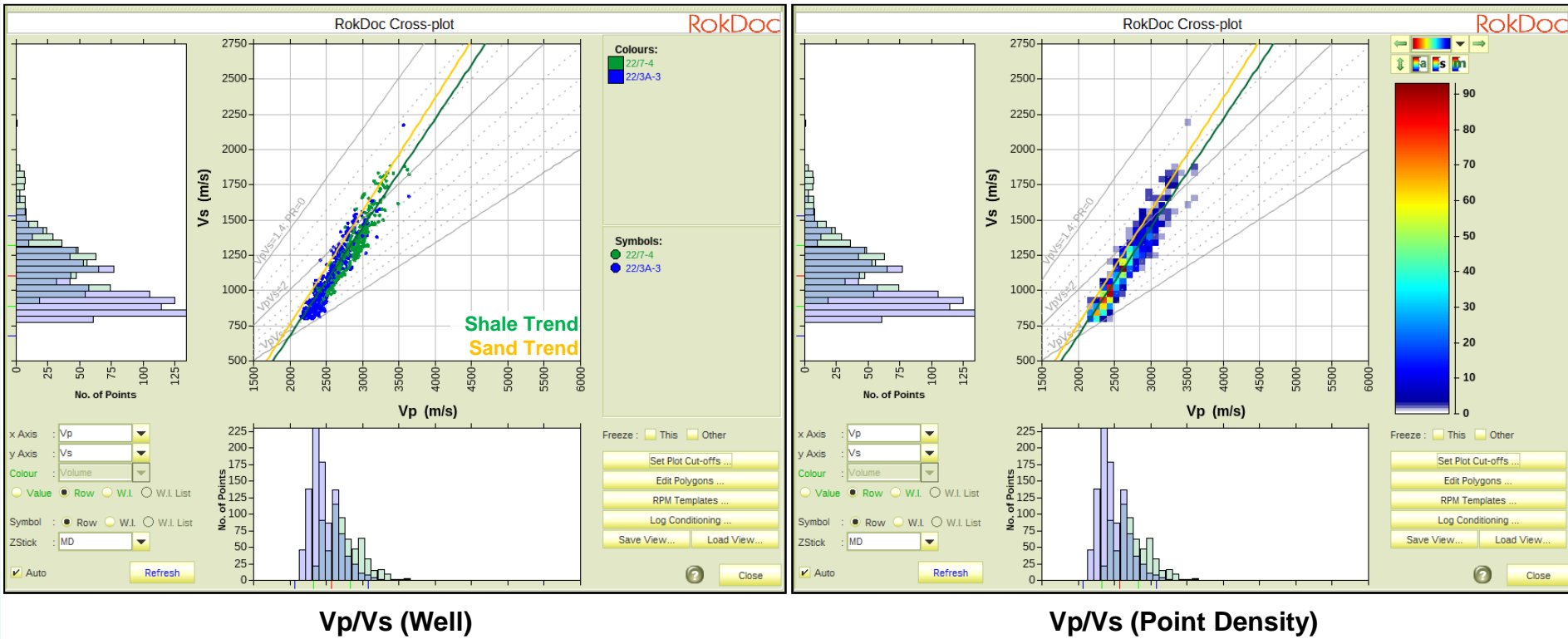
Vp/Vs (Point Density)

The sand data is generally faster than the shales, and the magnitude to the velocities suggest a degree of contact cement is present. The Greenberg-Castagna sandstone trend, an established rock physics trend, matches the data quite well, so this trend will be used:

$$Vs(\text{km/s})_{\text{sand}} = 0.80416 * Vp(\text{km/s}) - 0.85588$$

2.2 Vp/Vs Cross-plot

Shales

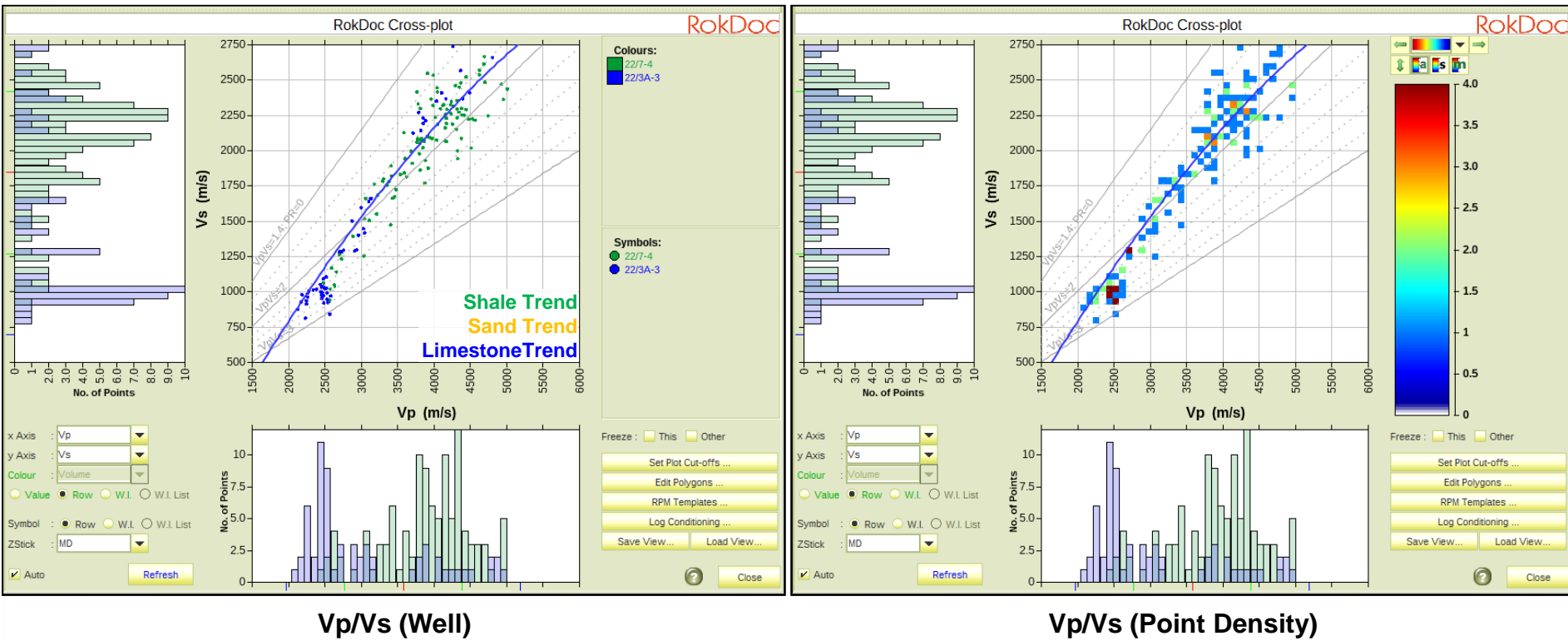


The shale data is slower than the sands. The Greenberg-Castagna shale trend, an established rock physics trend, matches the data quite well, so this trend will be used:

$$Vs(\text{km/s})_{\text{shale}} = 0.76969 * Vp(\text{km/s}) - 0.86735$$

2.2 Vp/Vs Cross-plot

Limestone



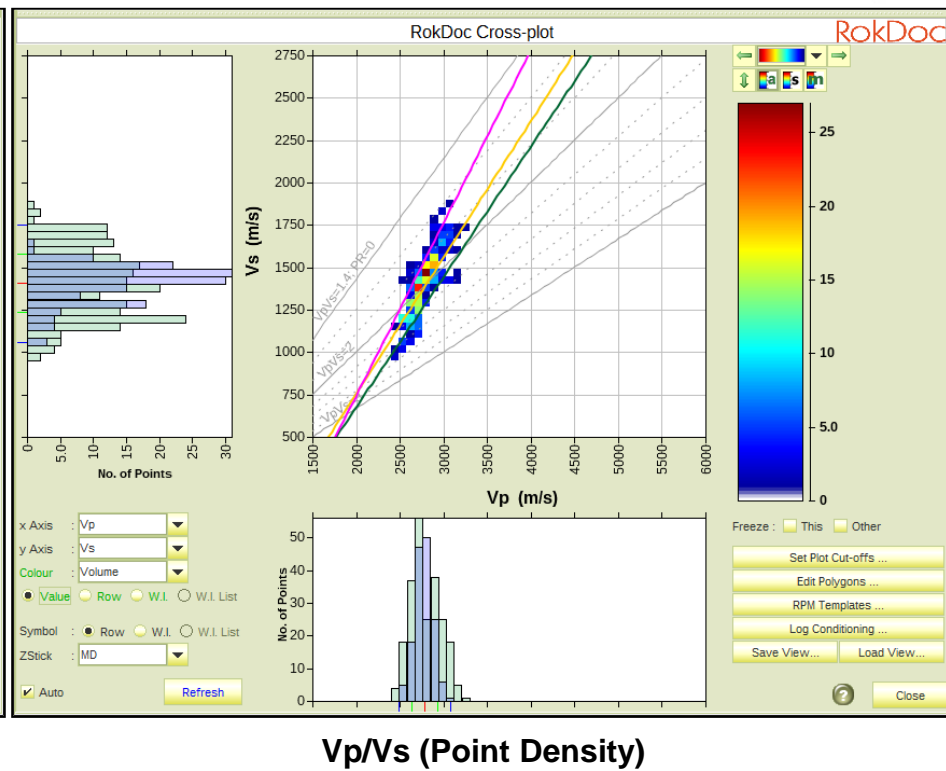
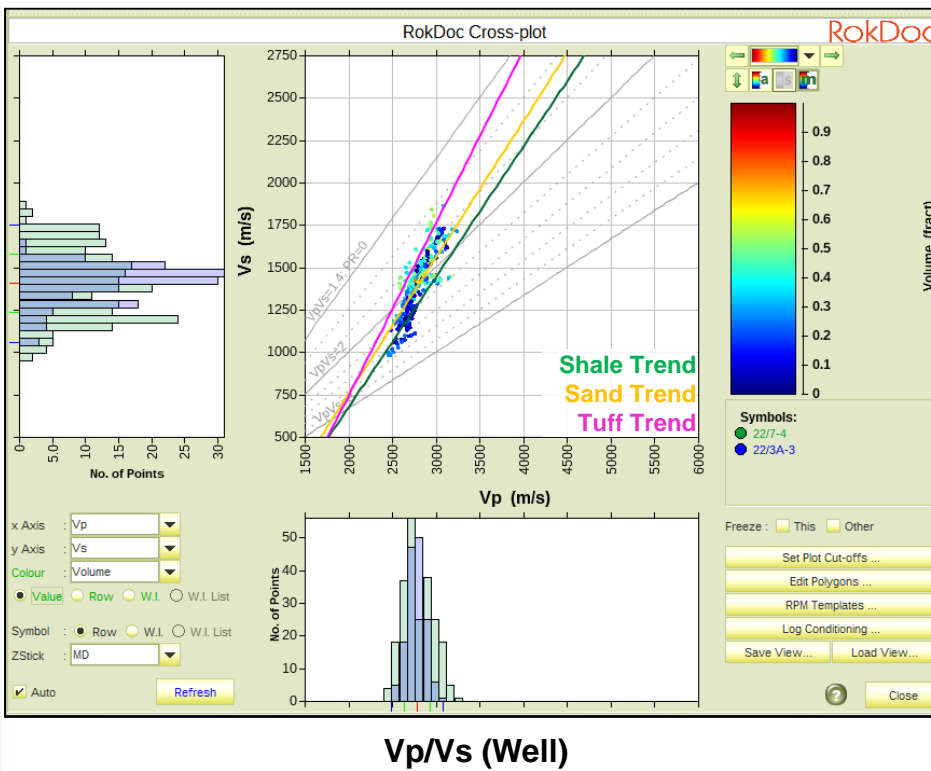
There is a lack of clean end-member quality limestone because most the limestone data in 22/7-4 and 22/3A-3 is composed of thin limestone stringers.

The Greenberg-Castagna limestone trend, an established rock physics trend, matches the data quite well, so this trend will be used:

$$Vs(\text{km/s})_{\text{limestone}} = 1.01677 * Vp(\text{km/s})^2 - 0.05508 * Vp(\text{km/s}) - 1.03049$$

2.2 Vp/Vs Cross-plot

Tuff



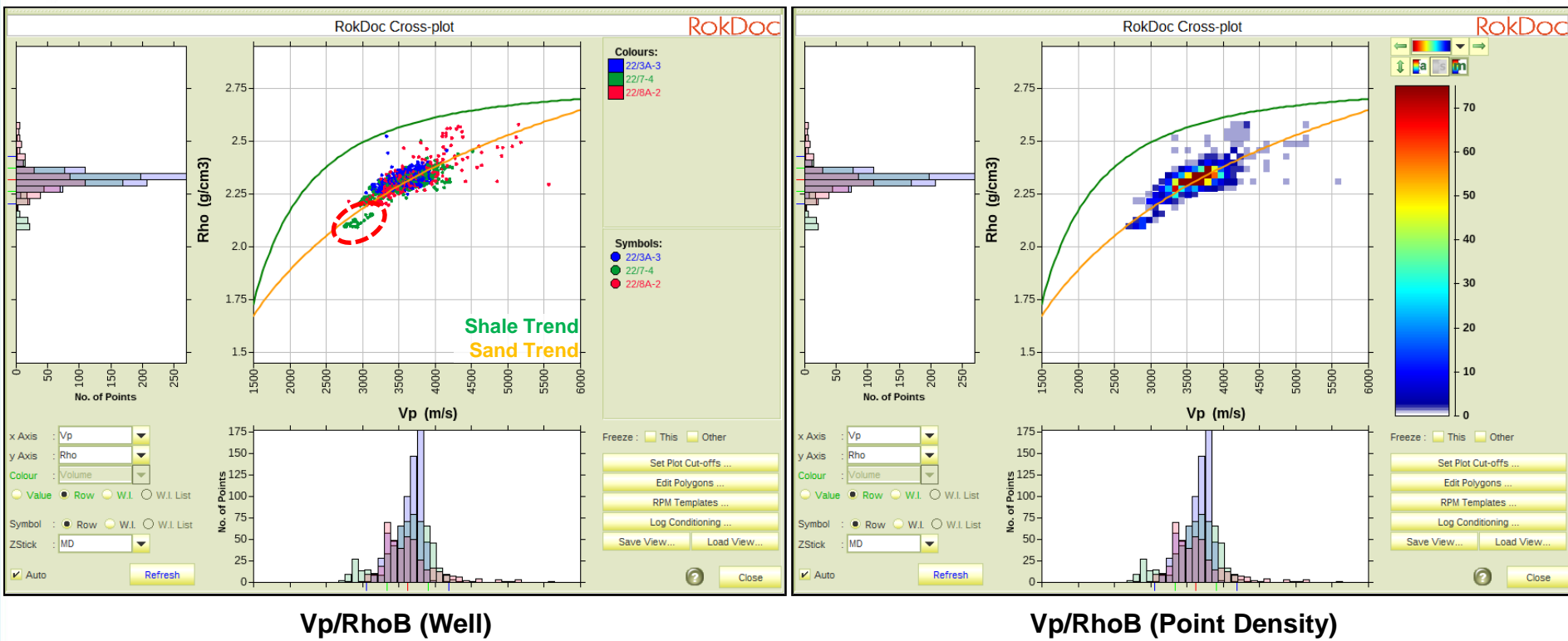
There are no clean sections of Tuff in the study, but a Vp/Vs trend for Tuff is needed to model Vs in 22/8A-2. Therefore the tuff trend was defined on the very edge of the Tuffaceous shale data and will be tested on the two wells with measured Vs.

The following trend was derived:

$$Vs(\text{km/s})_{\text{tuff}} = 1.0199 * Vp(\text{km/s}) - 1.300$$

2.3 Vp/RhoB Cross-plot

Sands



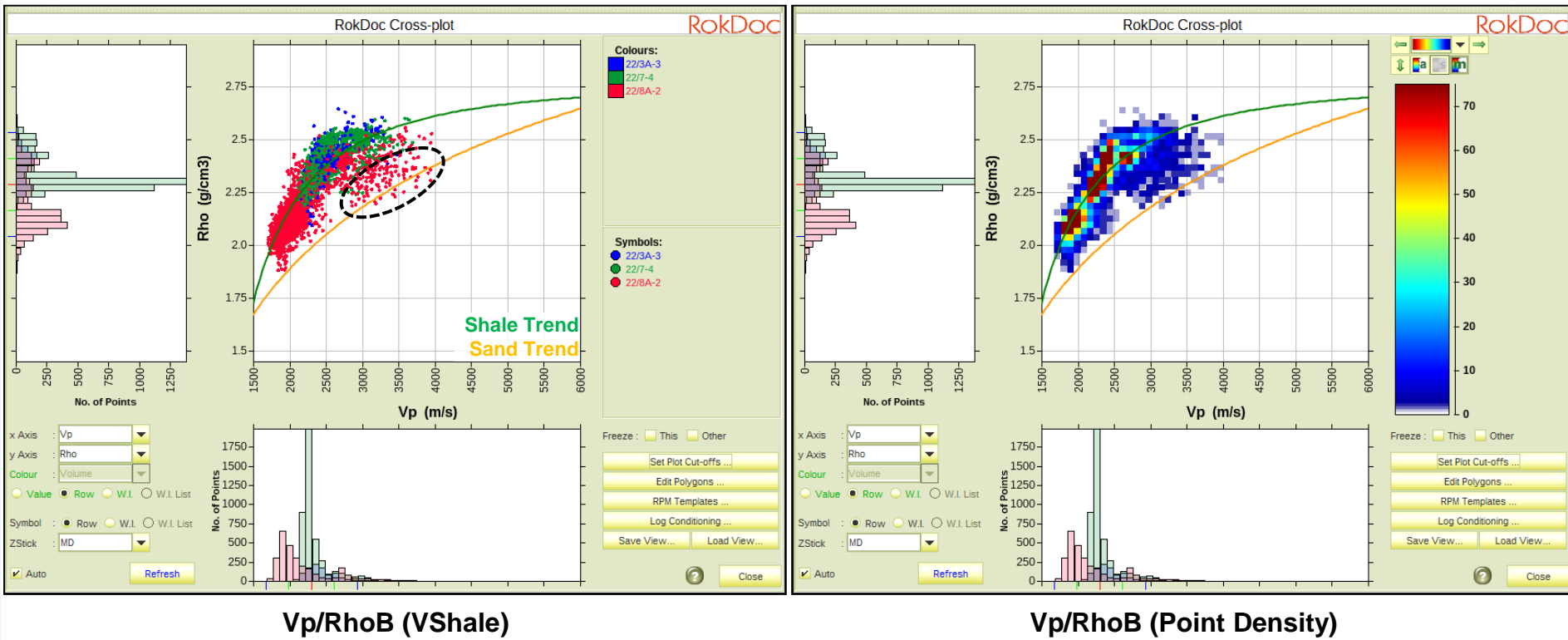
$$\text{RhoB(g/cc)}_{\text{sand}} = -6.6400 * \text{Vp(km/s)}^{\wedge} -0.1208 + 7.9933$$

Vsh < 0.1 cut-off used to isolate cleanest end-members.

The Balder sand plots off-trend and is circled in red.

2.3 Vp/RhoB Cross-plot

Shales



$$\text{RhoB(g/cc)}_{\text{shale}} = -2.2420 * \text{Vp(km/s)} ^ {-1.8770} + 2.7767$$

The effects of poorly resolved shale/sand interbeds are circled in **black**, where the shale data move towards the sand trend..

2.4 Rock Physics Cross-plot Analysis

Summary



- Vp/Vs and Vp/RhoB trends were derived for end-member sands and shales, using log data from all 3 wells in the study. The end-member log data were generally consistent across all wells.
- The Vp/Vs trends will be used for modelling Vs in 22/28A-2, so additional trends were needed for limestone and tuff. The following trends were derived:
- $Vs(\text{km/s})_{\text{sand}} = 0.80416 * Vp(\text{km/s}) - 0.85588$
- $Vs(\text{km/s})_{\text{shale}} = 0.76969 * Vp(\text{km/s}) - 0.86735$
- $Vs(\text{km/s})_{\text{limestone}} = 1.01677 * Vp(\text{km/s})^2 - 0.05508 * Vp(\text{km/s}) - 1.03049$
- $Vs(\text{km/s})_{\text{tuff}} = 1.0199 * Vp(\text{km/s}) - 1.300$
- The Vp/RhoB are generally consistent across all wells, although data quality is noticeably poorer in 22/8A-2, compared to 22/3A-3 and 22/7-4. The following trends were derived:
- $RhoB(\text{g/cc})_{\text{sand}} = -6.6400 * Vp(\text{km/s})^{-0.1208} + 7.9933$
- $RhoB(\text{g/cc})_{\text{shale}} = -2.2420 * Vp(\text{km/s})^{-1.8770} + 2.7767$

3. Vs Modelling

3.1 Introduction

3.2 Vs Modelling



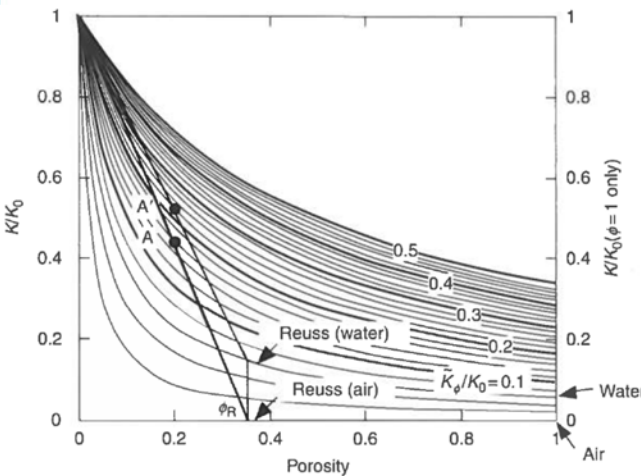
3.1 Vs Modelling

Introduction

- A Vs log is vital for understanding the AVO response at a well.
- 2 of the wells in this study contain measured Vs, 22/3A-3 and 22/7-4, so the derived Vp/Vs trends will be tested first at these two wells, before modelling Vs at the remaining well without measured Vs: 22/8A-2.
- Modelling Vs in thick reservoir sands with insitu hydrocarbons is more difficult than modelling Vs in non-reservoir lithologies because the fluid effect has to be taken into account.
- A useful method of doing this is with the Modified Gassmann method, in which the fluid effect is estimated using a linearized form of the Gassmann equation.
- The goal of this stage is a full set of elastic logs for each well.

3.1 Vs Modelling

Modified Gassmann



The linear form follows from the graphical construction shown on the left. A line is drawn from the mineral point ($\phi = 0$) through a point representing the rock modulus saturated with the initial pore fluid (A). The line intersects the Reuss average for the pore fluid at ϕ_R , this is a measure of pore stiffness. The rock modulus for a new pore fluid (A') fall along a second line drawn from the mineral point intersecting the the Reuss average for the new pore fluid at ϕ_R .

$$\Delta K_{Gass.}(\varphi) = \frac{\varphi}{\varphi_R} \Delta K_R(\varphi_R)$$

$\Delta K_R(\varphi_R)$ is the difference in the Reuss average for the two fluids evaluated at the intercept porosity ϕ_R and equals the Gassmann predicted change in saturated rock bulk modulus $\Delta K_{Gass.}(\varphi)$.

As the pore-fluid moduli are much smaller than the mineral moduli the Reuss average can be approximated as:

$$K_R(\varphi_R) \approx \frac{K_{fl}}{\varphi_R}$$

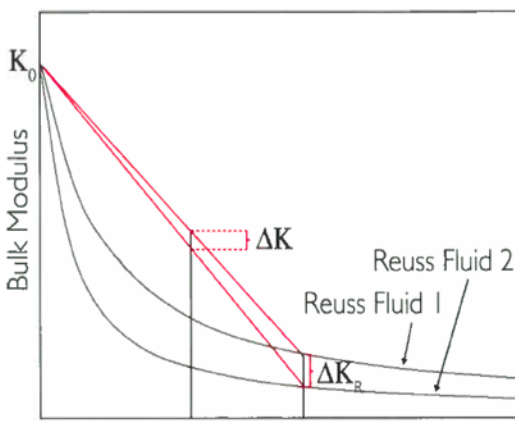
The linear form of Gassmann's relations can be approximated as:

$$\Delta K_{Gass.}(\varphi) \approx \frac{\varphi}{\varphi_R^2} \Delta K_{fl}$$

As Gassmann's relations predict no change in shear modulus the linear form can also be written in terms of P-wave modulus ($M = V_p^2 \rho$):

$$\Delta M_{Gass.}(\varphi) = \Delta K_{Gass.}(\varphi) \approx \frac{\varphi}{\varphi_R^2} \Delta K_{fl}$$

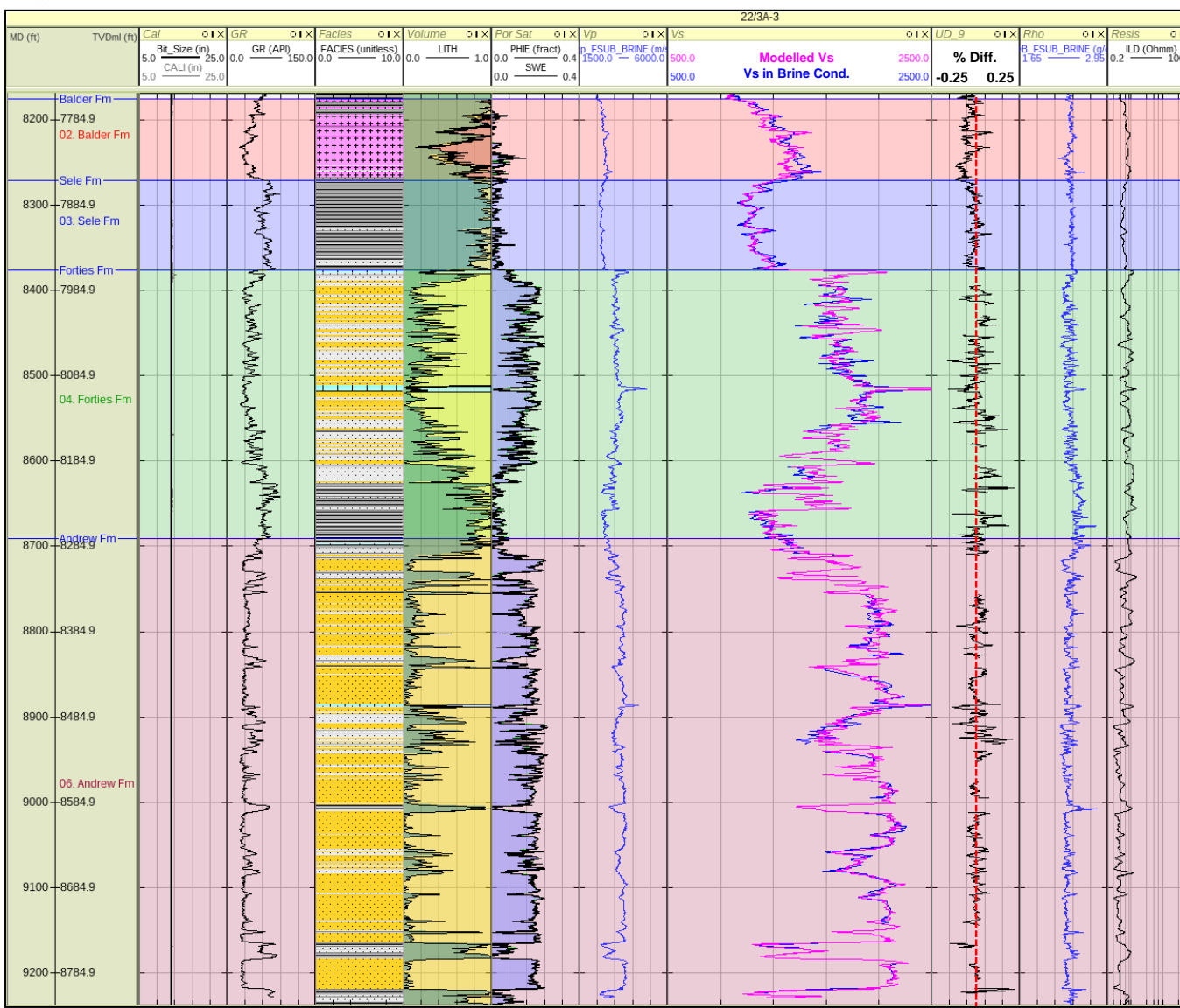
The linear relation above is used to predict a brine saturated V_p , at which point a V_s value can be predicted (using the calibrated G/C coefficients). The conventional Gassmann equation is then used to replace the insitu hydrocarbons. The term ϕ_R is the intercept porosity and should be close to the critical porosity of the rock.



NH15515

3.2 Vs Modelling at Wells with Measured Vs

22/3A-3



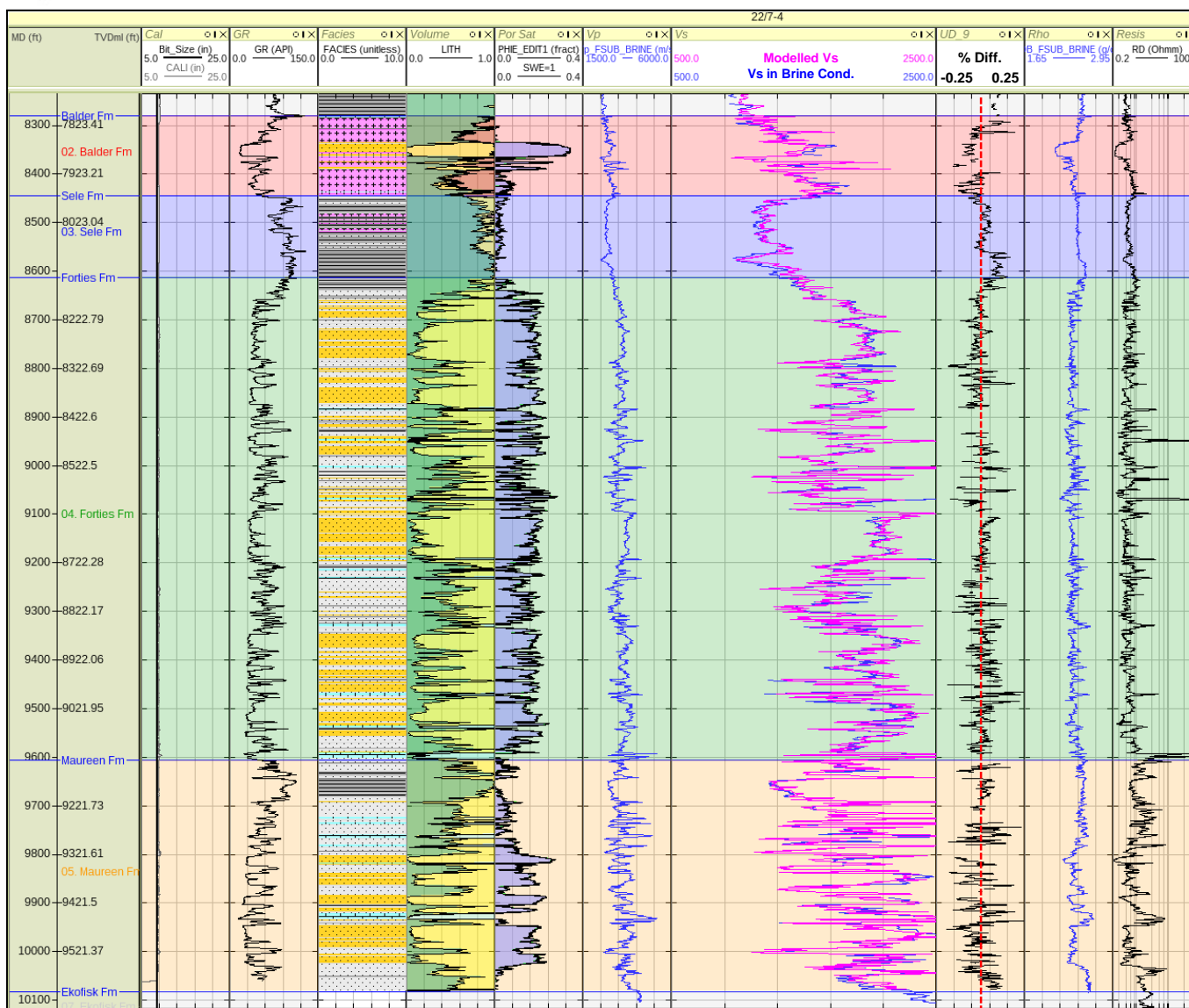
The Vs prediction is shown in the 4th track from the right in **pink**, along with the measured Vs (in insitu brine conditions), in **blue**.

Overall, the prediction looks accurate, showing a very good match to the Vs in brine conditions throughout the interval of interest.

$$\% \text{ Diff} = (\text{Modelled Vs} - \text{Measured Vs}) / \text{Measured Vs}$$

3.2 Vs Modelling at Wells with Measured Vs

22/7-4



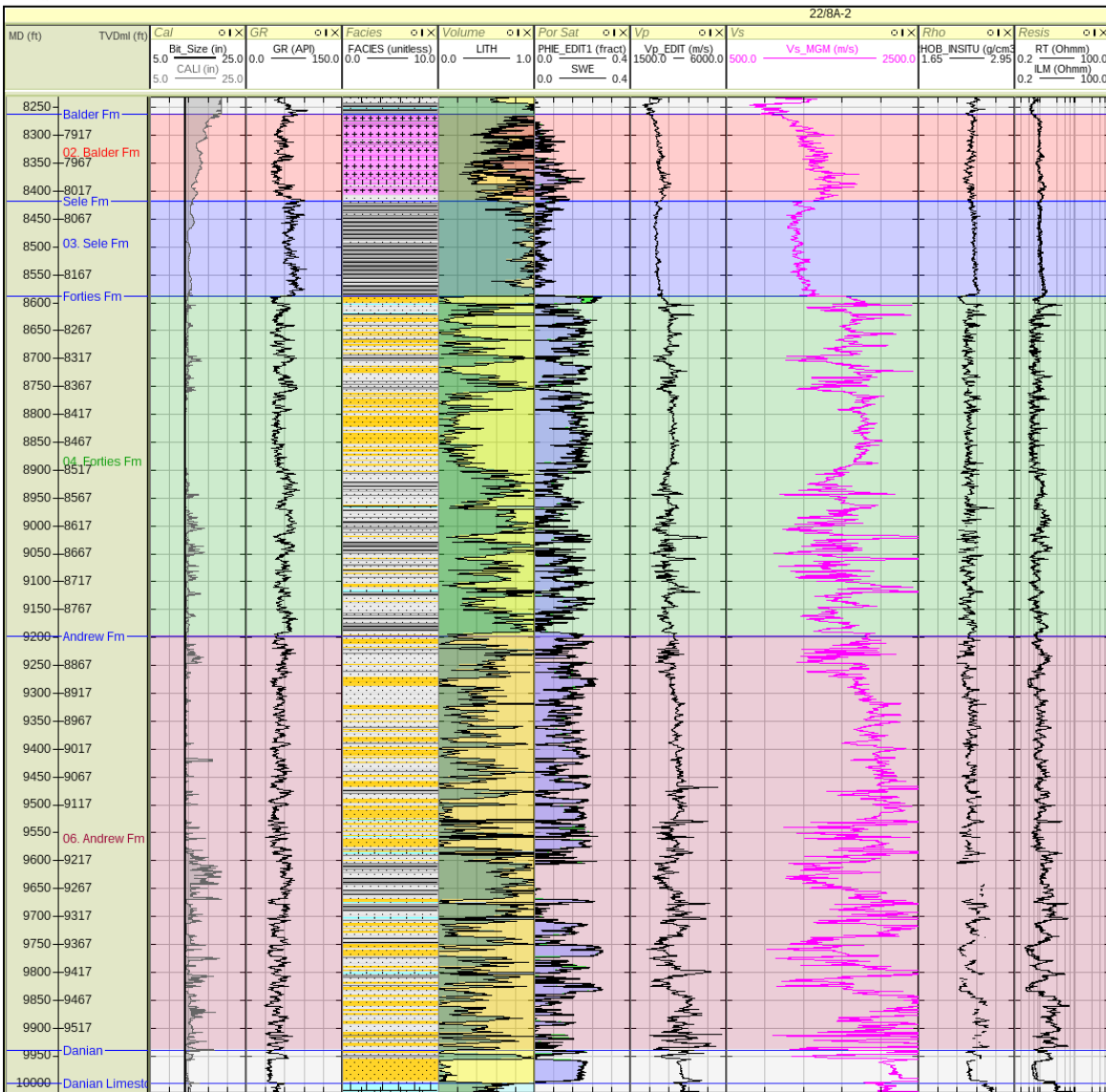
The Vs prediction is shown in the 4th track from the right in **pink**, along with the measured Vs (in insitu brine conditions), in **blue**.

Overall, the prediction looks accurate, showing a very good match to the Vs in brine conditions throughout the interval of interest.

$$\% \text{ Diff} = (\text{Modelled Vs} - \text{Measured Vs}) / \text{Measured Vs}$$

3.2 Vs Modelling at Wells with Measured Vs

22/8A-2



A Modified Gassmann approach will be used to model Vs in 22/8A-2 because the well contains small amount of insitu oil at the top of the Forties Fm.

The Vs prediction from Modified Gassmann is shown in the 3rd track from the right in pink.

As detailed earlier PorR is a fitting parameters and needs to be optimised to determine the pore stiffness and understand the fluid effect.

The optimised PorR is within the range expected for a sandstone, so the calculation is behaving as expected and the results are reliable.

Select Vp Log ... Vp EDIT

Input PorR Value

Initial	Final
0.40	0.39

Input Minimise Parameters

Max Tries	F Tolerance	X Tolerance
100	0.00010000	0.00010000

Optimise

Minimise Results

Number of Iterations : 13
 Actual F Tolerance : 3.099254908356386E-5
 Actual X Tolerance : 1.953124999982236E-5
 Optimisation Value : 15.300636747231287

4. Log Modelling & Gap filling

4.1 Introduction

4.2 Log Modelling & Gap-filling

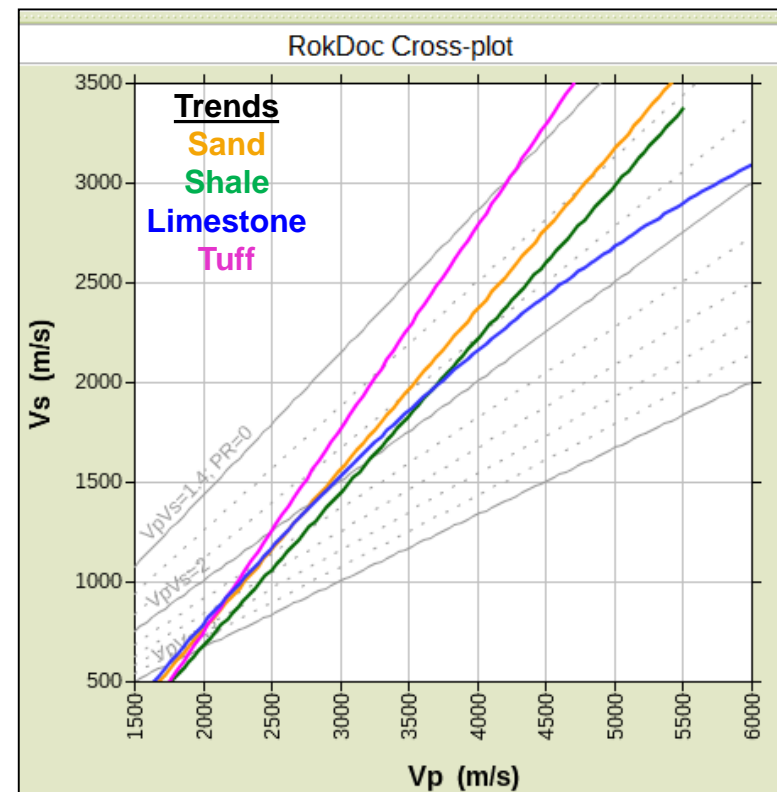
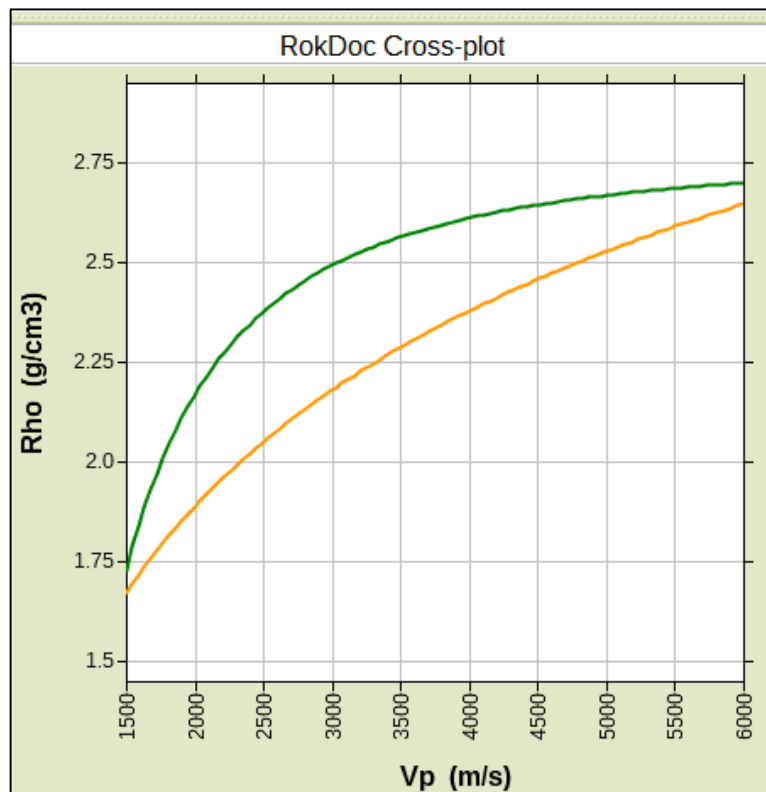
4.3 Summary



4.1 Log Modelling

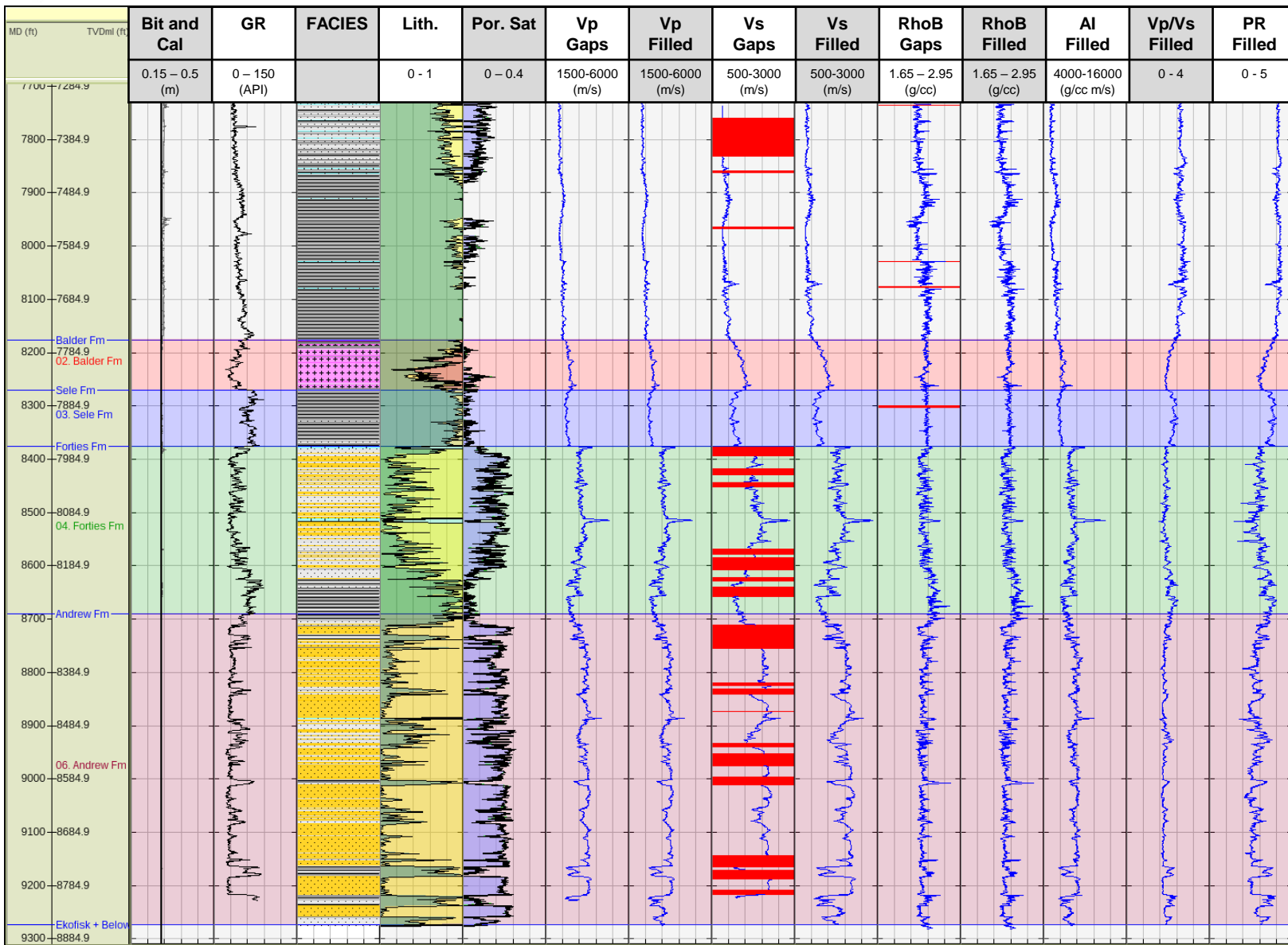
Introduction

- Vp/RhoB and Vp/Vs trend have now been derived for the end-member lithologies, using the log data from the 3 wells where the data are in insitu brine conditions.
- Synthetic logs can now be generated from the trends, which will be used to fill gaps in the logs, modelling RhoB from Vp, Vp from RhoB and Vs from Vp.
- The goal of this section is a full set of continuous elastic logs for each well. Note that gaps are only present in brine sections, so no fluid substitution is needed at this stage.



4.2 Log Modelling & Gap-filling

22/3A-3



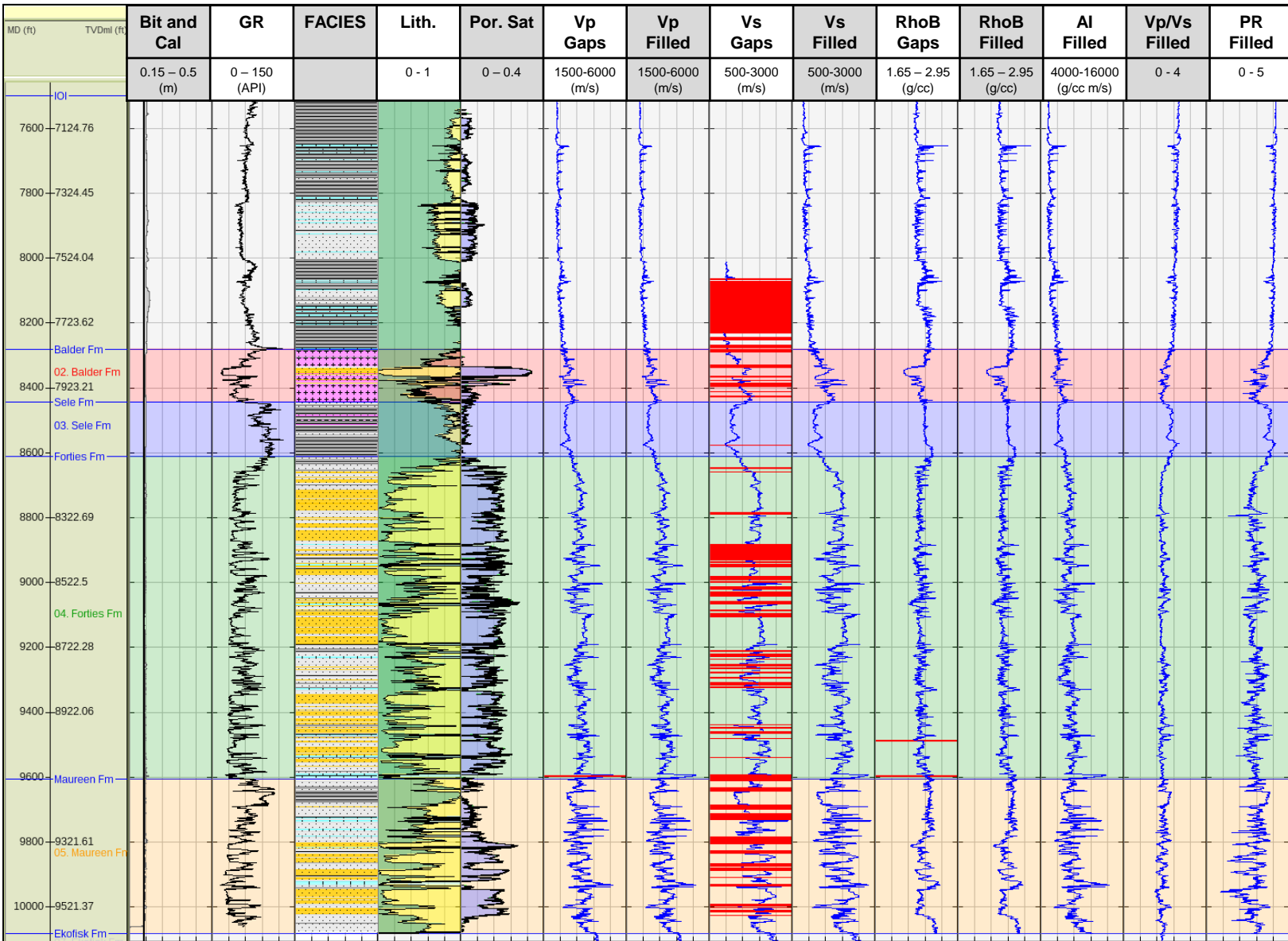
A number of small gaps at the top of the Vp run were filled with spline interpolations but these are outside of the interval of interest anyway.

Small gaps in RhoB were filled with spline interpolations and a larger gap in the Sele Fm was filled with the synthetic RhoB log.

The Vs log contained many gaps that were mostly filled with the synthetic Vs log.

4.2 Log Modelling & Gap-filling

22/7-4

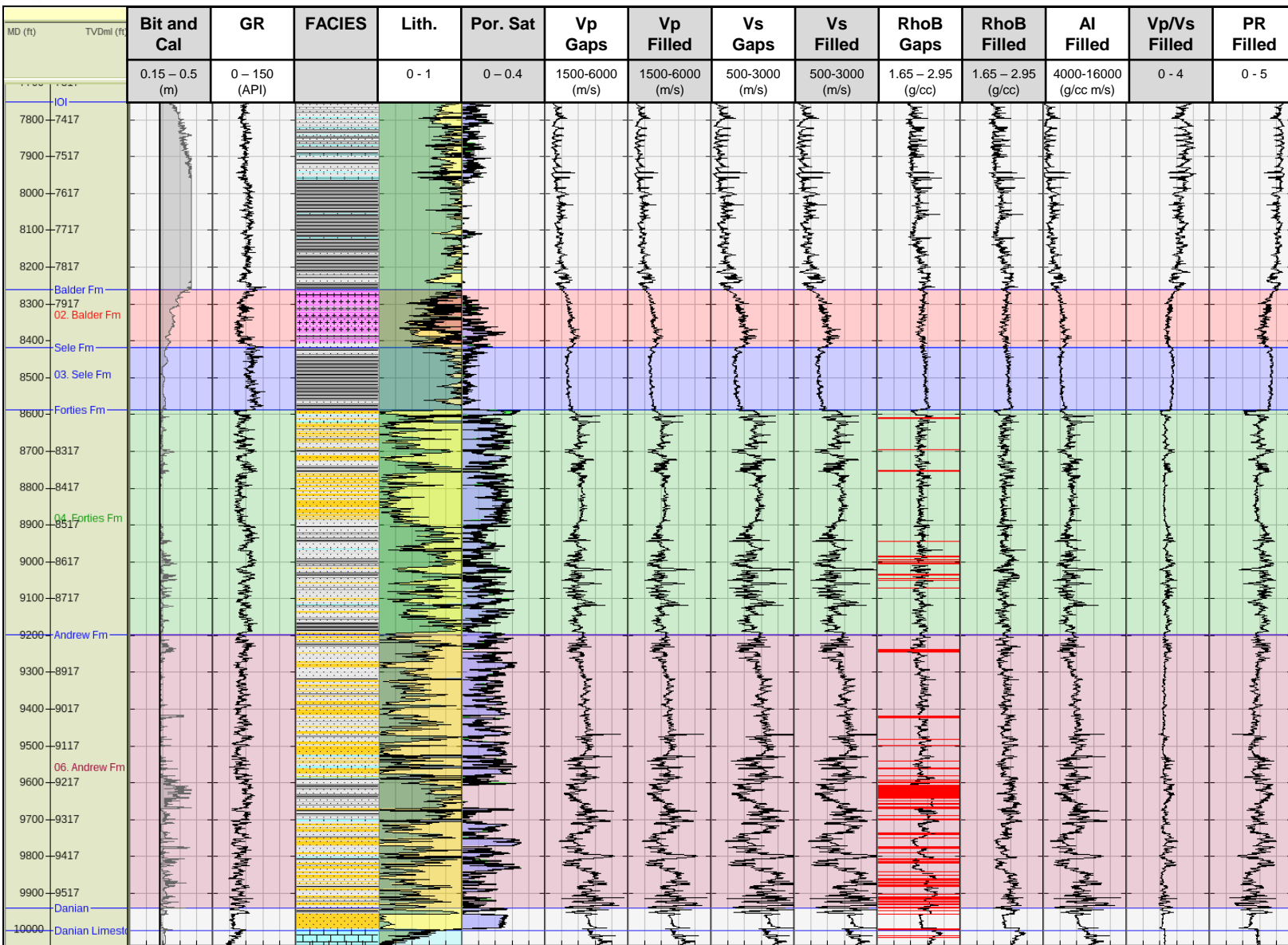


A small number of number of gaps in the Vp and Rhob logs were filled with spline interpolations.

The Vs log had been heavily edited and the large number of gaps were mainly filled with the synthetic Vs log.

4.2 Log Modelling & Gap-filling

22/8A-2



A small number of number of gaps in the Vp, above the interval of interest, were filled with spline interpolations.

The Rhob log had been heavily edited, and the gaps were mostly filled with the synthetic Rhob log, with some smaller gaps being filled with spline interpolations.

The Vs log contained no gaps because it was predicted from the gap-filled Vp log.

4.3 Vs Modelling Summary

- The Vp/RhoB and Vp/Vs trends have been used to model logs and fill any gaps present in the measured data.
- All wells now contain a full set of continuous elastic logs.
- 22/3A-3 and 22/7-4 are in brine conditions.
- 22/8A-2 contains trace oil and the logs will be fluid substituted to brine conditions in the next section.

5. Fluid Substitution & Elastic Attributes

5.1 Introduction

5.2 Introduction to Dry Rock Plots

5.3 Fluid Substitution to Brine and Hydrocarbon Conditions

5.1 Fluid Substitution

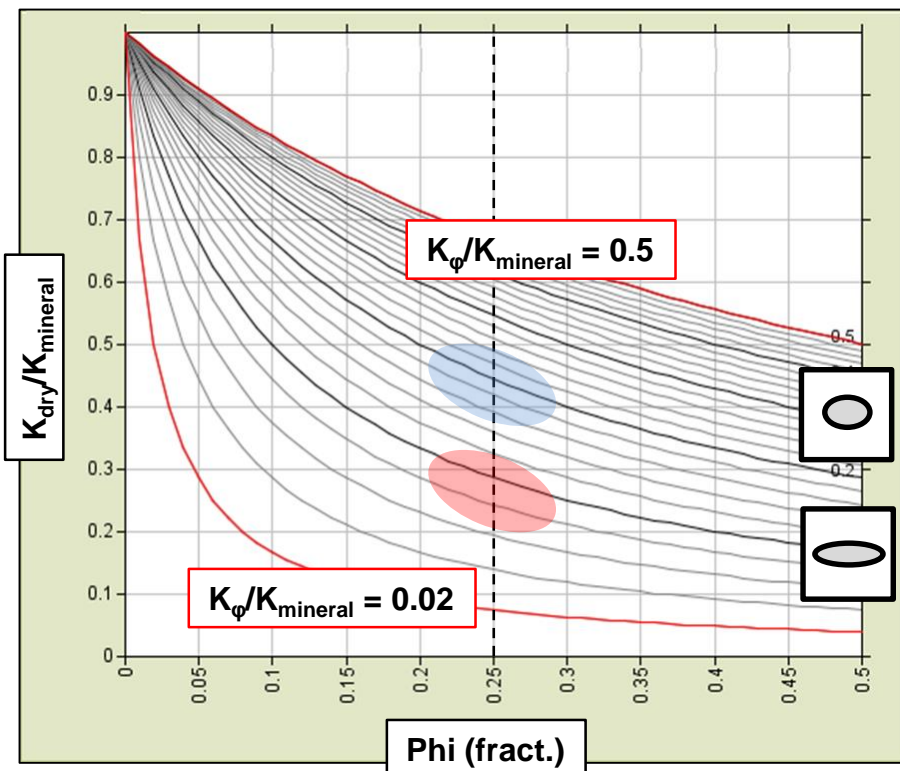
Introduction

- All 3 wells now have either a modelled or measured Vs log.
- The Vs logs in 22/3A-3 and 22/7-4 are in insitu brine conditions but the Vs log in 22/8A-2 is not and needs to be fluid-substituted to brine reference conditions, to remove the fluid effect.
- The elastic logs will then be fluid substituted to the following hydrocarbon saturations: 90% gas-saturated, 10% (residual) gas-saturated and 80% oil-saturated.
- This is also the first opportunity to look at dry rock plots, which are an important QC tool because they bring together the petrophysics, the elastic logs and the fluid and mineral properties.
- The goal of this section is a full set of continuous elastic logs in brine and hydrocarbon conditions for each well.

5.2 Introduction to Dry Rock Plots

Dependence of Rock Compressibility on Pore Fluid

Dry rock compressibility can be expressed as the sum of the **mineral compressibility** and the **compressibility of the pore space**. The effect of fluid compressibility in the pores on the bulk rock compressibility (1/bulk modulus) is dependant on the pore space compressibility.



Therefore the magnitude of the **fluid effect** is not uniquely related to porosity, but **porosity and pore-space stiffness**. The stiffer the pore, the lower the effect of pore fluid on the response at equivalent porosity:

$$\frac{1}{K_{sat}} \approx \frac{1}{K_{mineral}} + \frac{\varphi}{K_{\phi} + K_{fluid}}$$

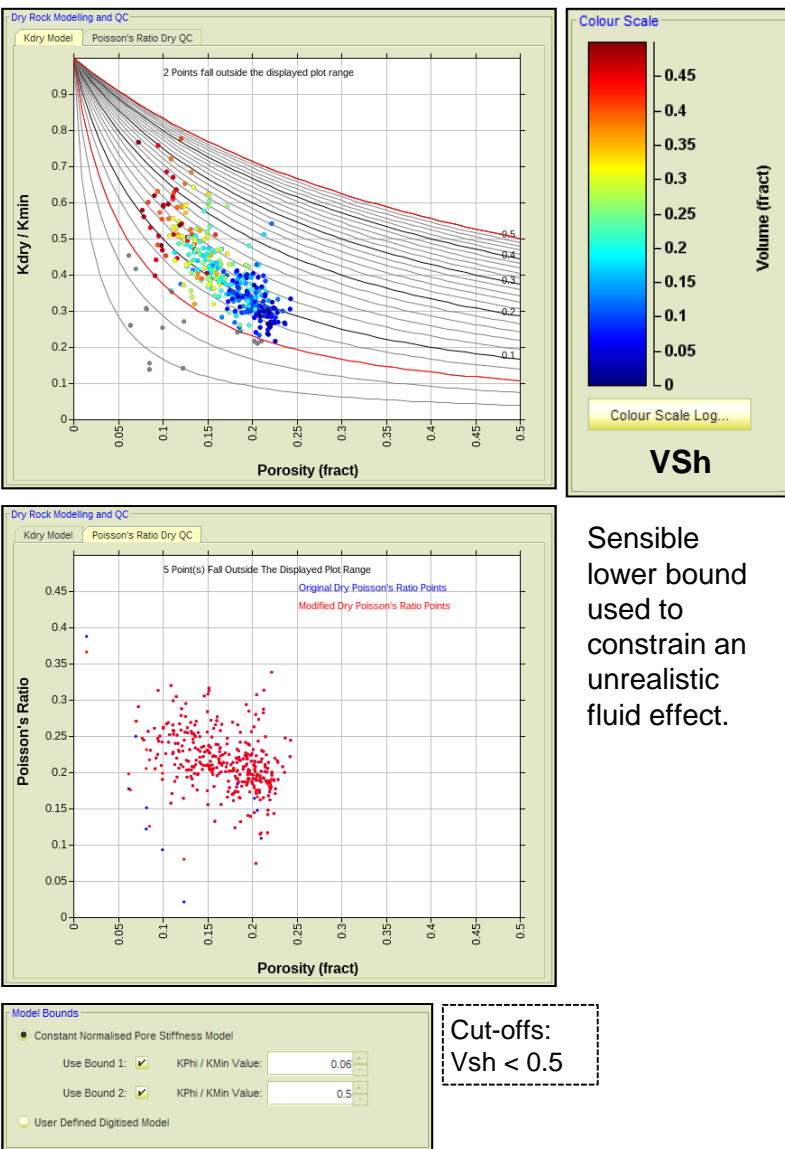
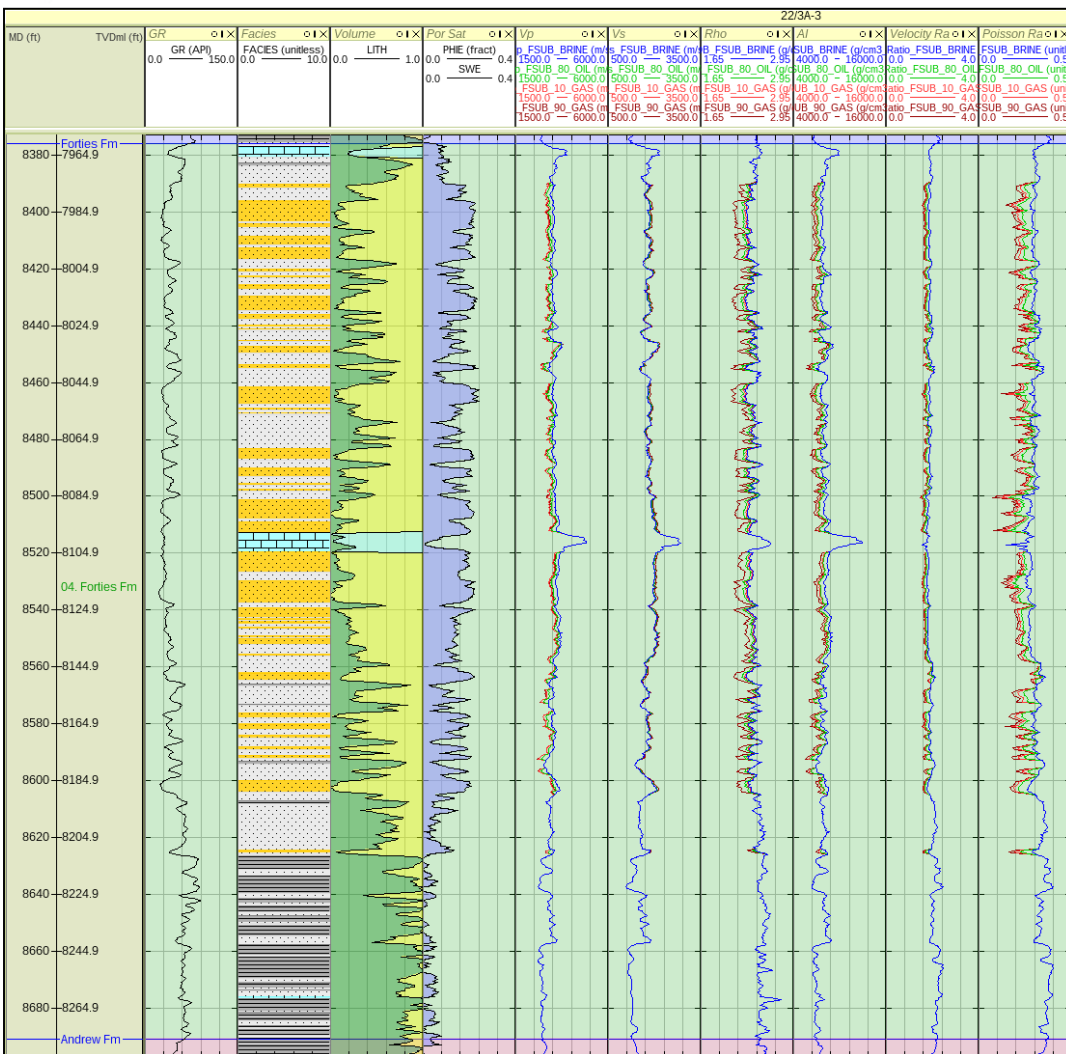
Points in the blue ellipse will exhibit a smaller fluid effect than points that fall in the red ellipse, as they have stiffer pores at equivalent porosity.

Pore stiffness can be related to pore aspect ratio, where stiffer pores are rounder and therefore have larger aspect ratios.

K_{ϕ} = pore space compressibility = change in pore volume as a function of an incremental pressure increase. Contours on the plot therefore represent constant pore stiffness.

5.3 Fluid Substitution – 22/3A-3

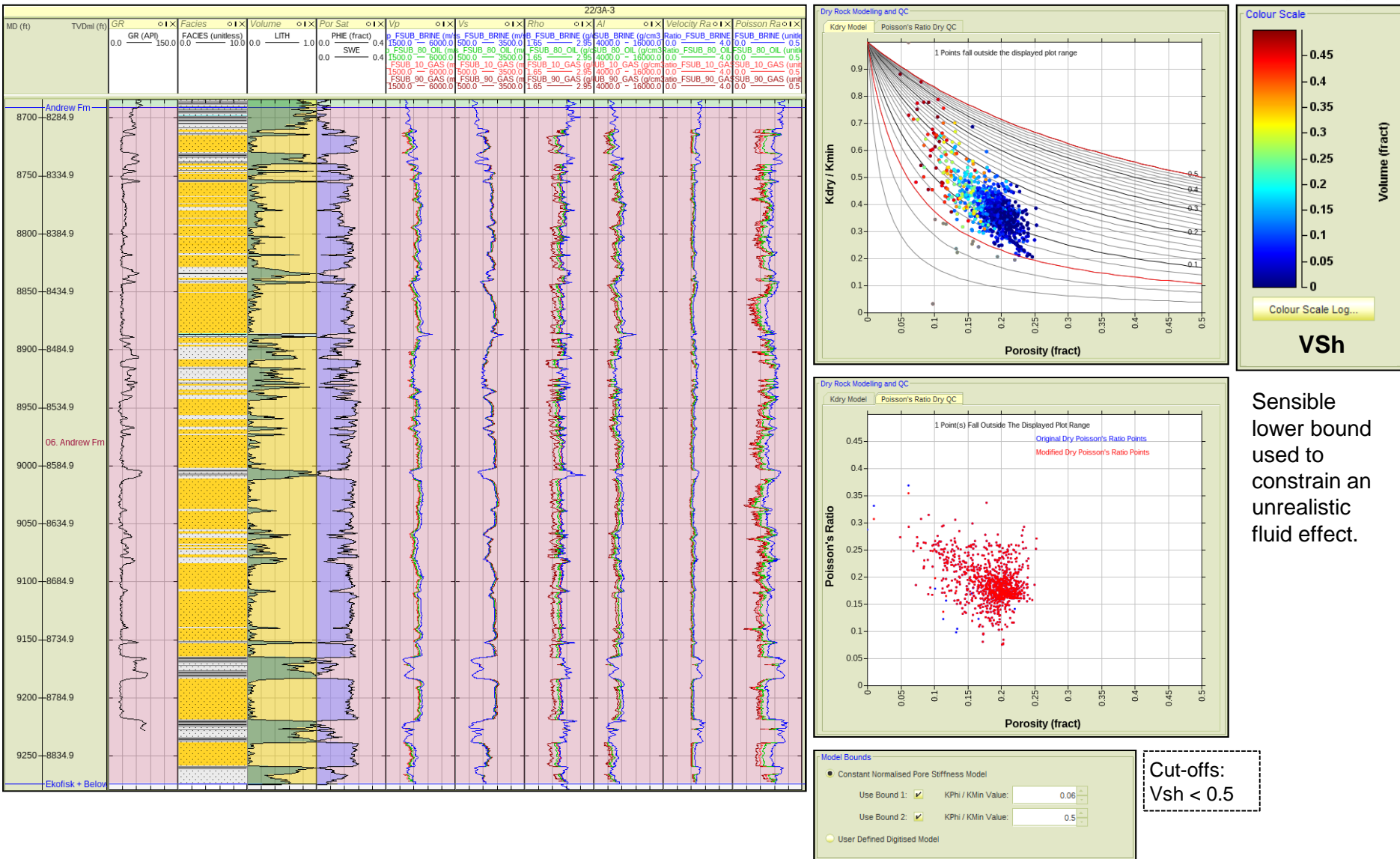
Forties



Sensible lower bound used to constrain an unrealistic fluid effect.

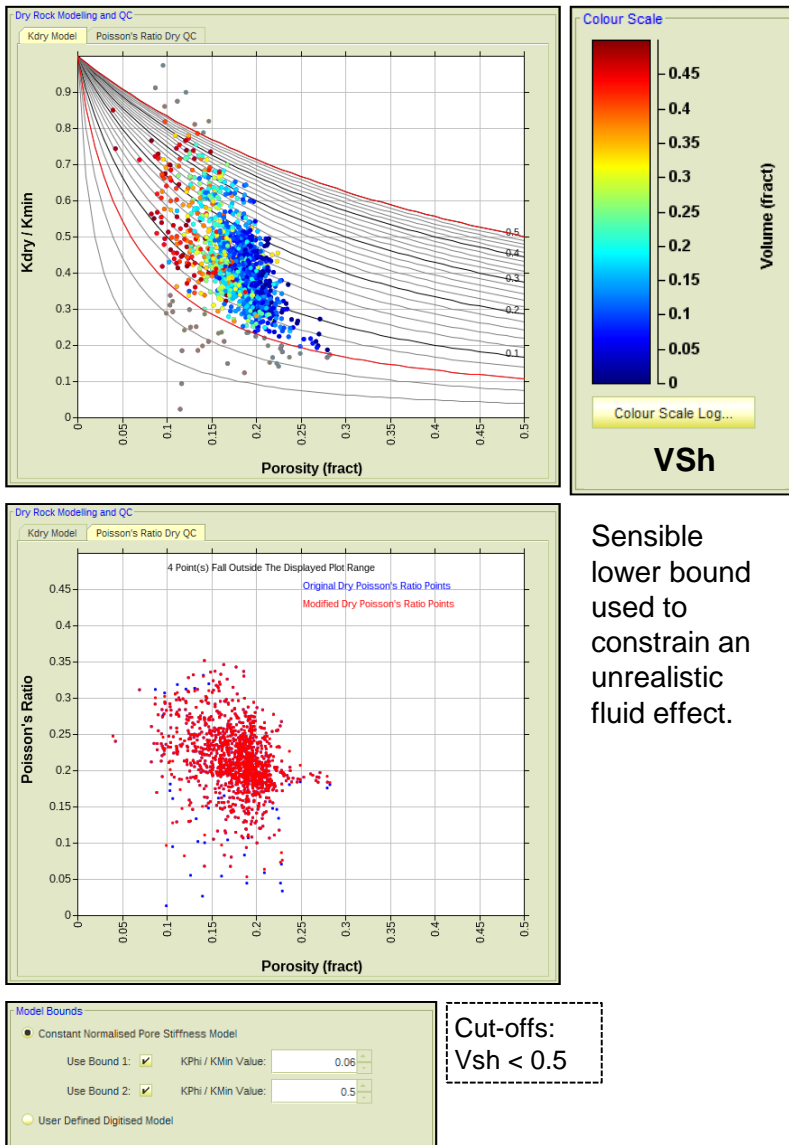
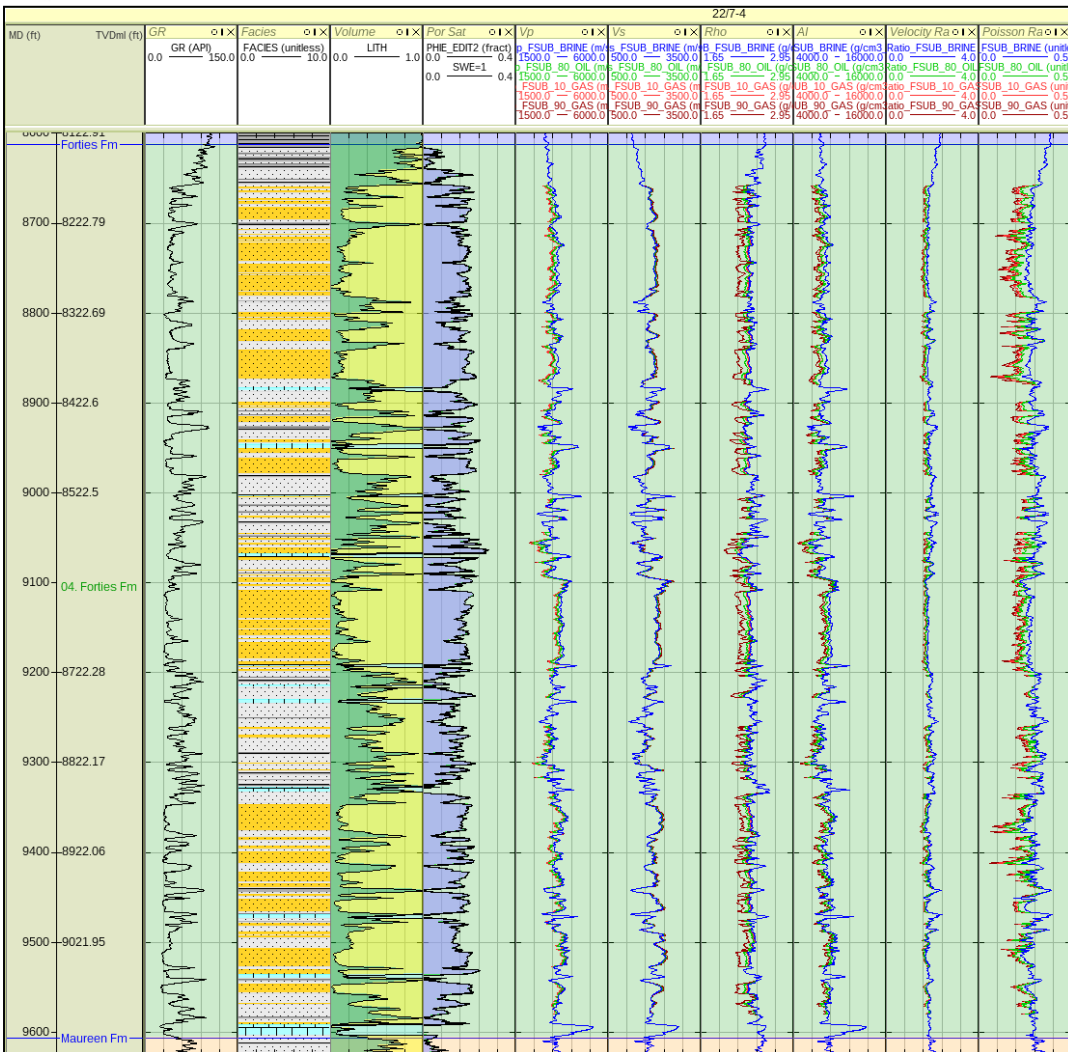
5.3 Fluid Substitution – 22/3A-3

Andrew



5.3 Fluid Substitution – 22/7-4

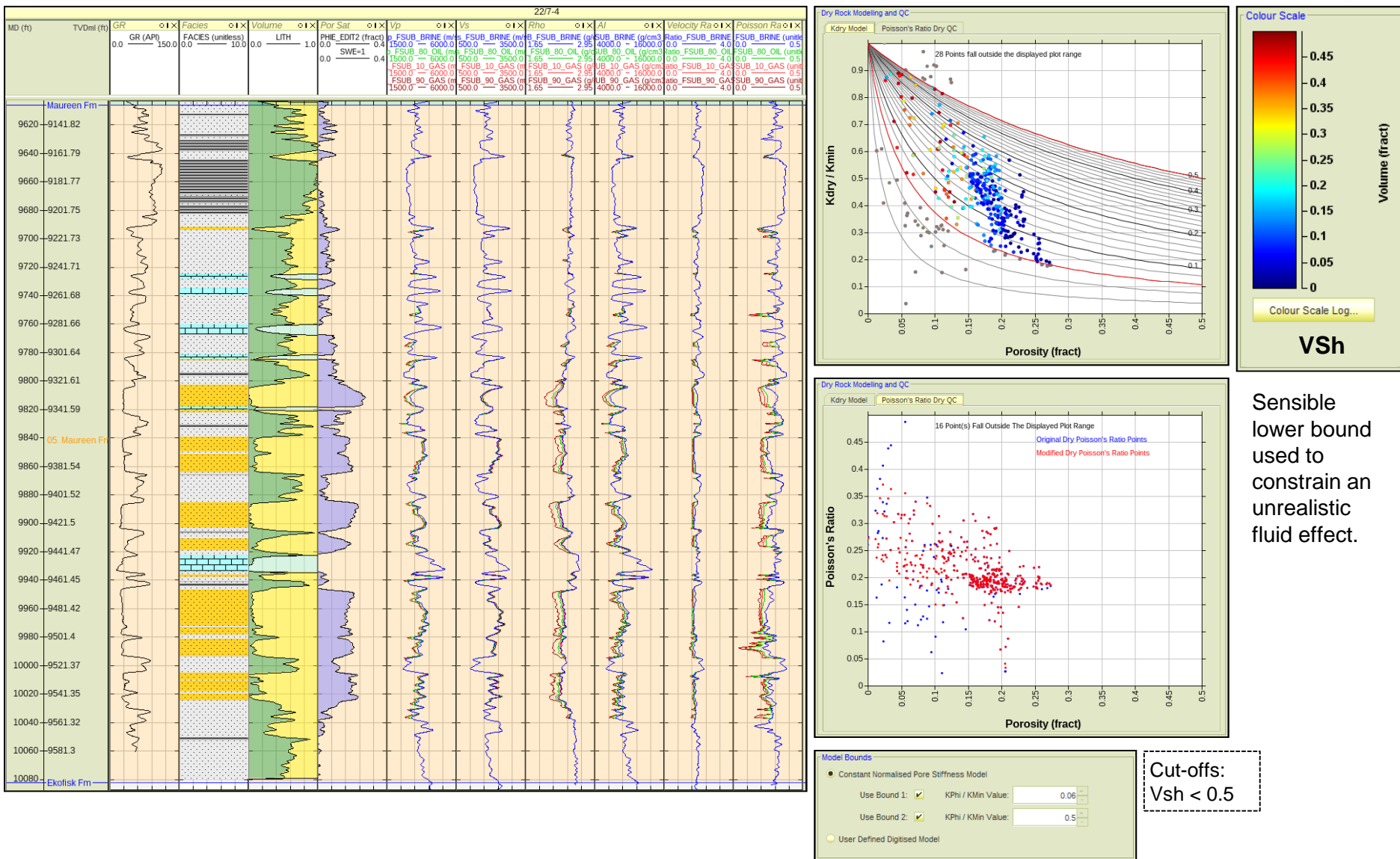
Forties



Sensible lower bound used to constrain an unrealistic fluid effect.

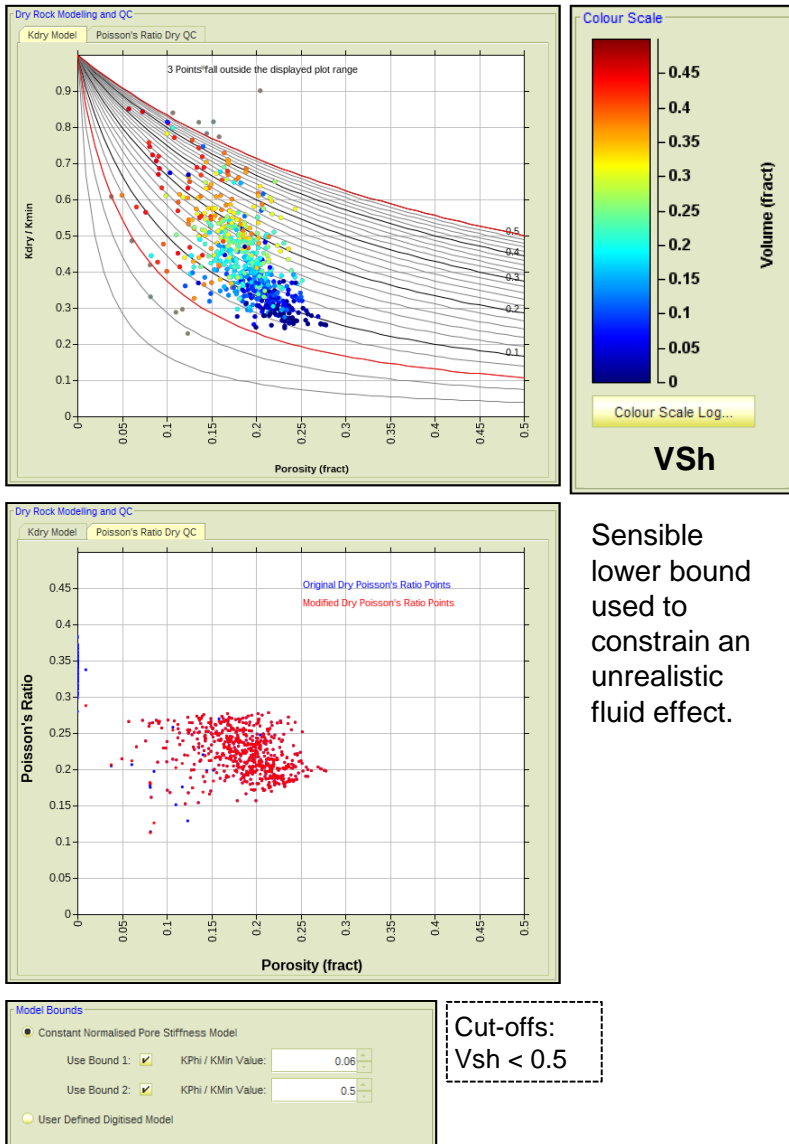
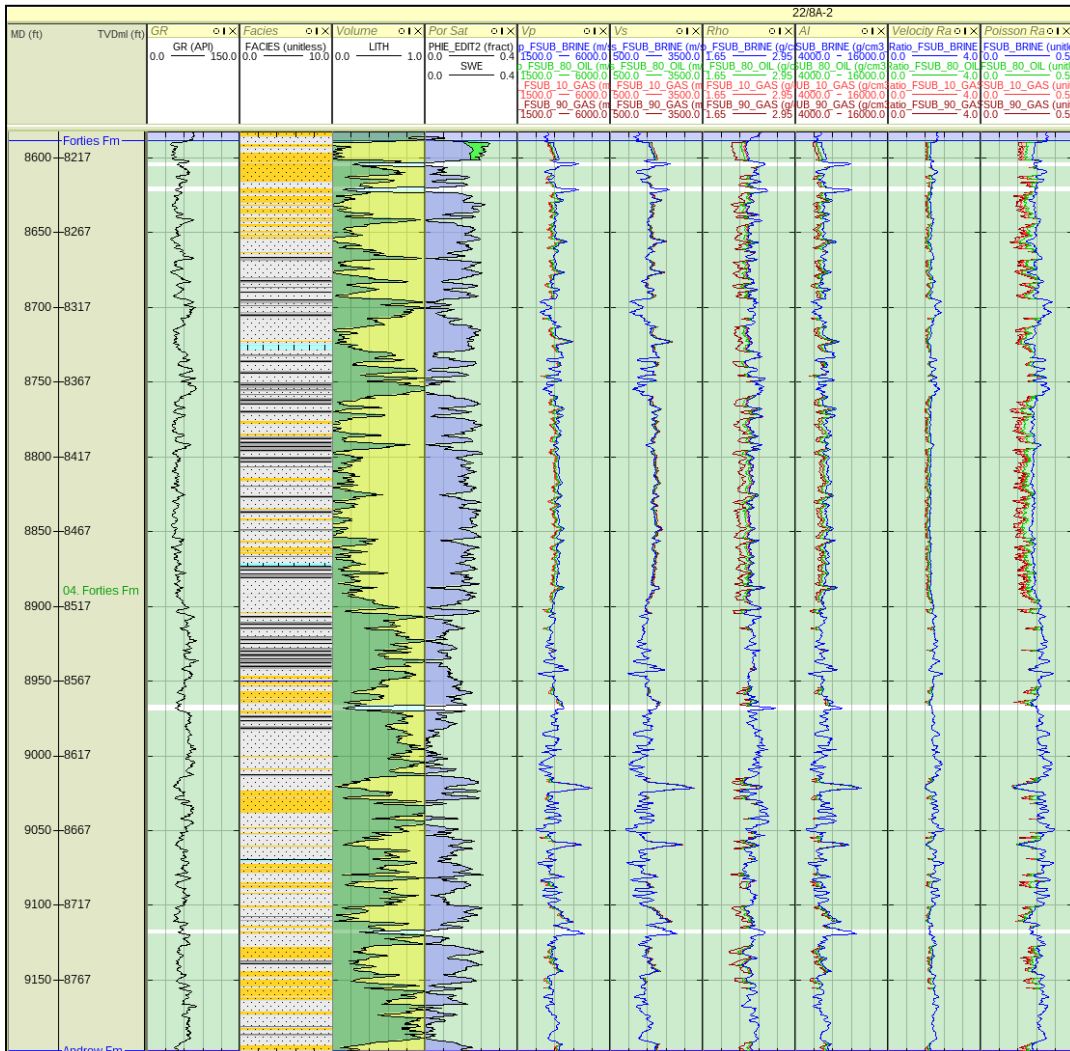
5.3 Fluid Substitution – 22/7-4

Maureen



5.3 Fluid Substitution – 22/8A-2

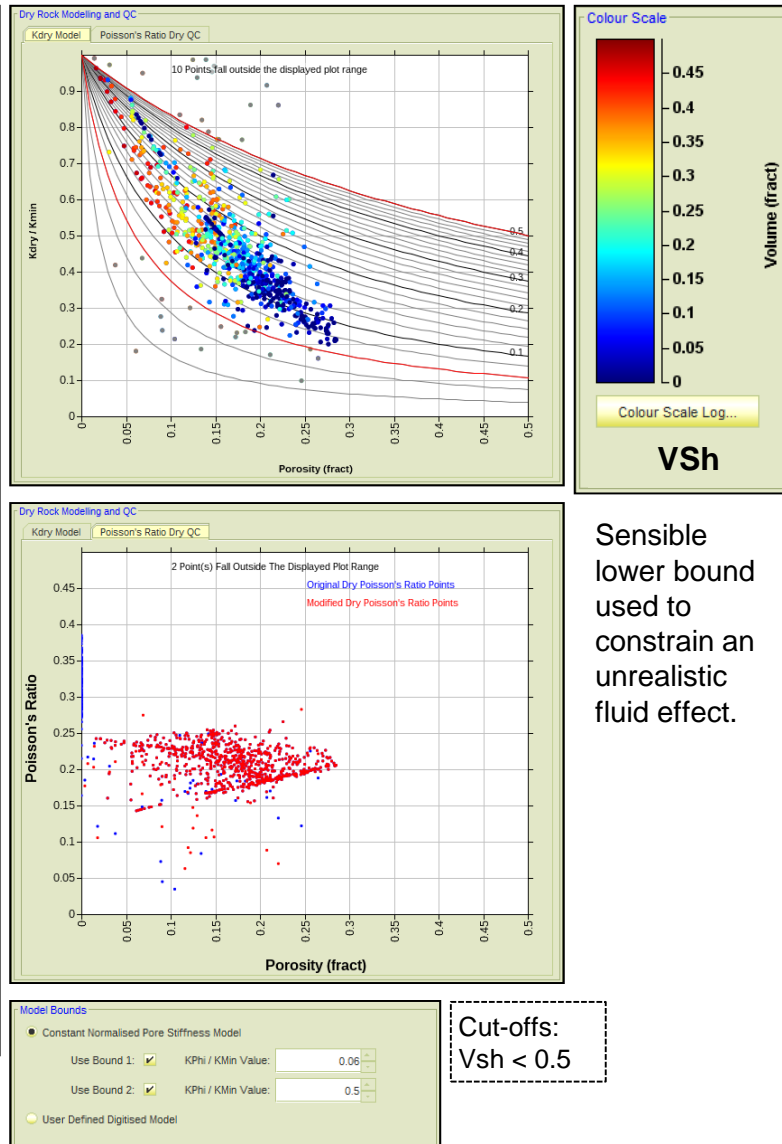
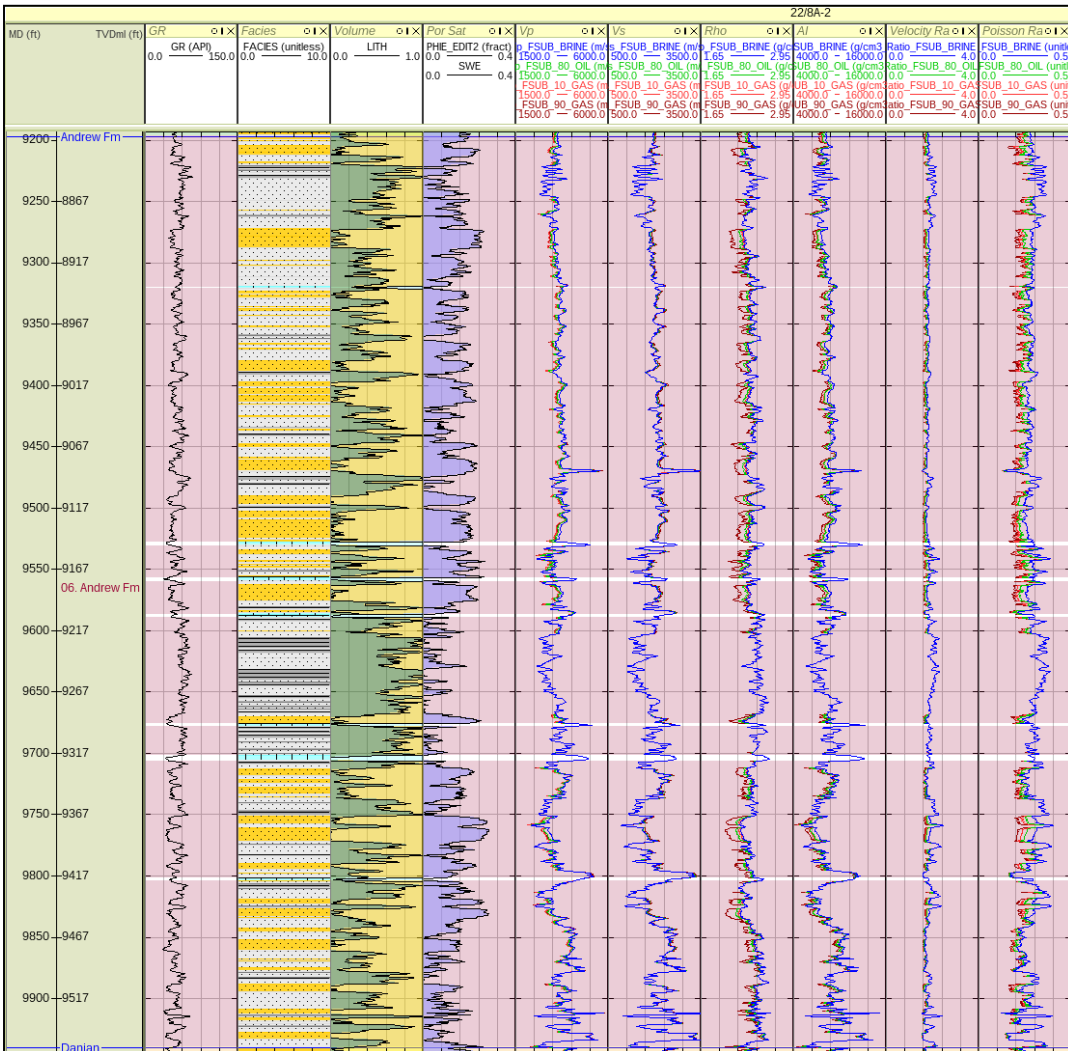
Forties



Sensible lower bound used to constrain an unrealistic fluid effect.

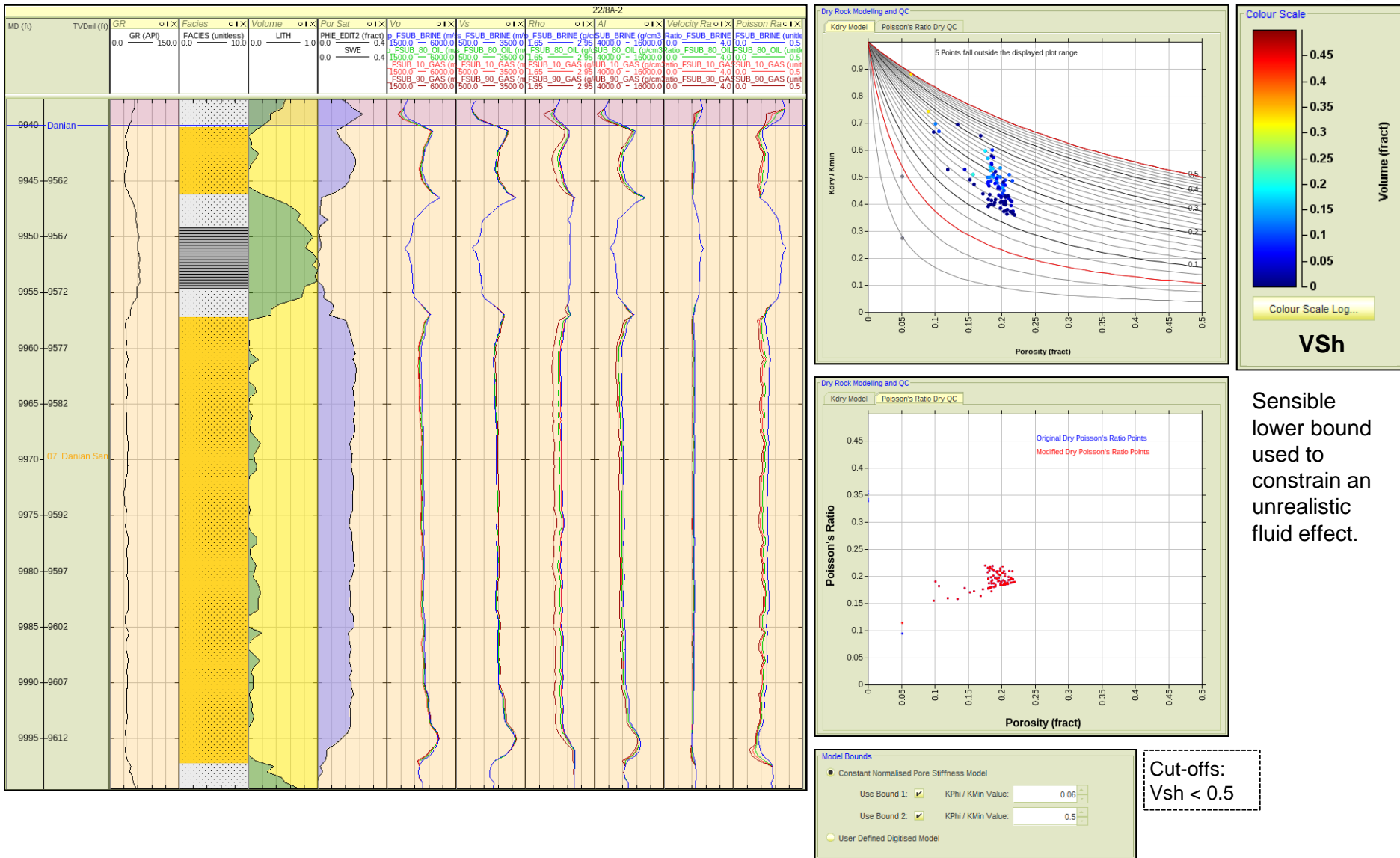
5.3 Fluid Substitution – 22/8A-2

Andrew



5.3 Fluid Substitution – 22/8A-2

Danian



6. Synthetic Gathers

6.1 Introduction, Wavelet & Backus Averaging

6.2 Average Sets

6.3 Synthetic Gathers

6.4 Summary

6.1 Synthetic Gathers

Introduction

Introduction

- Synthetic gathers are generated from the conditioned elastic log data by calculating reflectivity for a range of incidence angles, for each TWT sample point. The Zoeppritz equations are used to calculate reflectivity coefficients for each fluid case, and the wavelet is convolved with these to make the gather.
- Amplitude is extracted at each interface of interest, analysed and compared to the appropriate AVO half-space model. AVO half-space (or blocky) models are generated using average V_p, V_s and RhoB values for each formation under investigation.

Wavelet

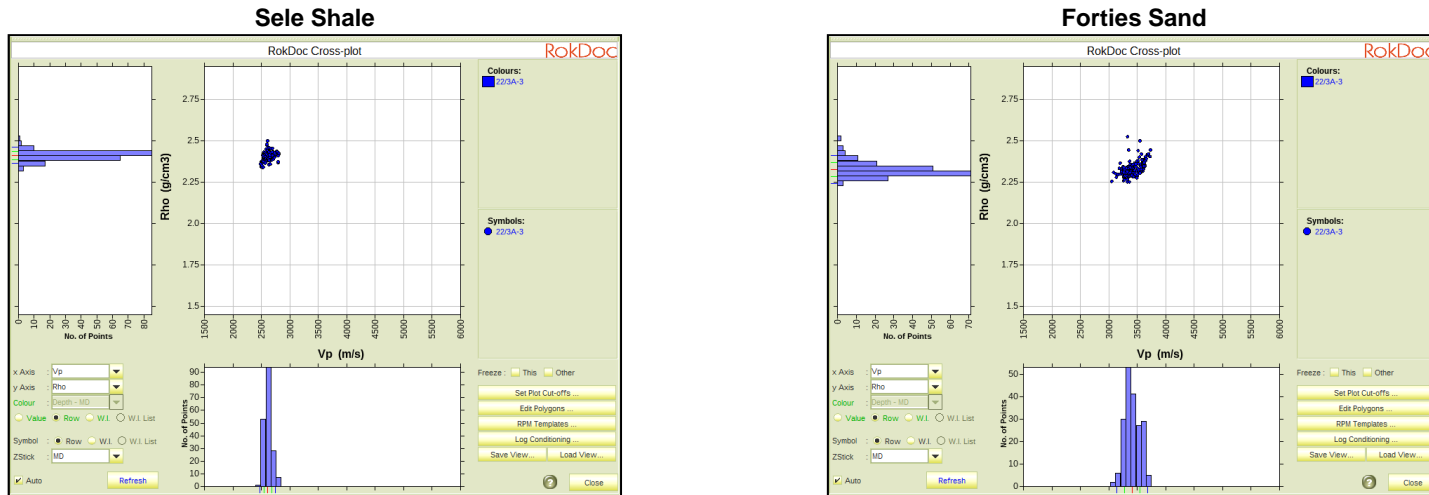
- A **25Hz Ricker wavelet** is used in the synthetic gathers.
- The wavelet is in **SEG Reverse Polarity**, so **an increase in impedance produces a negative trough**.

Backus Averaging

- The elastic logs undergo Backus averaging before synthetic gather generation, in order to remove any unrealistic artefacts in the synthetic traces, which could result from thin high-contrast layers – for example, calcite stringers.
- Backus averaging was applied to the logs, with a window **length of 15m**, which is appropriate for the depth of the well log data.

6.2 Average Sets

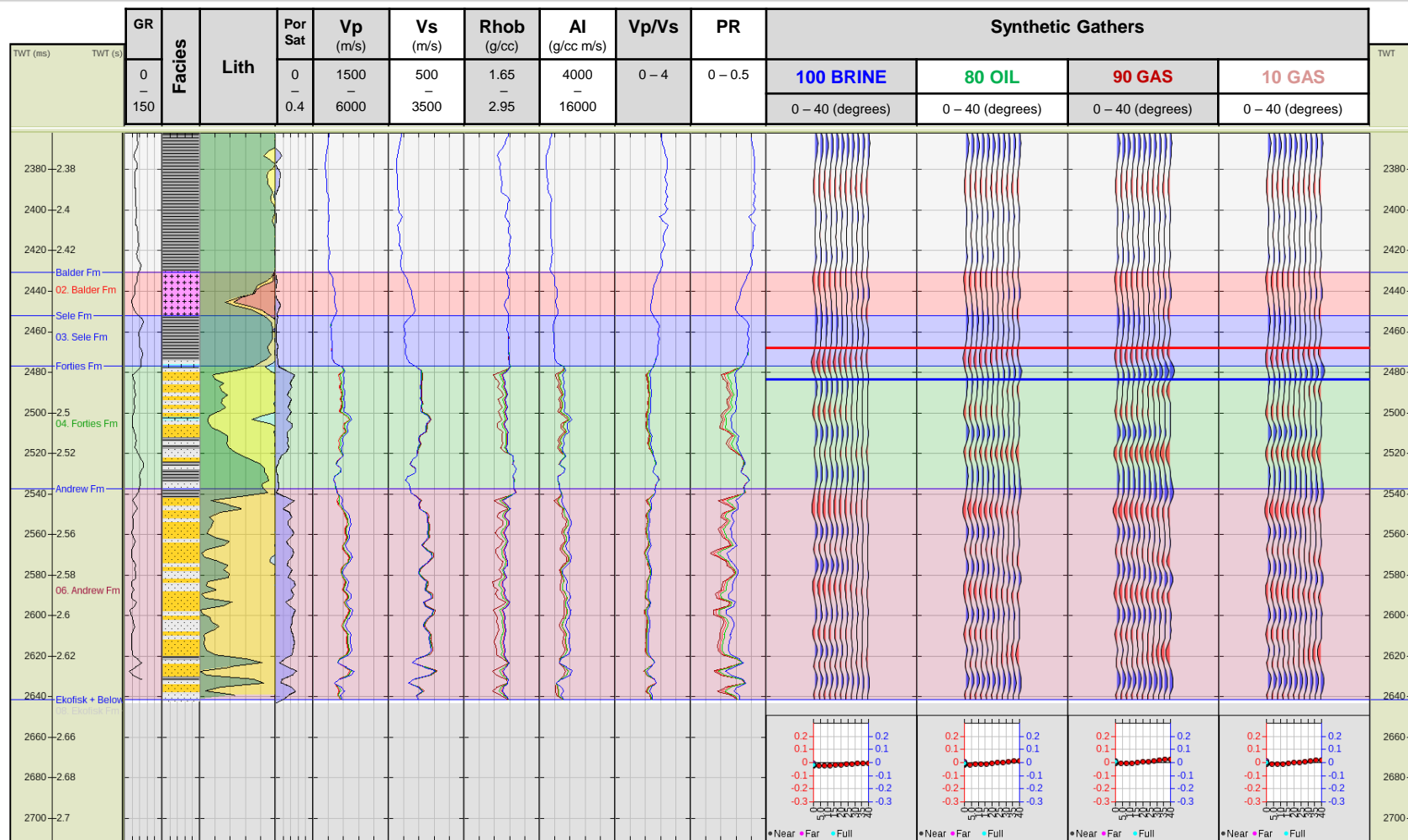
- Representative Vp, Vs and Rho values for each lithology are needed as inputs to the blocky models – AVO half-space models – and these are saved in RokDoc as *average sets*.
- The average sets were derived by analysing Histogram plots on Vp/Rho and Vp/Vs cross-plots, which are shown on the following slides.
- Example:



Average Set	Vp (m/s)	Vs (m/s)	Rhob (g/cc)
Sele Shale	2617.26	1168.38	2.41
Forties Brine Sand	3416.27	1865.98	2.33
Forties Oil Sand	3234.44	1885.68	2.28
Forties Gas Sand	3163.61	1929.08	2.18
Forties Gas Sand (Residual)	3130.78	1872.68	2.31

6.3 Synthetic Gathers

22/3A-3 (40Hz Ricker) – Forties Fm



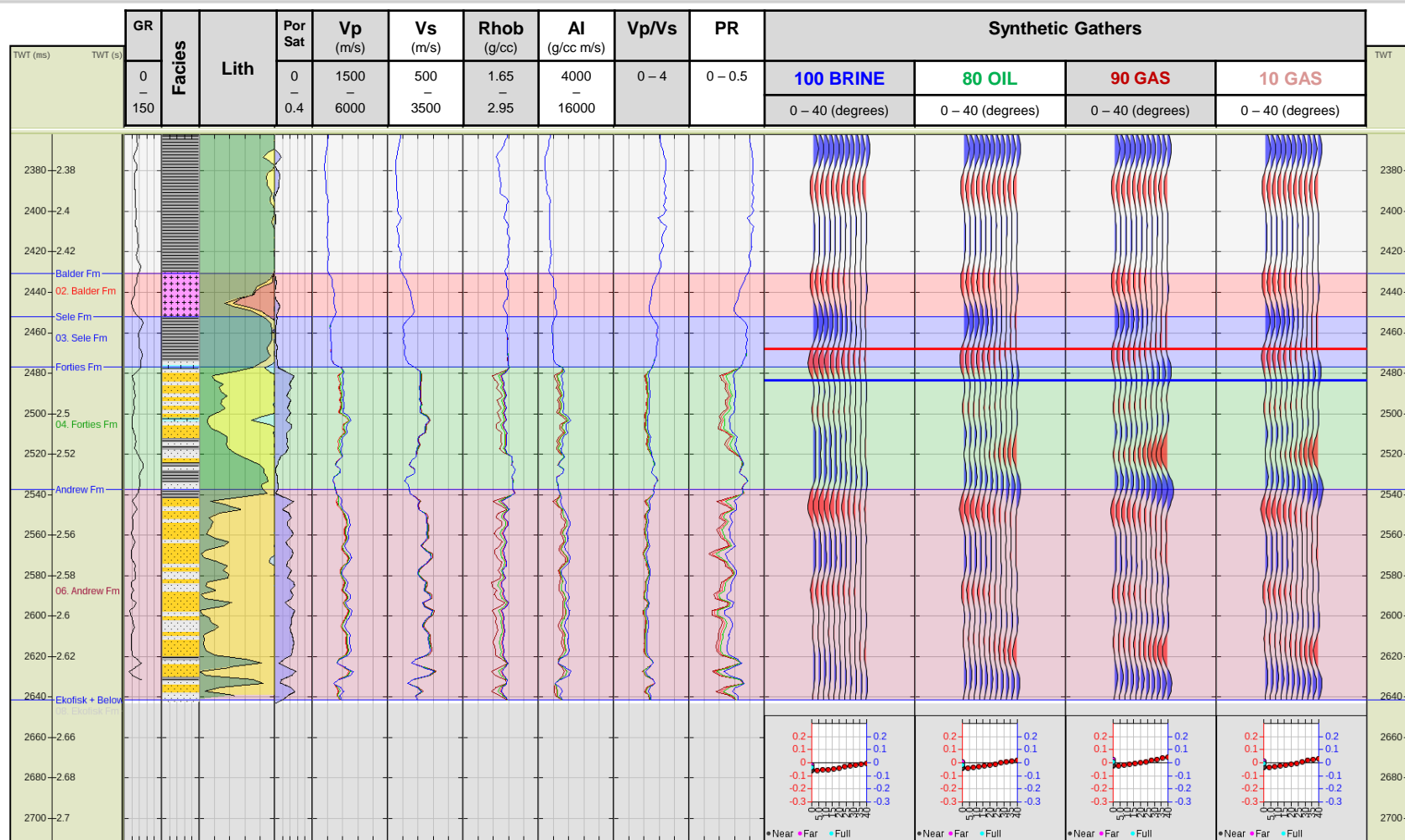
The AVO response is extracted as an average amplitude within the window in the gather track (red to blue bars).

Both the Forties and Andrew sands in 22/3A-3 are harder than their overlying shales when brine bearing, which should result in a negative response at zero offset that dims with increasing offset – a **Class I AVO response**. However, the response at the top of the Forties is complicated by thin layering of the presence of a calcite stringer between the Sele shale and the Forties shale/sand.

The sands become acoustically softer when hydrocarbon saturates the pore space, and the gradient becomes steeper. The result is a **class IIp** for the oil case, and a **class II** for the gas cases.

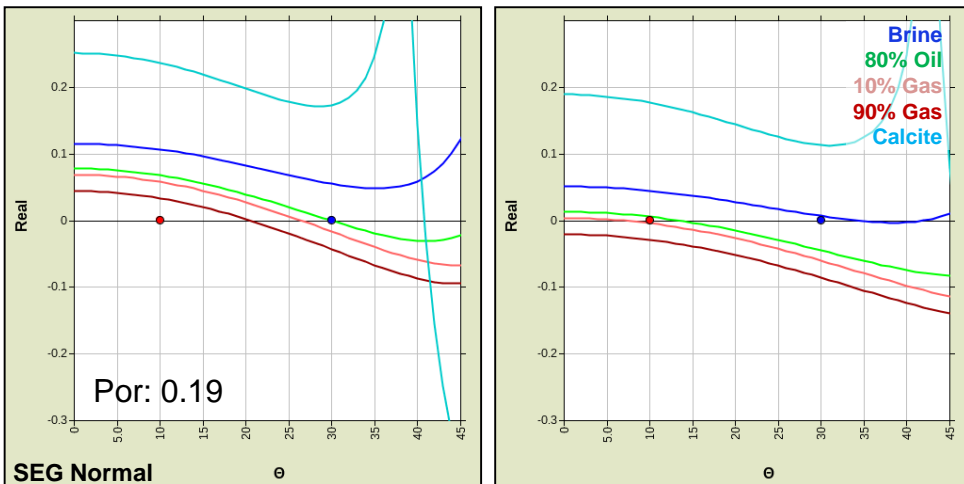
6.3 Synthetic Gathers

22/3A-3 (25Hz Ricker) – Forties Fm



6.3 Synthetic Gathers

22/3A-3 – AVO Half-space Model Comparison – Forties Fm



Interface	Fluid Fill	Half-space Model	Synthetic Gather
Sele Shale / Forties Sand	Brine	Class I	N/A
	Hydrocarbons	Class IIp	N/A
Sele Shale / Forties Calcite	N/A	Class I	Class I
Forties Shale / Forties Sand	Brine	Class I	Class I
	Hydrocarbons	Class IIp – Class II	Class IIp – Class II
Forties Shale / Forties Calcite	N/A	Class I	Class I

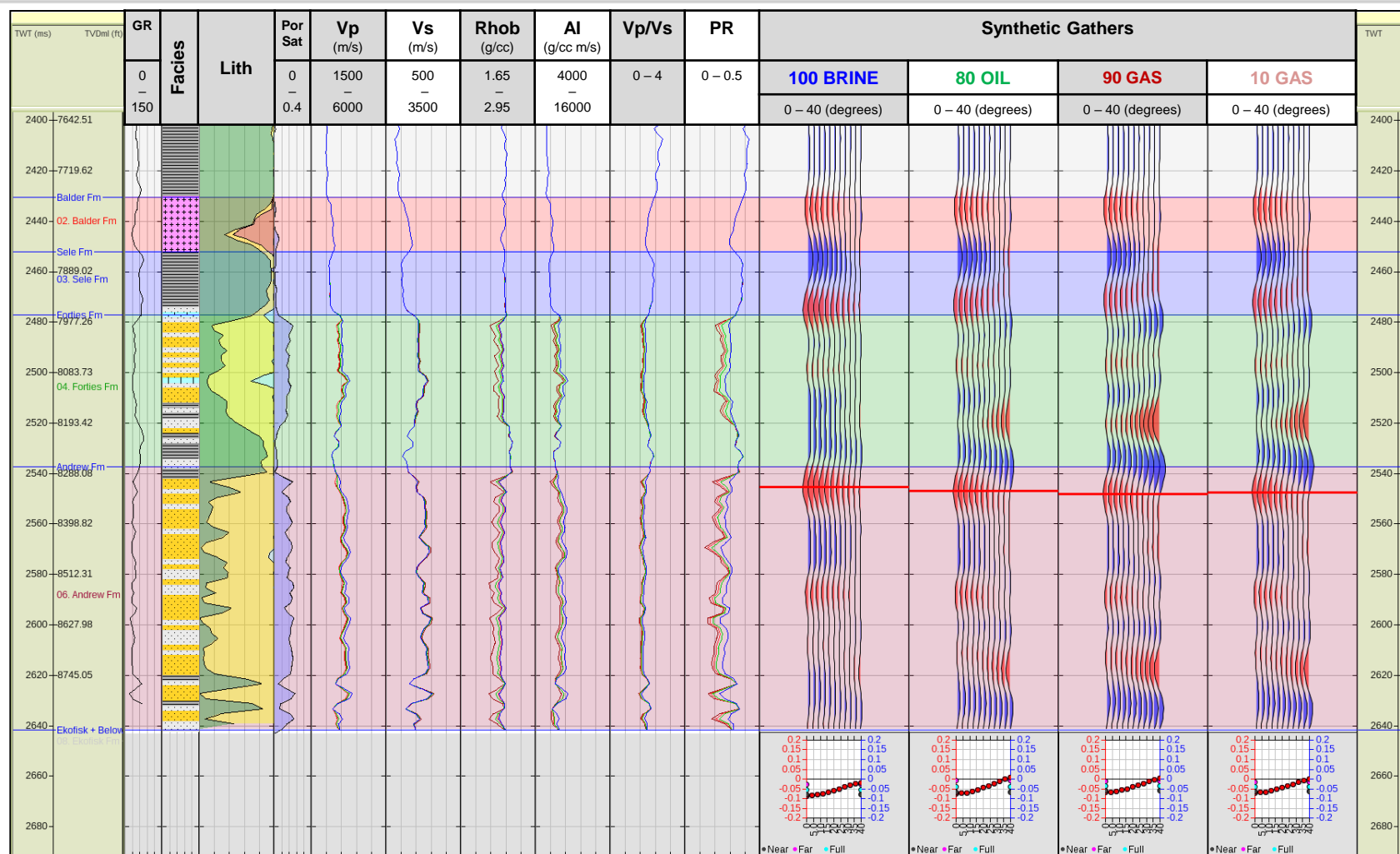
Interface at
2500ms TWT.



- The AVO half-space model for a Sele Fm shale overlying a Forties Fm sand shows a **Class I AVO response** for the brine case. Due to the complicated layering at the top of the Forties Fm in 22/3A-3, there is no direct analogue in the synthetic gather. Hydrocarbon saturation softens the sand and increases the AVO gradient, so that the responses dim with offset and cross the zero axis to become **Class IIp AVO responses**.
- The Top Forties Fm in 22/3A-3 consists of a Sele Fm Shale overlying a Forties Fm calcite stringer. The calcite stringer is much harder than the underlying shale and both the synthetic gather and the half-space model show a **Class I AVO response**.
- Underlying the Top Forties response is a Forties Fm shale/sand interface (blue line on the synthetic gathers), which is difficult to observe on the synthetic gathers (for the brine case especially) due to the bright response from the overlying Top Forties interface. The half-space model shows a weak Class I AVO response for the brine case, which correlates with the Class I AVO response in the synthetic gather. Hydrocarbon saturation softens the sand and increase the AVO gradient, with the oil and residual gas cases becoming **Class IIp AVO responses**, and the gas case changing polarity to become a **Class II AVO response**.
- A half-space model for a Forties Fm shale/calcite interface produces a **Class I AVO response**, which correlates with the response at ~2500ms TWT in the synthetic gather.

6.3 Synthetic Gathers

22/3A-3 (25Hz Ricker) – Andrew Fm

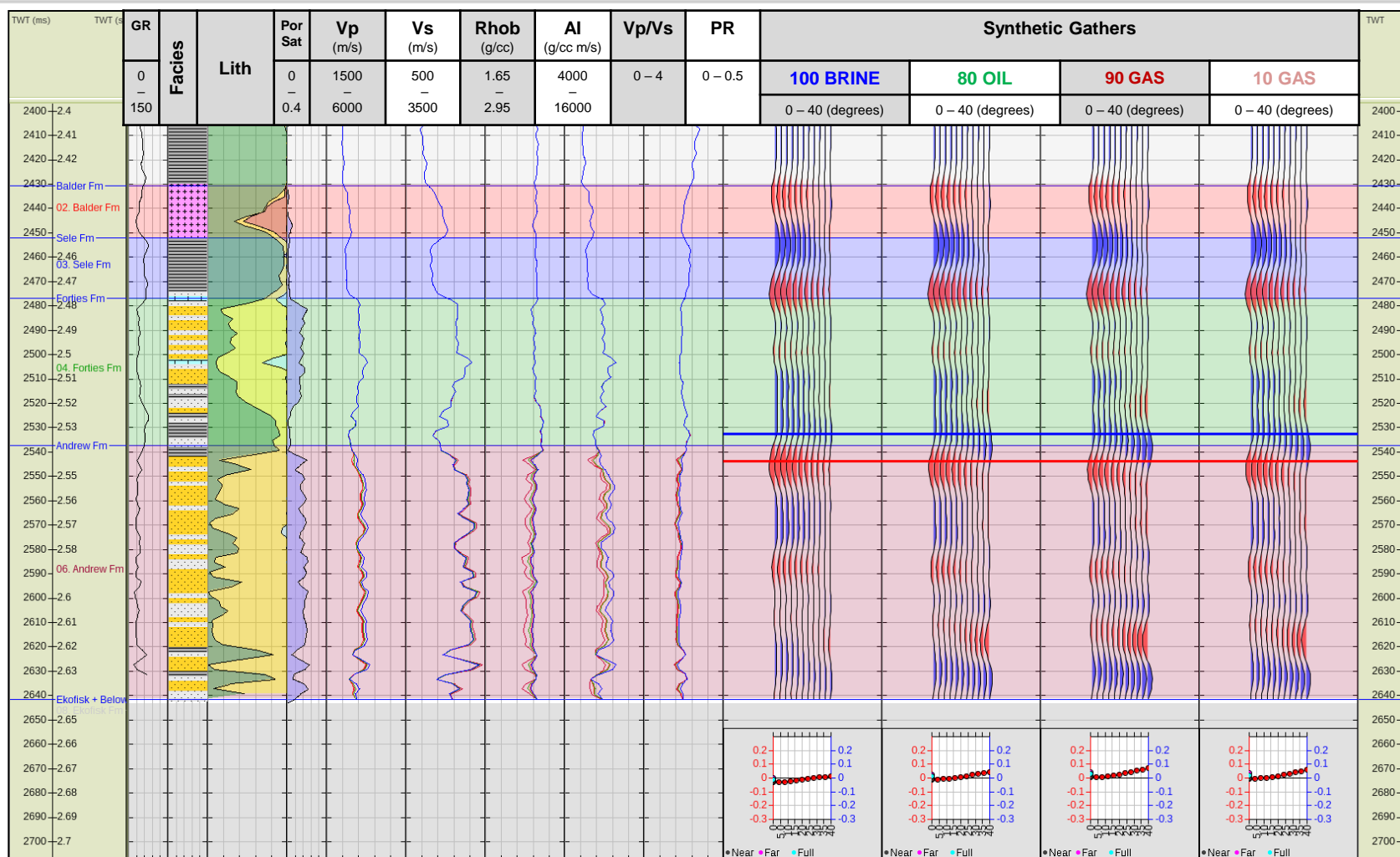


The Andrew Fm brine sand is harder than the overlying Forties Fm shale, which results in a negative amplitude at zero offset that dims with increasing offset (red line). This is a **Class I AVO response**.

Hydrocarbon saturation results in a slight dimming of the zero offset response, as the sand becomes softer. The AVO gradient becomes steeper, which results in all the hydrocarbon responses dimming with offset and crossing the zero axis to become **Class IV AVO responses**.

6.3 Synthetic Gathers

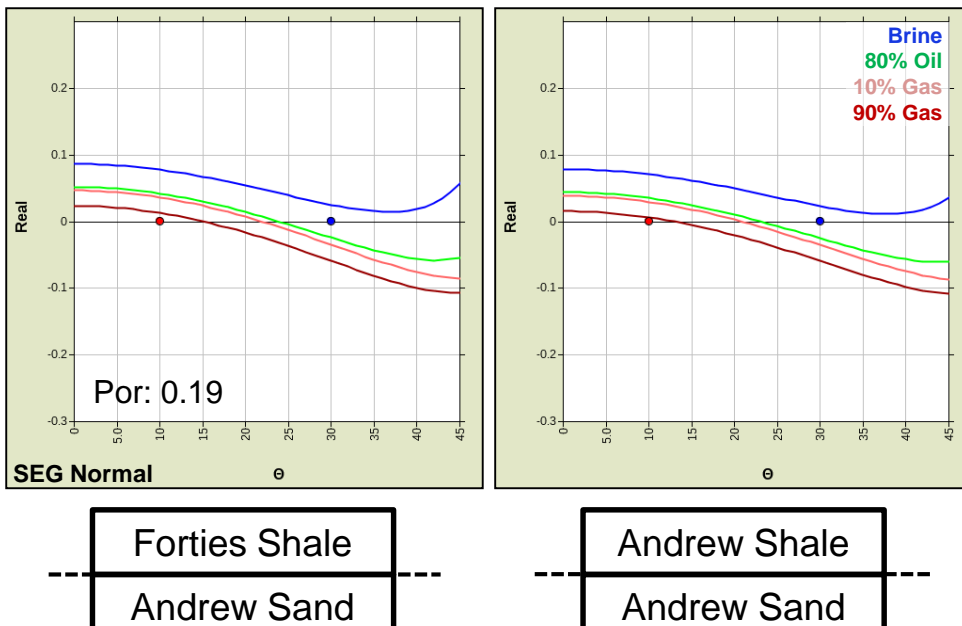
22/3A-3 (25Hz Ricker) – Andrew Fm (brine filled Forties)



Here the Forties is brine filled in all cases, with a 100% brine, 80% oil, 10% gas and 90% gas case in the Andrew sands. The response at the top Andrew shows a class I in the brine case, a class IIp in the oil case and a class II response in the gas cases.

6.3 Synthetic Gathers

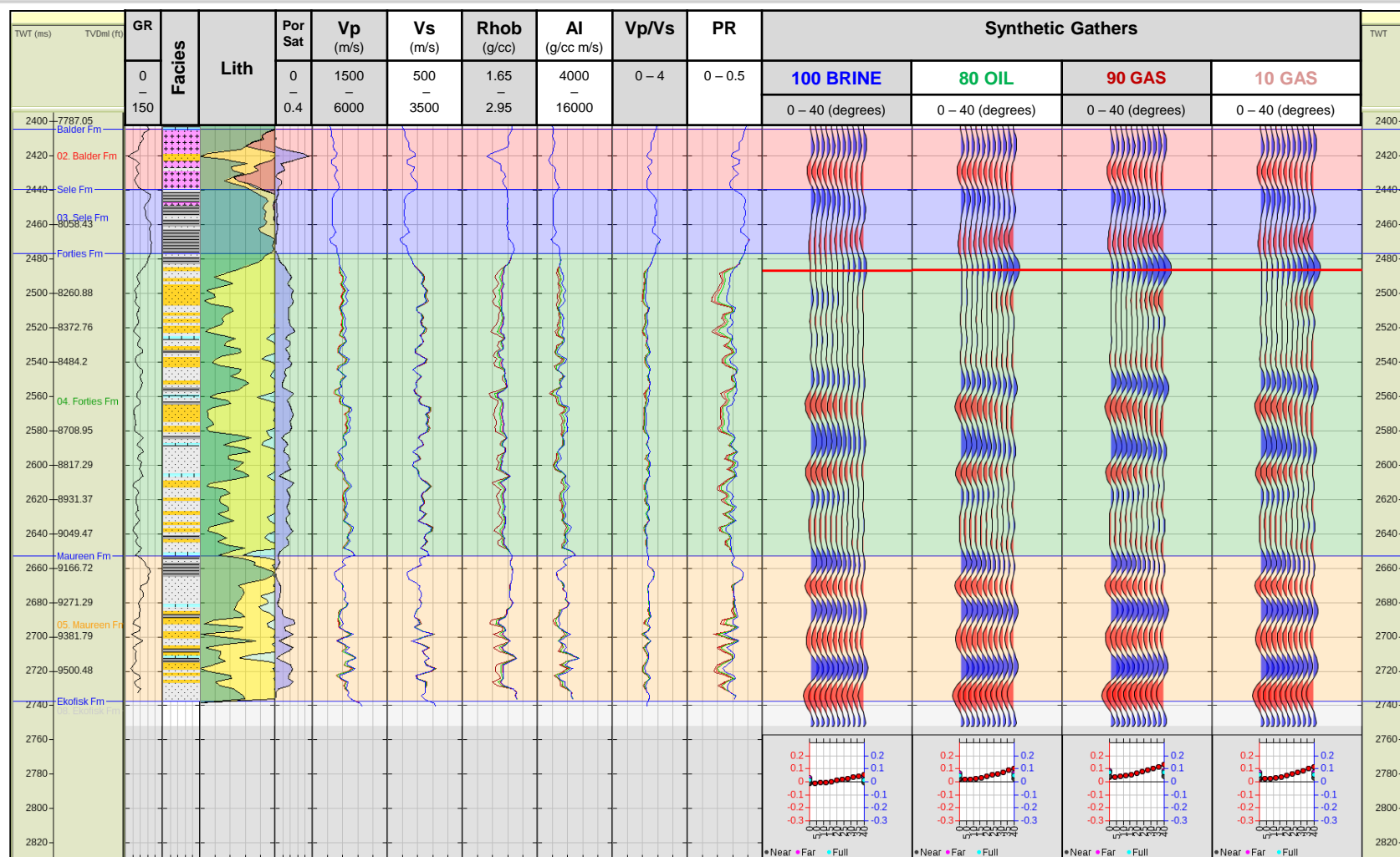
22/3A-3 – AVO Half-space Model Comparison – Andrew Fm



- The Top Andrew response in 22/3A-3 consists of a Forties Fm shale overlying an Andrew Fm sand. The sand is harder than the overlying shale, so the half-space model shows a positive amplitude at zero offset that dims with increasing offset, which is a **Class I AVO response**. This correlates with the response in the synthetic gather, which also shows a **Class I AVO response**. Hydrocarbon saturation softens the sand and increases the AVO gradient, so that all hydrocarbon responses become **Class IIp AVO responses**, which is also observed in the synthetic gathers.
- There is no clear Andrew Fm shale/sand interface in 22/3A-3. There are two clean shale towards the base of the formation but they are thin, so the interfaces are not properly resolved.
- The half-space model for an Andrew Fm shale/sand interface in 22/3A-3 shows the same response as the Forties Fm shale/Andrew Fm sand interface, which is a **Class I AVO response** for the brine case and a **Class IIp AVO response** for the hydrocarbon cases.

6.3 Synthetic Gathers

22/7-4 (25Hz Ricker) – Forties Fm



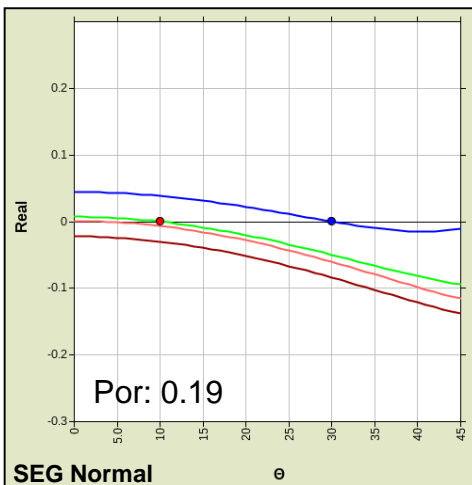
The Forties sand in 22/7-4 is slightly harder than the overlying Sele shale, which results in a **Class IIip AVO response** for the shale/brine sand interface. The response dims with offset before crossing the zero axis at 15 degrees and brightening.

Hydrocarbon saturation results in the sand becoming softer than the shale (for all hydrocarbon saturations), which causes the weak positive response at zero offset to become negative. These responses brighten with increasing offset and are **Class II AVO responses**. The AVO gradient is observed to slightly increase with hydrocarbon saturation.

There are a number of other synthetic responses within the Forties Fm but it is difficult to assign these to shale/sand interfaces due to the lack of intra-Forties clean shale.

6.3 Synthetic Gathers

22/7-4 – AVO Half-space Model Comparison – Forties Fm



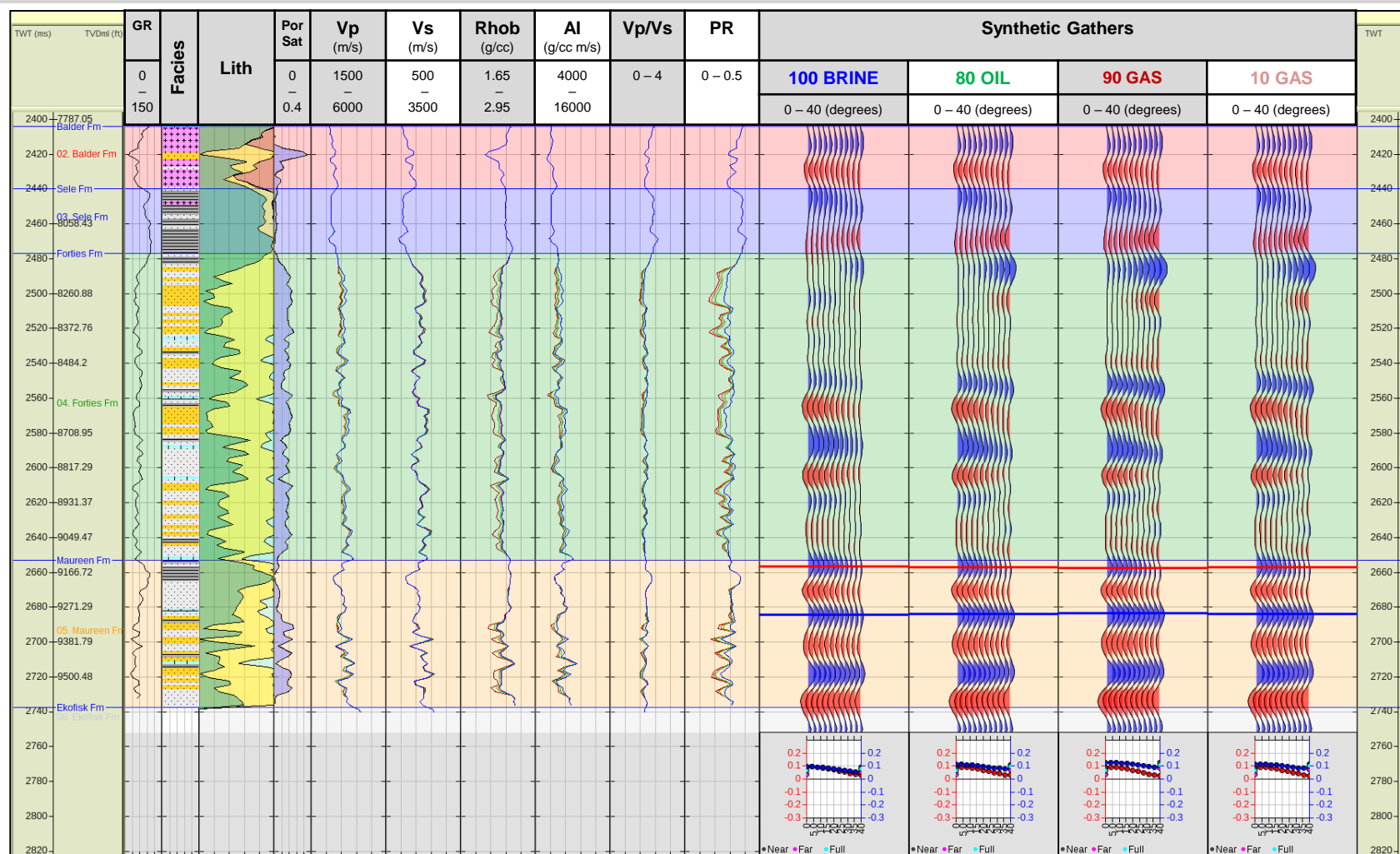
Interface	Fluid Fill	Half-space Model	Synthetic Gather
Sele Shale / Forties Sand	Brine	Class IIp	Class IIp
	Hydrocarbons	Class IIp- Class II	Class II
Forties Shale / Forties Sand	Brine	Class I	N/A
	Hydrocarbons	Class IIp – Class II	N/A



- The Top Forties response consists of a Sele Fm shale overlying a Forties Fm sand. The half-space model for the brine case is a **Class IIp AVO response**, which correlates with that observed in the synthetic gather. The response is dimmer than the equivalent response in 22/3A-3, which indicates that the shale and sand are more similar acoustically. Hydrocarbon saturation softens the sand and steepens the AVO gradient, with the oil and residual gas cases becoming **Class IIp AVO responses** and the gas case changing polarity to become a **Class II AVO response**.
- There is no clear Forties shale/sand interface in 22/7-4, due to the lack of thick end-member shales. The half-space model for this interface shows a Class I AVO response for the brine case. Hydrocarbon saturation softens the sand but it remains harder than the overlying shale, so the response remains a **Class IIp AVO response**.

6.3 Synthetic Gathers

22/7-4 (25Hz Ricker) – Maureen Fm



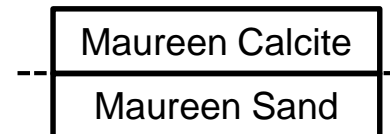
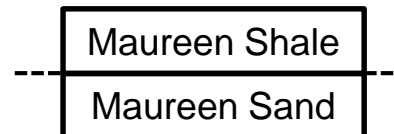
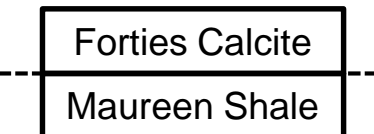
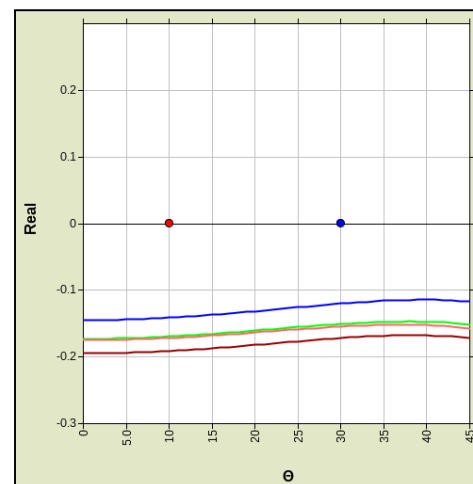
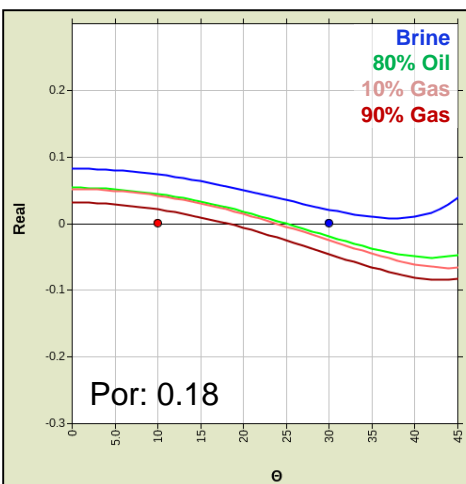
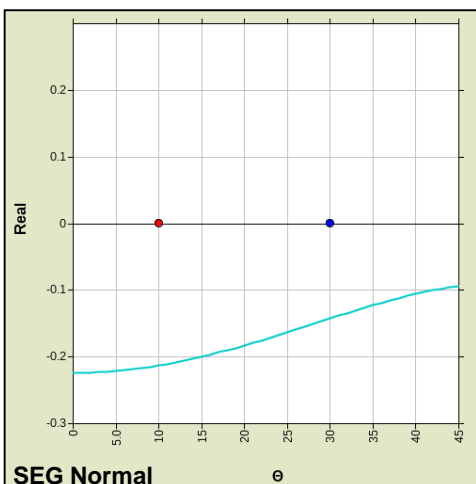
The top of the Maureen Fm is composed of a calcite stringer of the Forties Fm, overlying a Shale of the Maureen Fm (red line). The calcite stringer is much harder than the underlying shale, which results in a positive amplitude at zero offset that dims with increasing offset, which is a **Class IV AVO response**. There is no fluid effect associated with this interface.

Identifying a shale/sand interface response in the Maureen Fm is difficult because of thin layering and mixed lithologies. A possible top sand response is shown by the blue line. Here, the sand is softer than the overlying lithology, which results in a **Class IV AVO response**.

Hydrocarbon saturation results in the zero offset response dimming slightly and a reduction in AVO gradient. The presence of calcite in the upper layer is likely to be having an influence on the interface response.

6.3 Synthetic Gathers

22/7-4 – AVO Half-space Model Comparison – Maureen Fm

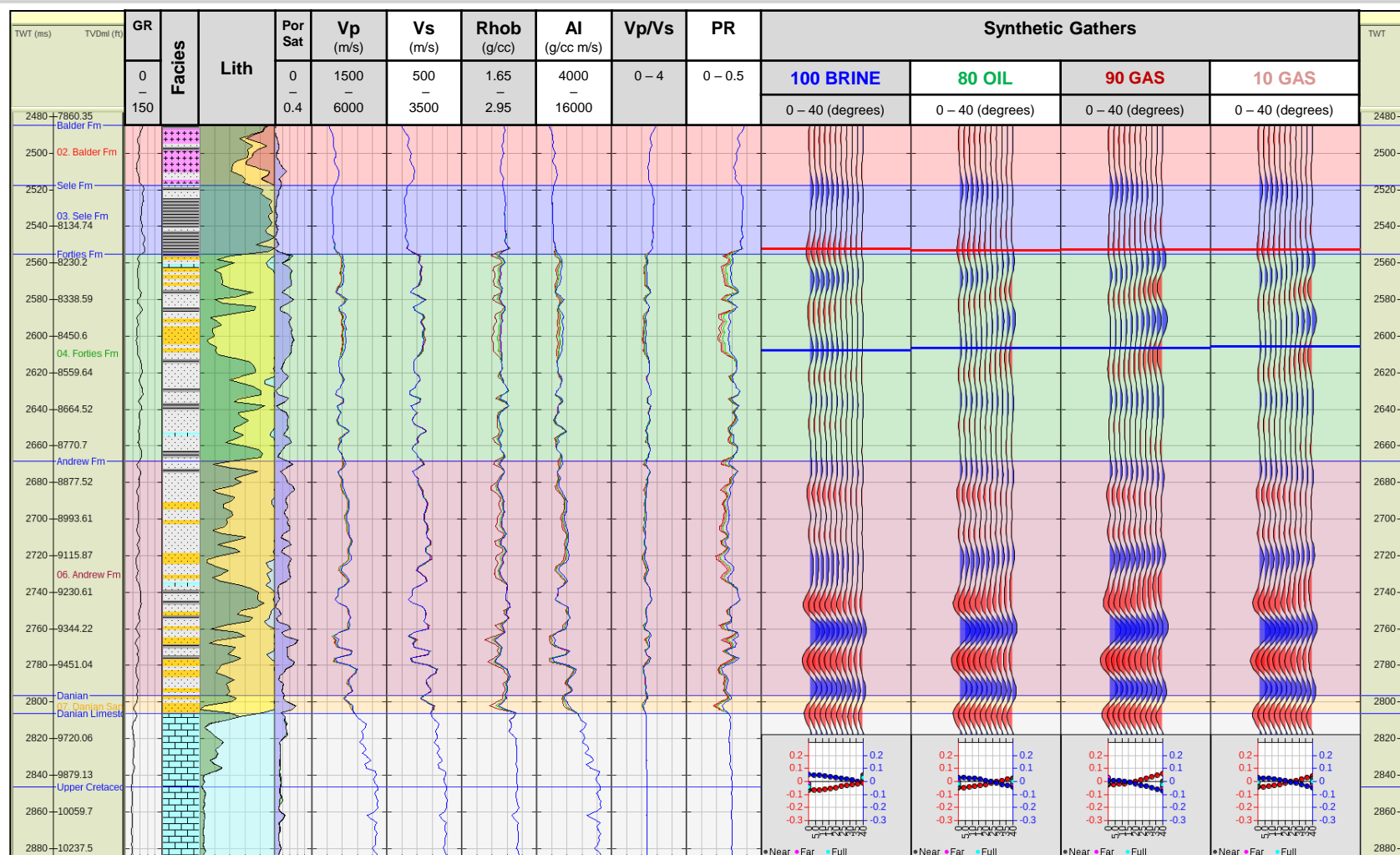


- The Top Maureen Fm response in 22/7-4 is a Forties Fm calcite stringer overlying a Maureen shale. The calcite stringer is much harder than the Maureen shale, so the half-space model shows a bright **Class I AVO response**, which correlates with the response observed in the synthetic gather.
- It is difficult to interpret other interfaces in the synthetic gather, due to a mixture of lithologies and thin layering.
- The blue line in the synthetic gather shows the response for a Maureen Fm calcite stringer overlying a Maureen Fm sand. The half-space model for this interface shows a **Class IV AVO response** for all fluid cases because the calcite stringer is much harder than the underlying sand. This correlates with the response observed in the synthetic gather, which also shows a **Class IV AVO response**.
- There is no clean Maureen Fm shale/sand interface in 22/7-4. The half-space model shows a **Class I AVO response** for the brine case because the sand is harder than the shale. Hydrocarbon saturation softens the sand and increases the AVO gradient but it remains harder than the shale, resulting in a **Class IIp AVO response** for all hydrocarbon cases.

Interface	Fluid Fill	Half-space Model	Synthetic Gather
Forties Calcite / Maureen Shale	N/A	Class IV	Class IV
Maureen Shale / Maureen Sand	Brine	Class I	N/A
	Hydrocarbons	Class IIp	N/A
Maureen Calcite / Maureen Sand	Brine	Class IV	Class IV
	Hydrocarbons	Class IV	Class IV

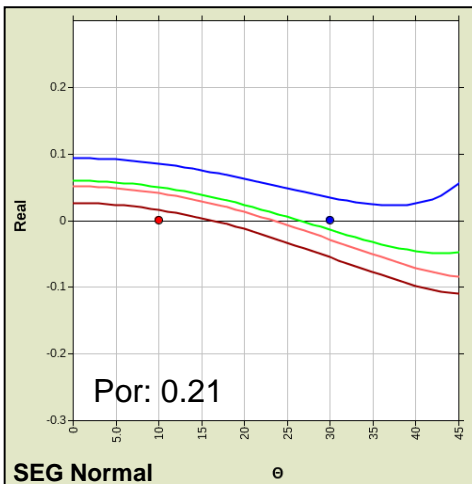
6.3 Synthetic Gathers

22/8A-2 (25Hz Ricker) – Forties Fm



6.3 Synthetic Gathers

22/8A-2 – AVO Half-space Model Comparison – Forties Fm



Interface	Fluid Fill	Half-space Model	Synthetic Gather
Sele Shale / Forties Sand	Brine	Class I	Class I
	Hydrocarbons	Class IIp	Class IIp
Forties Shale / Forties Sand	Brine	Class IIp	Class I*
	Hydrocarbons	Class IIp – Class II	Class IIp*

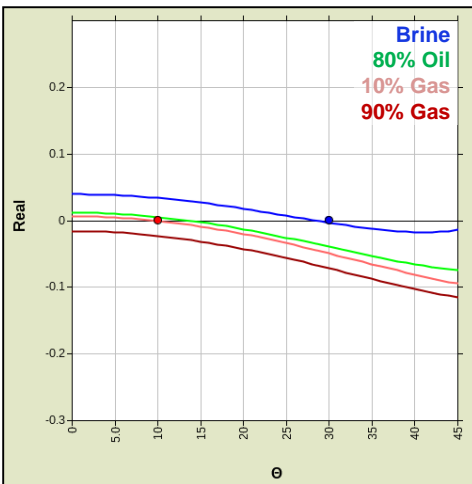
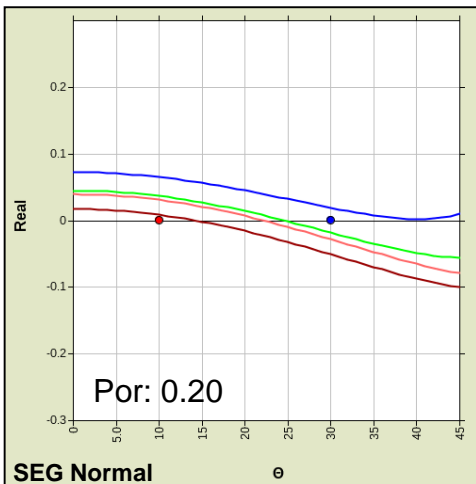
*the interface is present in the synthetic gather as a base response.



- The Top Forties Fm response in 22/8A-2 consists of a Sele Fm shale overlying a Forties Fm sand. The sand is harder than the overlying shale, so the half-space model for this interface shows a **Class I AVO response** for the brine case, which correlates with the response observed in the synthetic gather. Hydrocarbon saturation softens the sand and increases the AVO gradient but it remains harder than the overlying shale, so the response becomes a **Class IIp AVO response**. This is observed in both the synthetic gathers and the half space model.
- There is no clean Forties Fm shale/sand interface in 22/8A-2 but there is a clean sand/shale interface, which is a base response. This response can simply be inverted to understand what a shale/sand interface would produce. The half-space model for this interface shows a **Class IIp AVO response** that crosses the zero axis at ~35°, so could be considered a **Class I AVO response** and agrees with the synthetic gather. Hydrocarbon saturation softens the sand but it remains harder than the shale for the oil and residual gas cases, producing a **Class IIp AVO response**. The gas sand becomes softer than the shale, so the response changes polarity and becomes a **Class II AVO response**.

6.3 Synthetic Gathers

22/8A-2 – AVO Half-space Model Comparison – Andrew Fm



Interface	Fluid Fill	Half-space Model	Synthetic Gather
Forties Shale / Andrew Sand	Brine	Class I	N/A
	Hydrocarbons	Class IIp	N/A
Andrew Shale / Andrew Sand	Brine	Class IIp	N/A
	Hydrocarbons	Class IIp – Class II	N/A



- There are no clear sand/shale or shale/sand interfaces in the Andrew Fm of 22/8A-2. The Top Andrew Fm response is very weak due to the lack of thick, clean lithologies, and the synthetic gather is dominated by high amplitude responses towards the base of the formation. These appear to be associated with interbedded silt, sandstone and calcite but there are no clear interfaces of interest.
- The half-space model for a Forties Fm shale overlying an Andrew Fm sand shows a **Class I AVO response** because the sand is harder than the overlying shale. As in other wells, hydrocarbon saturation softens the sand and increases the AVO gradient, which results in a **Class IIp AVO response**.
- The half-space model for an Andrew Fm shale overlying an Andrew Fm sand shows a **Class IIp AVO response** that crosses the zero axis at 30°. Hydrocarbon saturation results in the oil and residual gas cases staying as **Class IIp AVO responses**, but the gas cases change polarity and become a **Class II AVO response**.

7. Inversion Feasibility

- 7.1 Introduction
- 7.2 Al/VpVs Cross-plots
- 7.3 LMR Cross-plots
- 7.4 LnAl/LnGI Cross-plots – chi angle calculation (EEI log for lithology and fluid discrimination)
- 7.5 Well panels, logs comparison
- 7.6 Summary

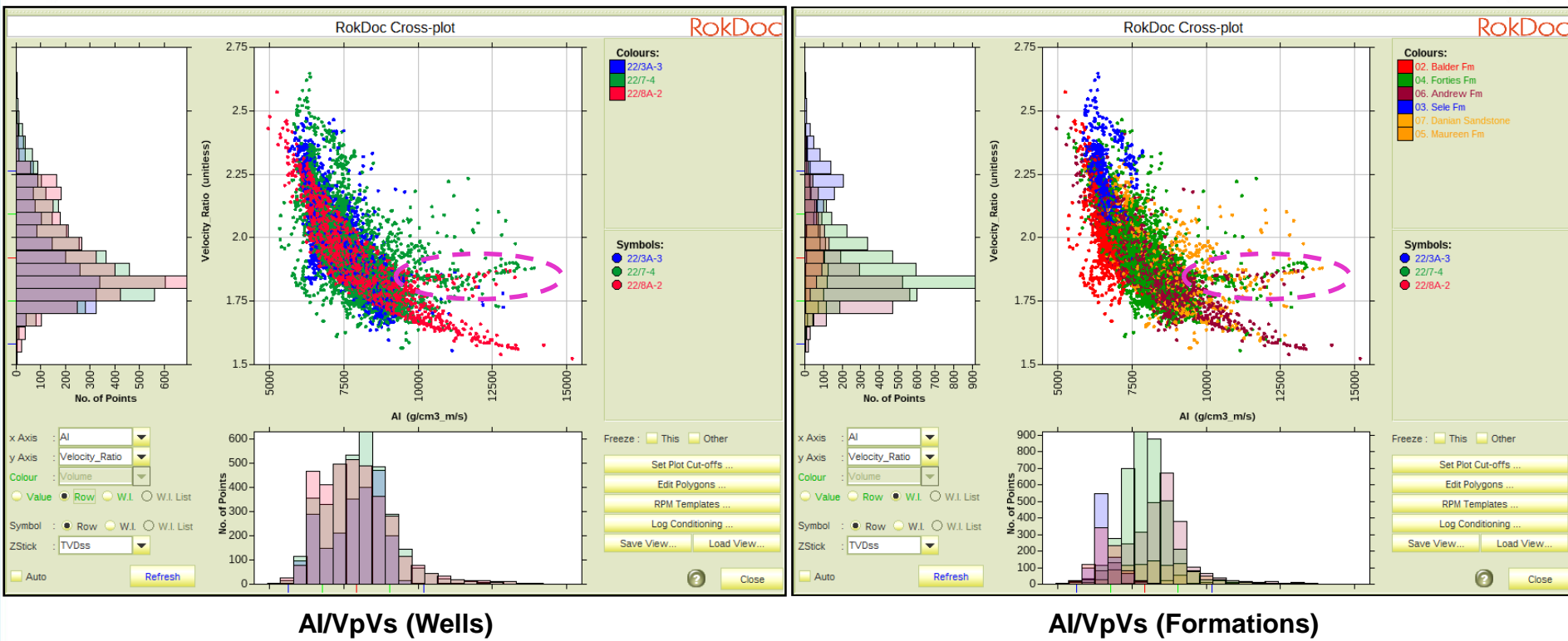
7.1 Inversion Feasibility

Introduction

- Cross-plots for AI-Vp/Vs, LambdaRhob/MuRhob will be generated to investigate which impedance attributes are the most suitable for discriminating lithology and fluid effects.
- Also, LnAI/LnGI cross-plots will be generated to estimate chi angles for both lithology and fluids discrimination. These chi angles will be used to calculate EEI logs.
- These cross-plots will be done at log-scaled and up-scaled (using Backus averaging with a window length of 15m). Up-scaling is also performed by the application of band-pass filters. The band-limited logs are shown at the well locations to produced a modelled 'best case' inversion result, this is done with fully band-limited logs (relative inversion)and high-cut filtered logs (absolute inversion) that retain the low frequency information.

7.2 AI/VpVs Cross-plots – log-scaled

All wells, brine substituted conditioned logs

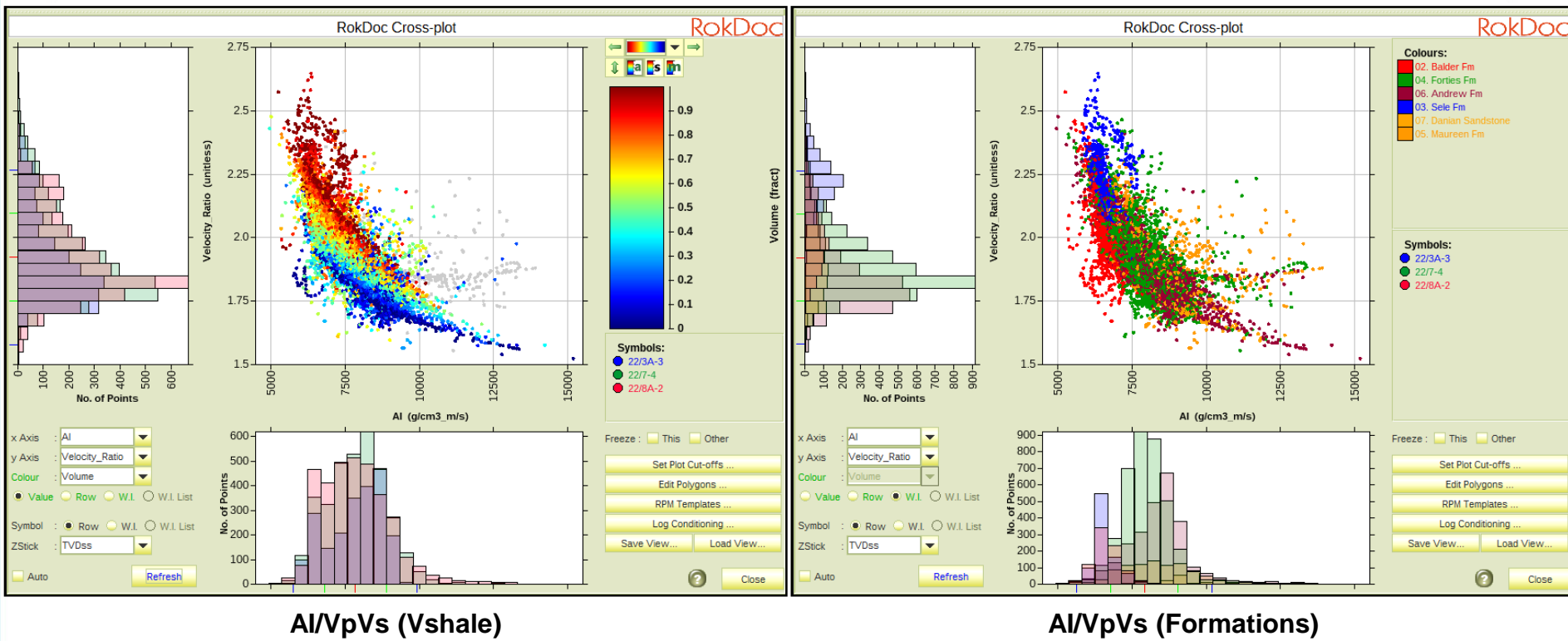


The cross-plot on the left-hand side shows the data coloured by wells and on the right-hand side coloured by formations. We can observe that wells 22/7-4 and 22/8A-2 shows points with high AI values in Forties and Maureen formations. These points (circle in pink) corresponds with thin limestones.

Also we can observe that the data for wells 22/3A-3 and 22/7-4 are more scattered than the data for well 22/8A-2, this is because Vs log for the later well was modelled from Vp log.

7.2 AI/VpVs Cross-plots – log-scaled

All wells, brine substituted conditioned logs

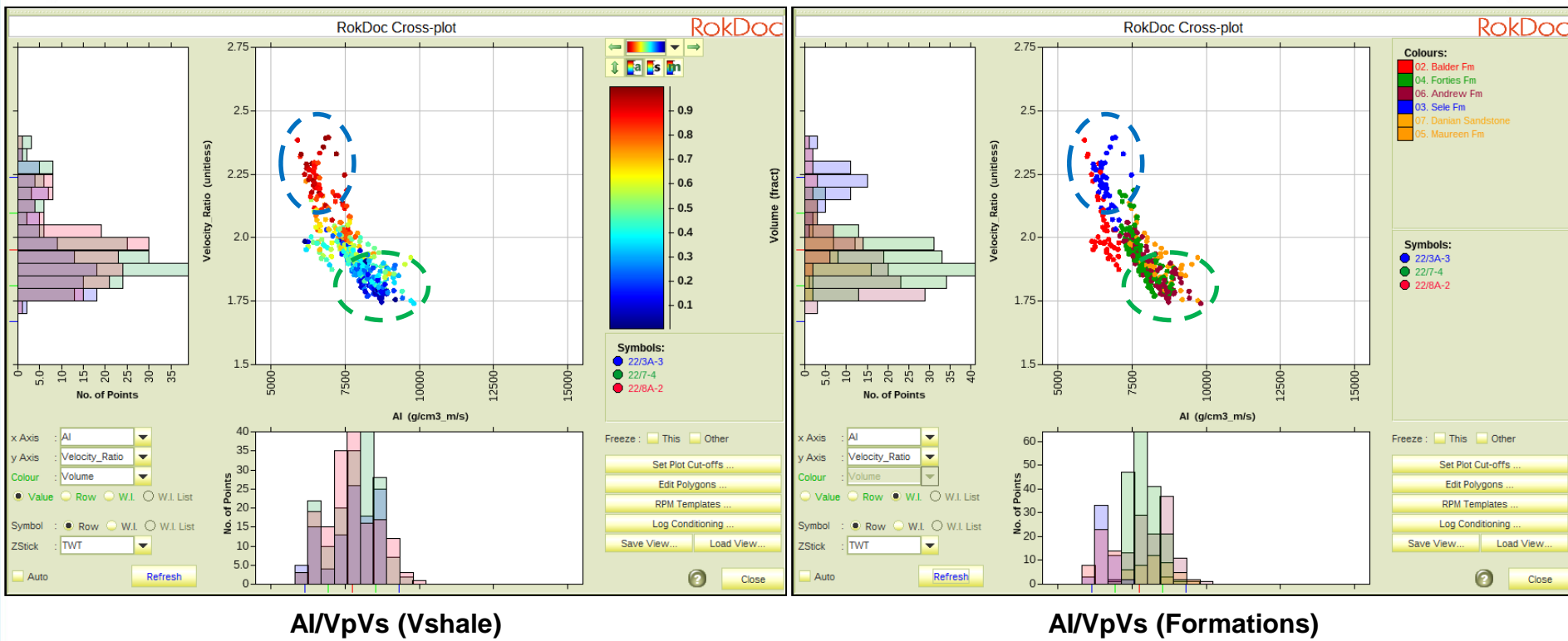


The cross-plot on the left-hand side shows the data coloured by Vshale volume. We can observe a transition from clean shales (colour in red with high values of VpVs) to clean sand (colour in blue, with low values of VpVs). AI by itself is not good enough to discriminate lithologies but together with VpVs it can.

We can see that clean shale correspond mainly with data from Sele formation, clean sand correspond to data from Forties, Andrew, Maureen and Danian formations.

7.2 AI/VpVs Cross-plots – up-scaled

All wells, brine substituted conditioned logs



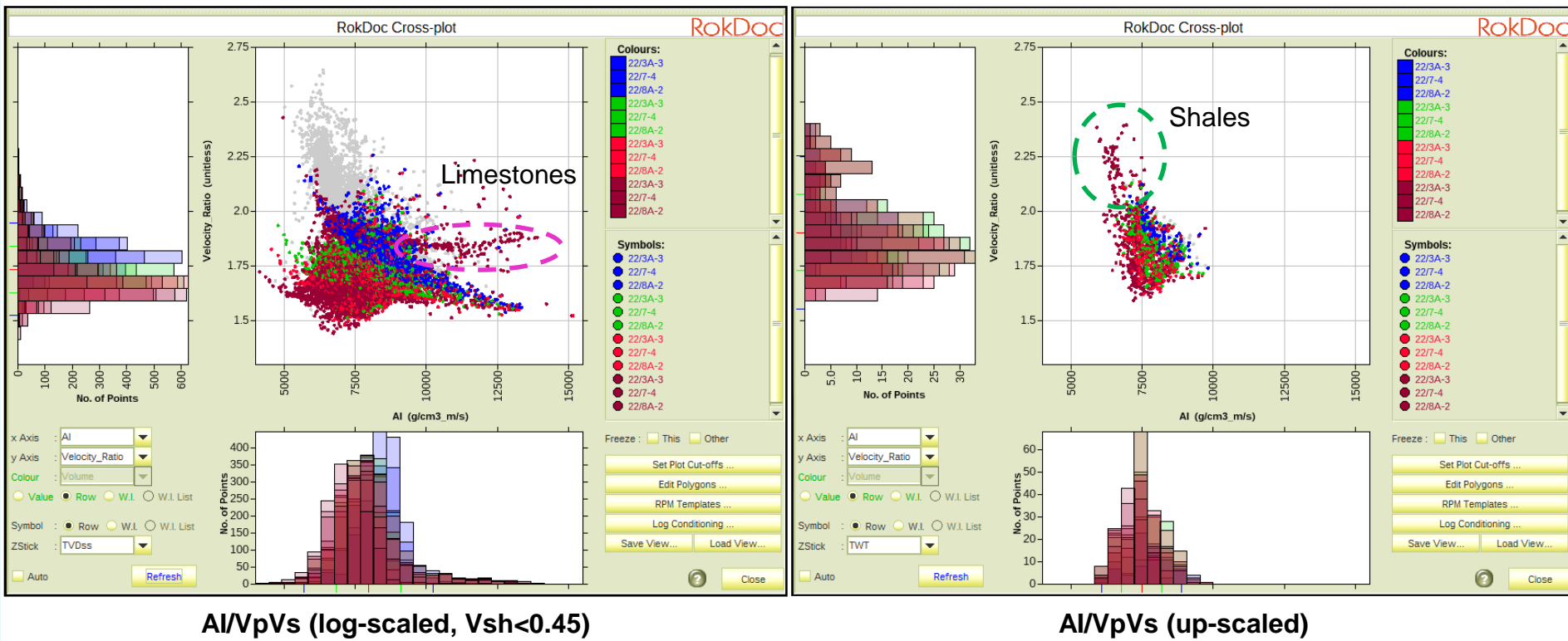
The cross-plot on the left-hand side shows the data coloured by Vshale volume and on the right-hand side by formation. Up-scaled data show a good separation between sand and shales in both AI and VpVs logs. Sands show high AI and low VpVs while shales have low AI and high VpVs.

We can see that clean shale (circle in blue) correspond with data from Sele and Balder formations, clean sand (circle in green) correspond to data from Forties, Andrew, Maureen and Danian formations.

7.2 AI/VpVs Cross-plots

All wells, different fluids,

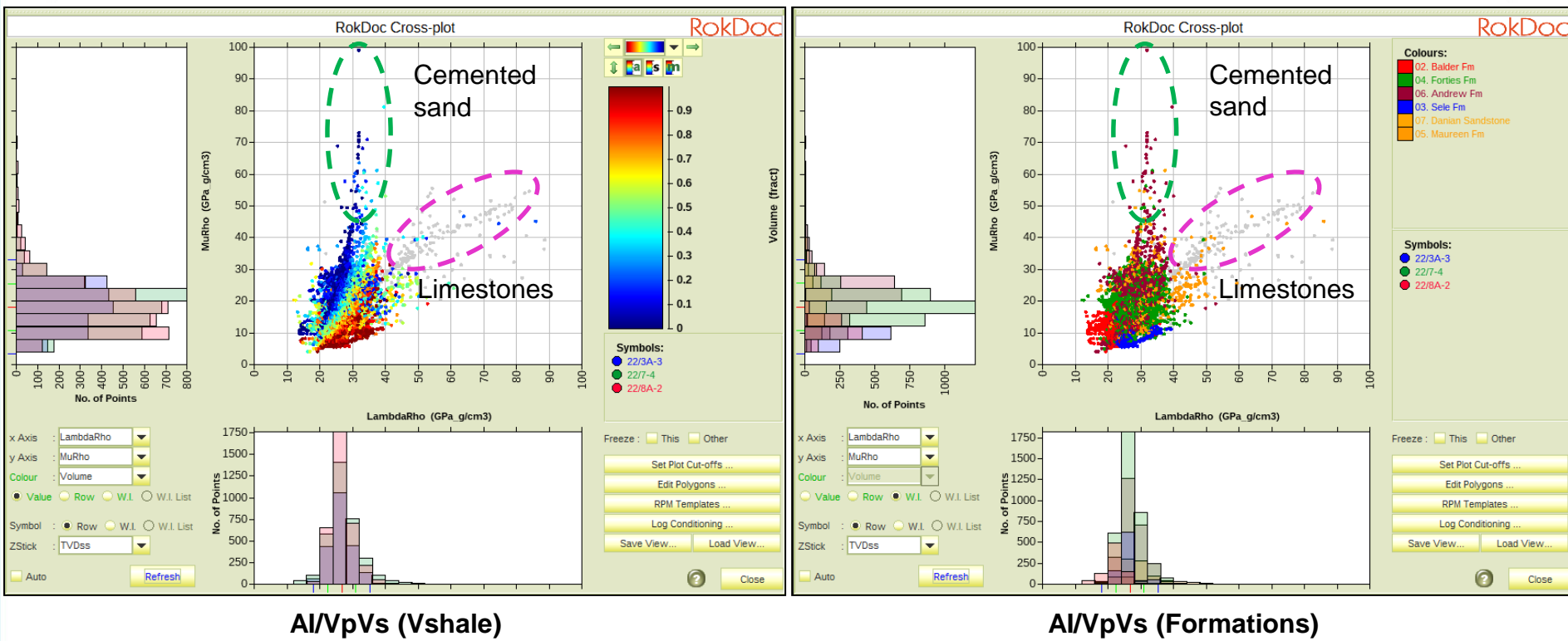
Brine
80% Oil
10% Gas
90% Gas



The cross-plot on the left-hand side shows the data log-scaled, with a Vshale cut-off applied of $V_{sh} < 0.45$ and coloured by fluids. The cross-plot on the right-hand side shows the data up-scaled, coloured by fluids. In both cases, we can observe that there is an overlap between the different hydrocarbons fluids. At log-scaled brine separates from hydrocarbon, however, it is not obvious to separate oil from different percentage of gas. Up-scaled data show an overlap between all the fluids, including brine.

7.3 LMR Cross-plots – log-scaled

All wells, brine substituted conditioned logs

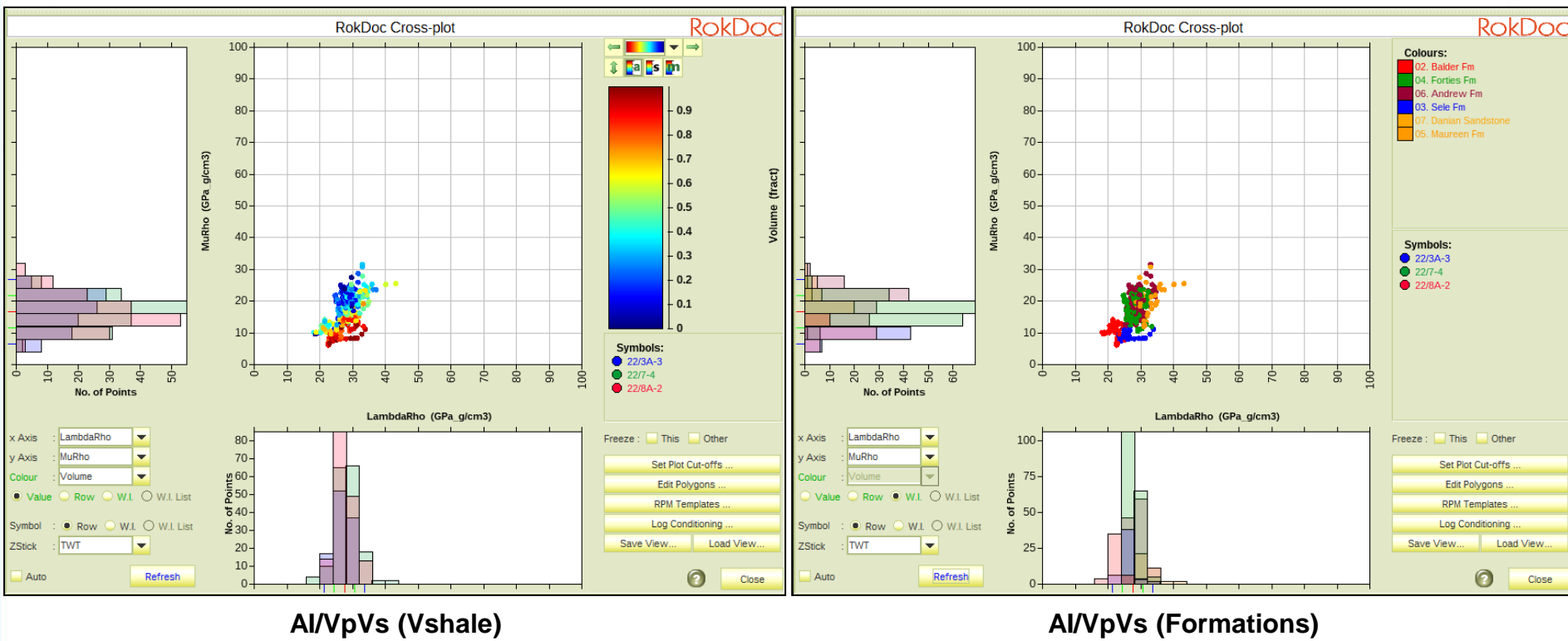


The cross-plot on the left-hand side shows the data coloured by Vshale volume and on the right-hand side coloured by formations.

The cross-plots show sands with low values of LambdaRho (LR) while shales show higher values. Clean sands have higher values of MuRho (MR) than shales.

7.3 LMR Cross-plots – up-scaled

All wells, brine substituted conditioned logs



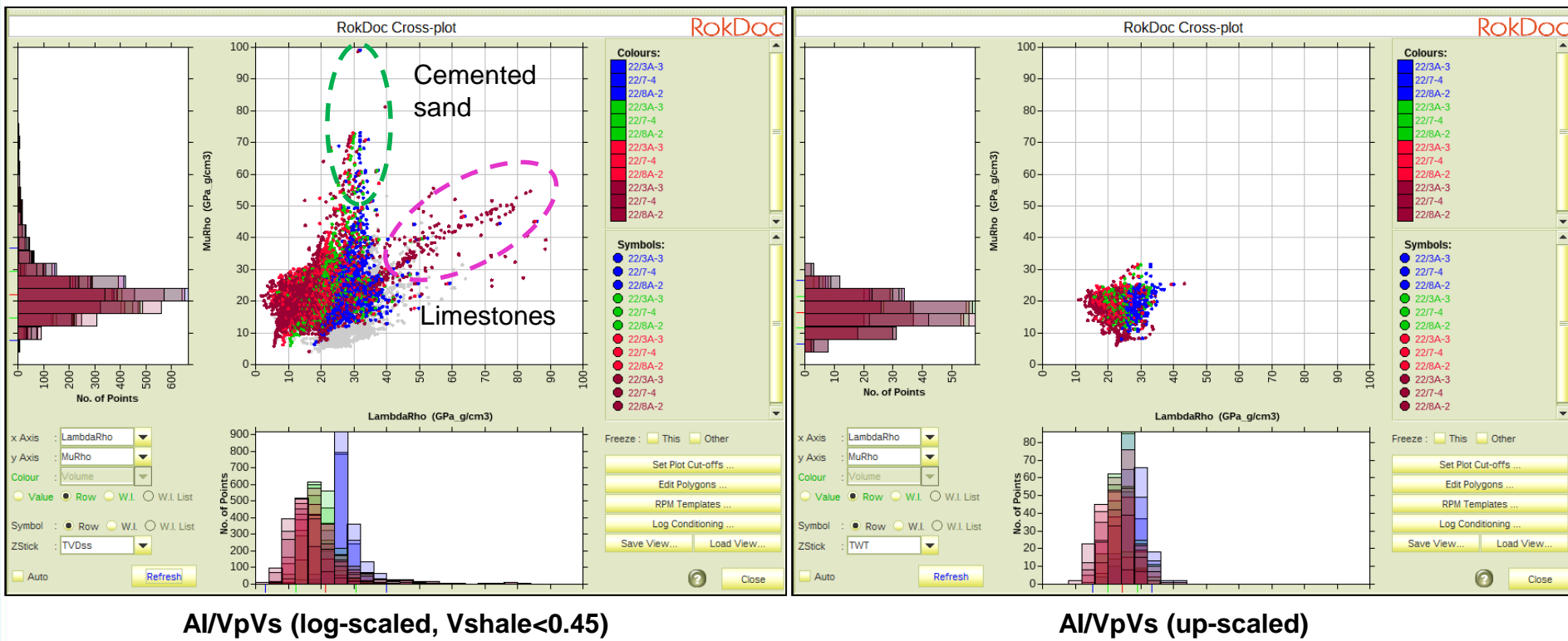
The cross-plot on the left-hand side shows the data coloured by Vshale volume and on the right-hand side coloured by formations.

Up-scaled data show good separation between sand and shales, with sands showing higher values of Murho than shales, but very similar range for LambdaRho.

7.3 LMR Cross-plots

All wells, different fluids

Brine
80% Oil
10% Gas
90% Gas



The cross-plot on the left-hand side shows the data log-scaled, with a Vshale cut-off applied of Vsh<0.45 and coloured by fluids. The cross-plot on the right-hand side shows the data up-scaled, coloured by fluids. In both cases, we can observe that there is an overlap between the different hydrocarbons fluids. At log-scaled brine separates from hydrocarbon, however, it is not obvious to separate oil from different percentage of gas. Up-scaled data show an overlap between all the fluids, including brine.

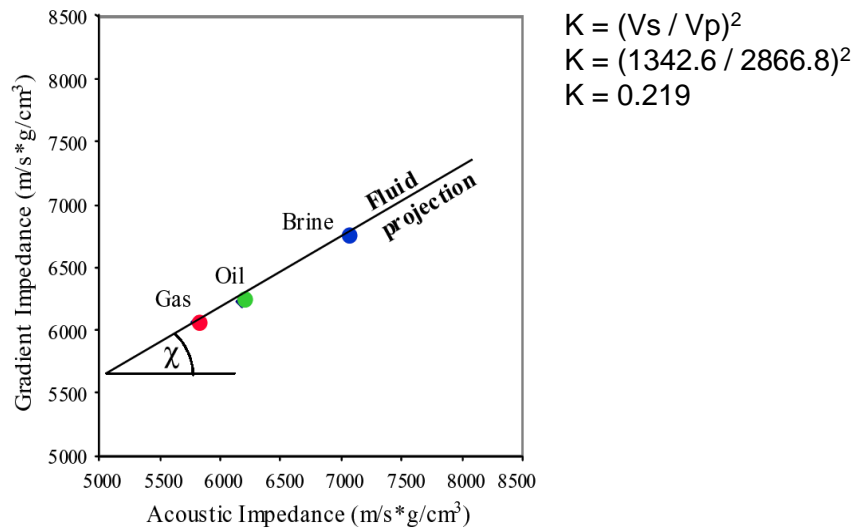
7.4 LnAI-LnGI Cross-plot

Estimation of chi angles

A rotation in intercept and gradient space (or AI-GI) can enhance fluid or lithological variation within the seismic dataset. This rotation is a combination of AI and GI logs and can be tuned to maximise a particular effect. The resulting impedance is known as Extended Elastic Impedance (EEI) and is generated at a specified Chi(χ) angle. As the rotation is a multiplication of impedance logs the plots are made in LnAI-LnGI space (an example projection is seen below).

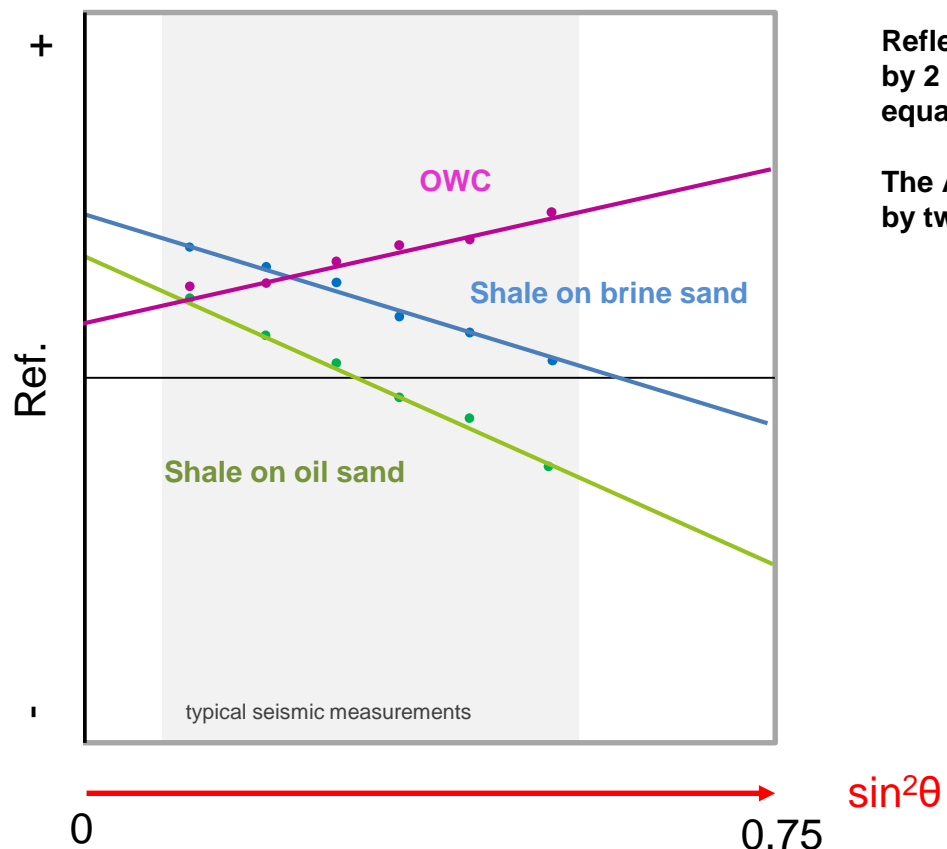
Once a rotation has been tuned to the data it can be extracted from the seismic via the generation of intercept and gradient from partial angle stack data, this is then rotated to the equivalent projection and inverted to relative impedance using a coloured inversion scheme.

The generation of EEI requires a K constant as well as a normalising average set, this is derived from the V_p, V_s, rhoB logs over the interval of interest.



The EEI Concept

Range of measurements



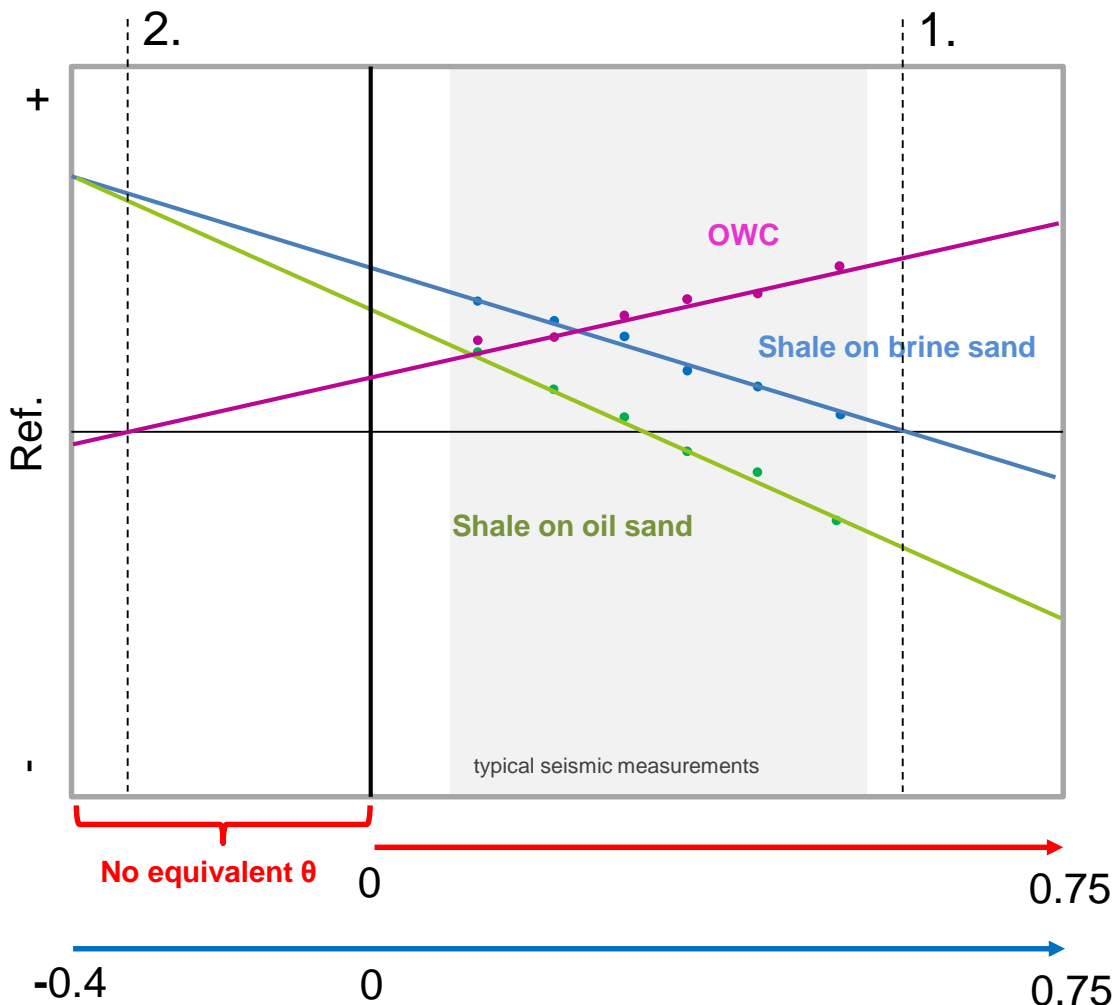
Reflectivity is linearized as a function of $\sin^2\theta$ by 2 term reflectivity equations (e.g. Shuey's equation).

The AVO behaviour can therefore be described by two parameters, intercept and gradient.

$$R(\theta) = I + G \sin^2\theta$$

The EEI Concept

Extension to non-physical angles



Extended Elastic Impedance allows the extension of the linearized AVO response to non-physical angles. Reflectivity is now determined as a function of $\tan X$.

Fluid effects dominate at positive X angles, and lithology effects dominate at negative X angles.

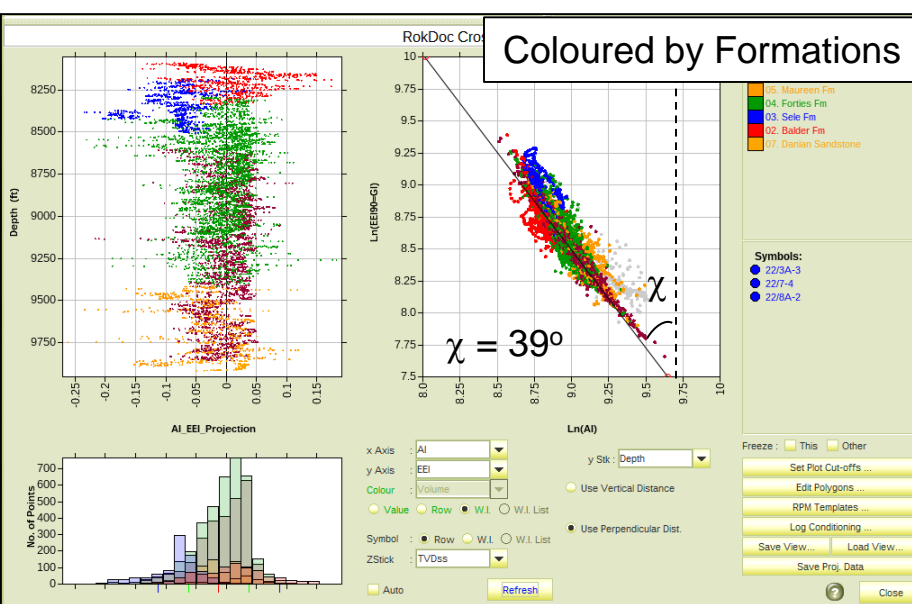
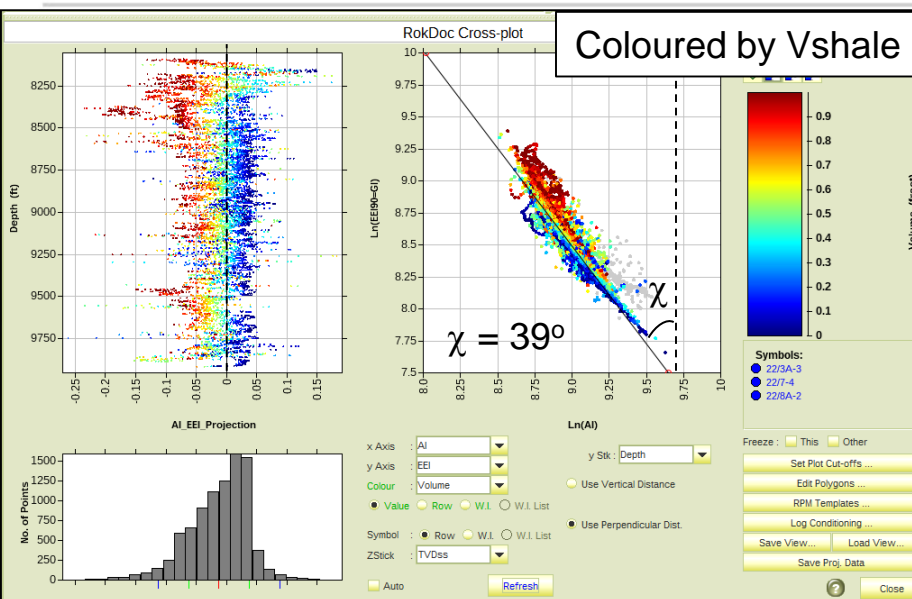
Examples

1. Shale/brine sand interface has minimal contrast, shale/oil sand interface is a strong negative response, and OWC is a positive response. This is therefore a fluid angle, where fluid effects are maximised.
2. Shale/brine sand and shale/oil sand have similar positive responses – no fluid effect. OWC shows no contrast. This is therefore a lithology angle where fluid effects are minimised.

$\sin^2\theta$

$\tan X$

7.4 EEI Cross-plot – log-scaled Estimation of chi angles – litho-fluid stack



The cross-plot shows $\ln(\text{EEI}90^\circ\text{G})$ v. $\ln(\text{AI})$, at log-scale. The natural logarithms of each impedance are taken as the impedance logs are multiplied to have a reflectivity equivalent.

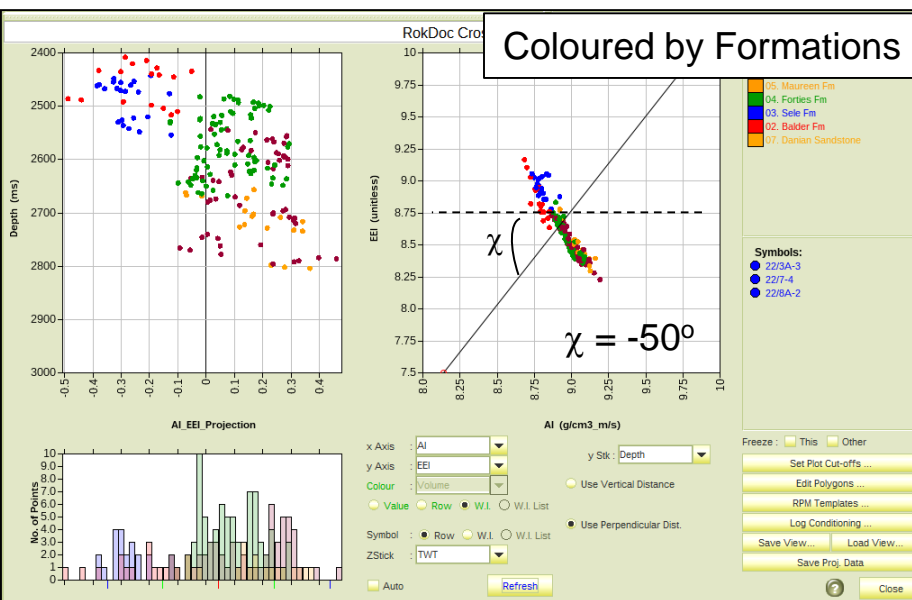
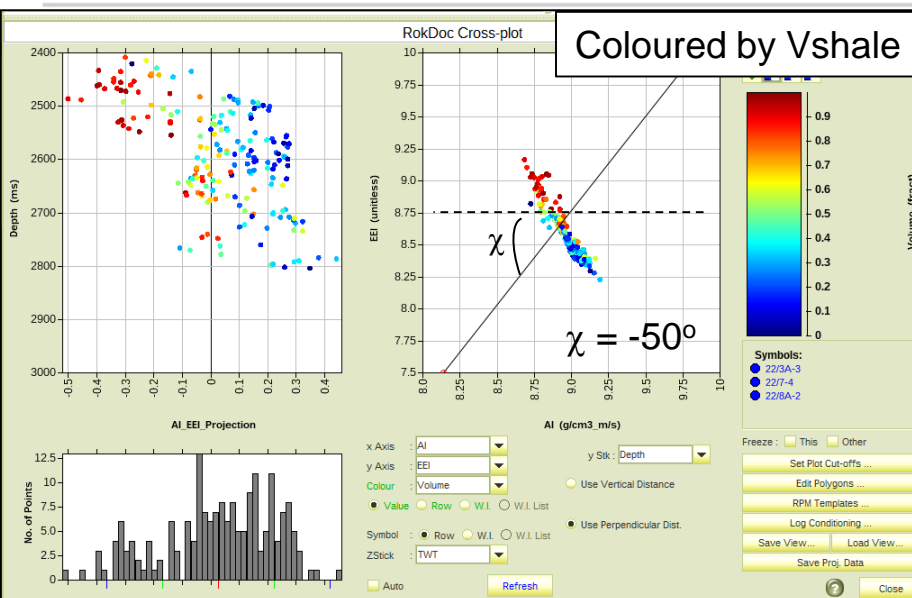
A projection line was added to separate sands from shales. The track on the left-hand side shows the projection as a function of depth (TVDss).

The projection separates shales with an opposite polarity kick to sands. Hydrocarbon saturation in the sands will increase the amplitude of the sand response, hence the attribute is referred to as a litho-fluid stack. The trend is parallel to the porosity trend in the sand, therefore the effect of changing porosity in this projection is minimised (i.e. low porosity sands have a similar response in the projection to high porosity sands at a given porosity).

A vertical, dotted line was added to the main cross-plot to determine an appropriate chi angle to separate sands from shales.

According to the plot, EEI log at 39°X should be a good litho-fluid discriminator.

7.4 EEI Cross-plot – up-scaled Estimation of chi angles – lithology stack



The cross-plot shows $\ln\text{EEI}90^\circ\text{X}$ ($\ln\text{GI}$) v. $\ln\text{AI}$, after up-scaling. The natural logarithms of each impedance are taken as the impedance logs are multiplied to have a reflectivity equivalent. The track on the left-hand side shows the projection as a function of time (TWT), sands and shales have opposite polarity responses in this relative attribute.

According to the plot, EEI log at 50°X should be a good lithology discriminator.

This trend crosses the porosity trend in the sands, so is sensitive to porosity, and can be thought of as a porosity indicator. A further complication with this type of high angle projection for these sands/shales is that higher porosity sands are closer to the projection line, and therefore have weaker response to the lower porosity sands.

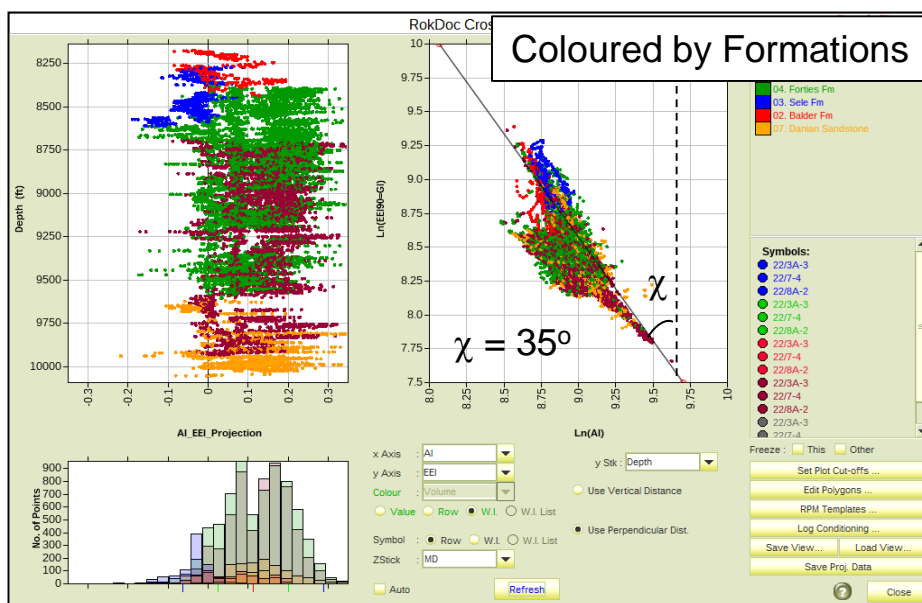
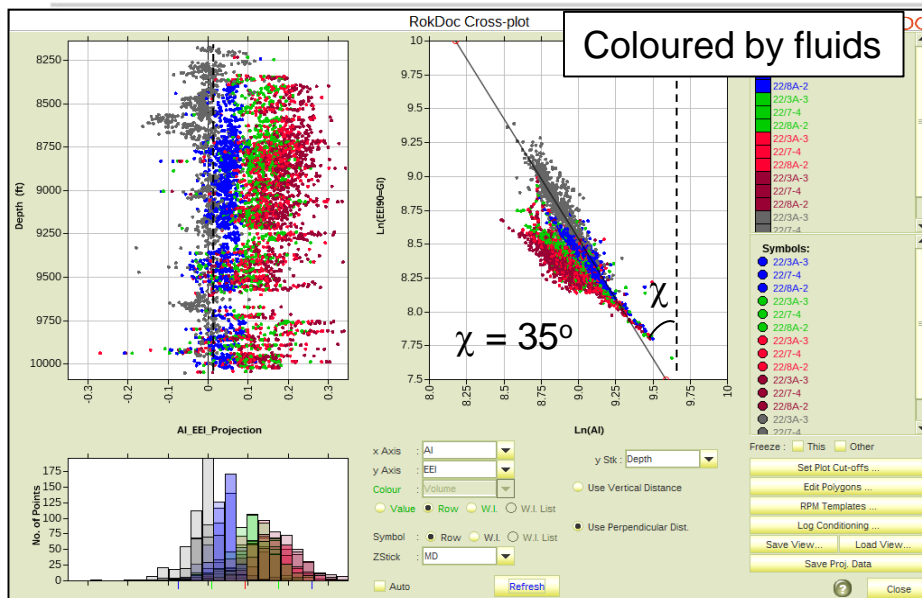
It is recommended that this type of stack is used in conjunction with the litho-fluid stack shown in the previous slide (i.e. the litho-fluid stack is used to identify sand packages, with the lithology attribute then investigated within those packages to see if it provides additional information).

This projection is parallel to the saturation trend in the sands, so the EEI -50°X is insensitive to saturating fluid in the sands.

7.4 EEI Cross-plot – log-scaled

Estimation of chi angles – fluid stack

Brine
80% Oil
10% Gas
90% Gas



The cross-plot shows $\text{LnEEI}90^\circ\text{X}$ (InGI) v. LnAI , at log scale. The natural logarithms of each impedance are taken as the impedance logs are multiplied to have a reflectivity equivalent. The track on the left-hand side shows the projection as a function of time (TWT), sands and shales have opposite polarity responses in this relative attribute.

According to the plot, an EEI stack at 35°X should be a good fluid discriminator.

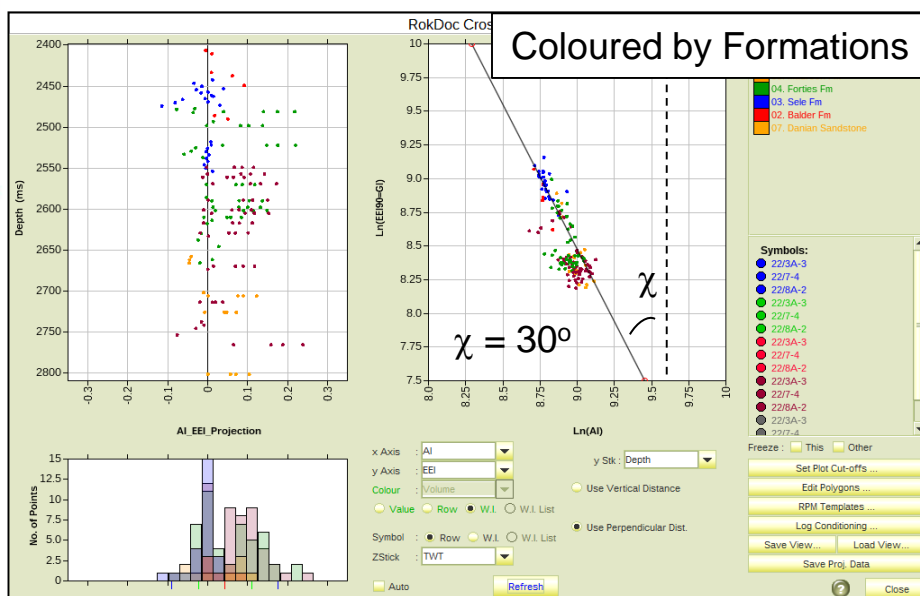
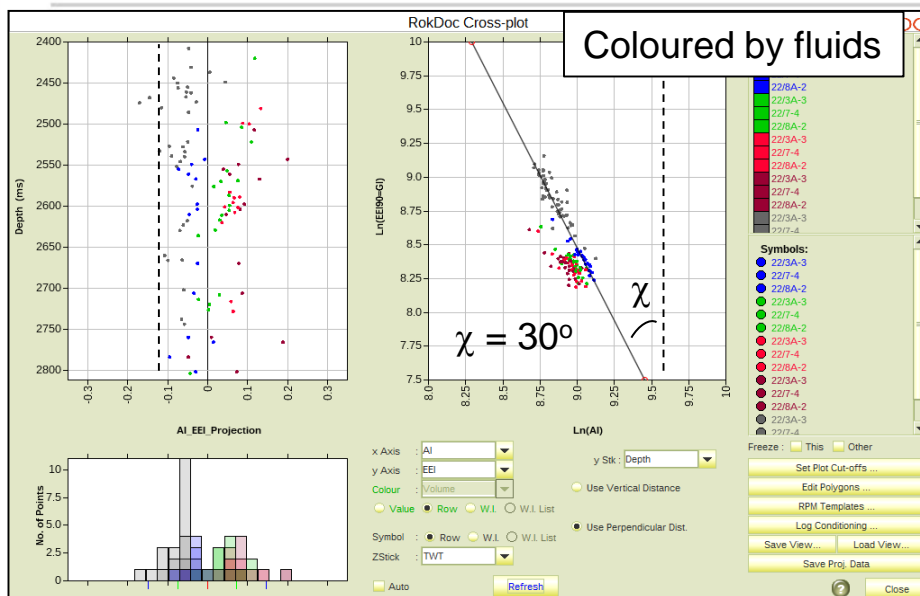
This projection is made orthogonally to the brine sand / shale trend. Points that fall to the left of the trend line are hydrocarbon bearing sands. This results in an attribute where minimal contrasts are seen between brine sands and shales, and bright responses are shown where pay sands are present..

Again it is recommended that this type of stack is used in conjunction with the litho-fluid stack shown previously (i.e. the litho-fluid stack is used to identify sand packages, with the fluid stack response then investigated within those packages to see if it provides additional information on fluid fill).

7.4 LnAI-LnGI Cross-plot – up-scaled

Estimation of chi angles - fluids

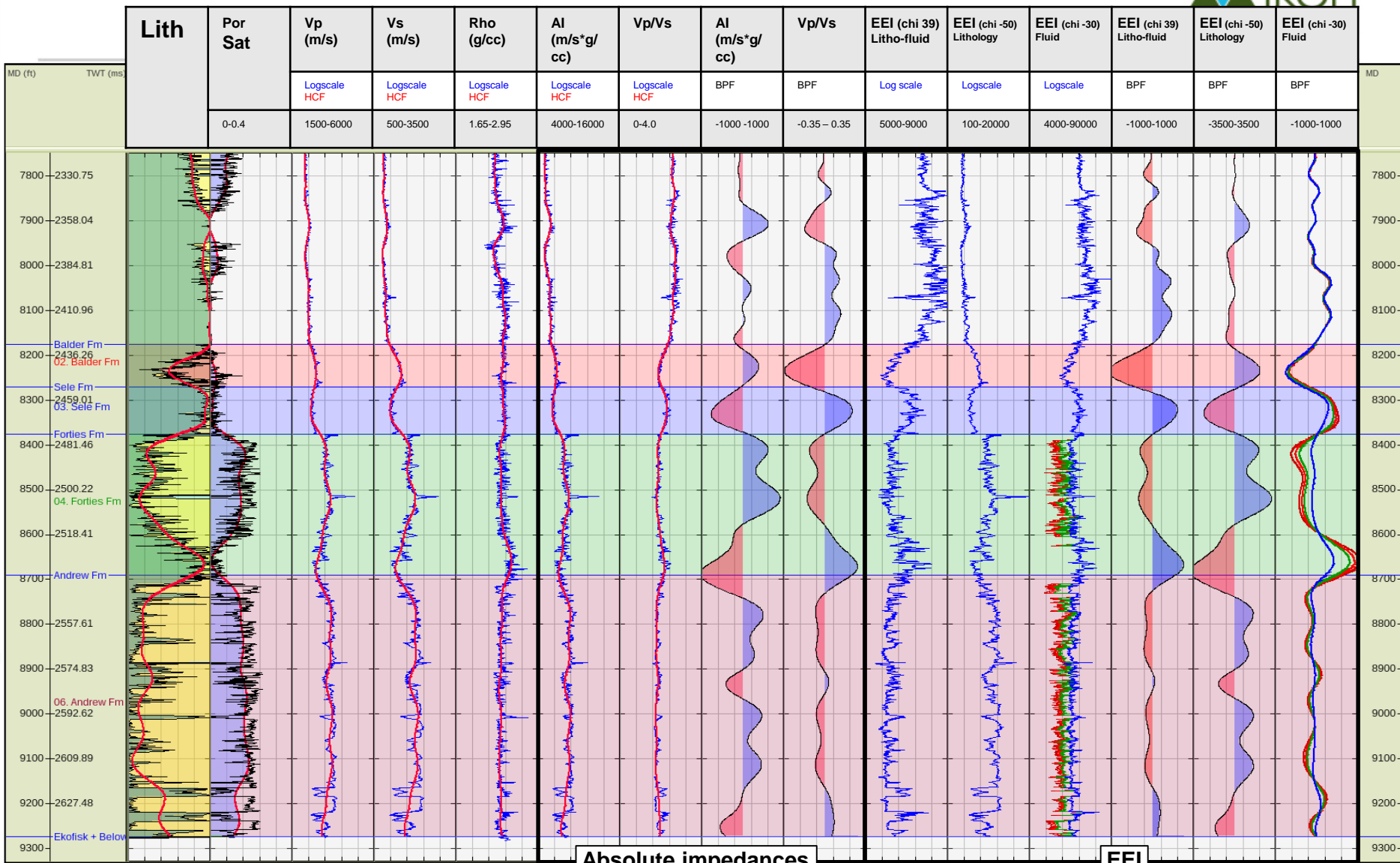
Brine
80% Oil
10% Gas
90% Gas



The cross-plot shows LnEEI90°X (lnGI) v. LnAI, at seismic scale. The natural logarithms of each impedance are taken as the impedance logs are multiplied to have a reflectivity equivalent. The track on the left-hand side shows the projection as a function of time (TWT), sands and shales have opposite polarity responses in this relative attribute.

At seismic scale the relationship of each facies response changes slightly and the EEI projection angle becomes clearer. An EEI projection of 30°X is appropriate as the optimum fluid stack at seismic scale, the projection is made orthogonally to the brine sand / shale trend.

7.5 Well panel – 22/3a-3

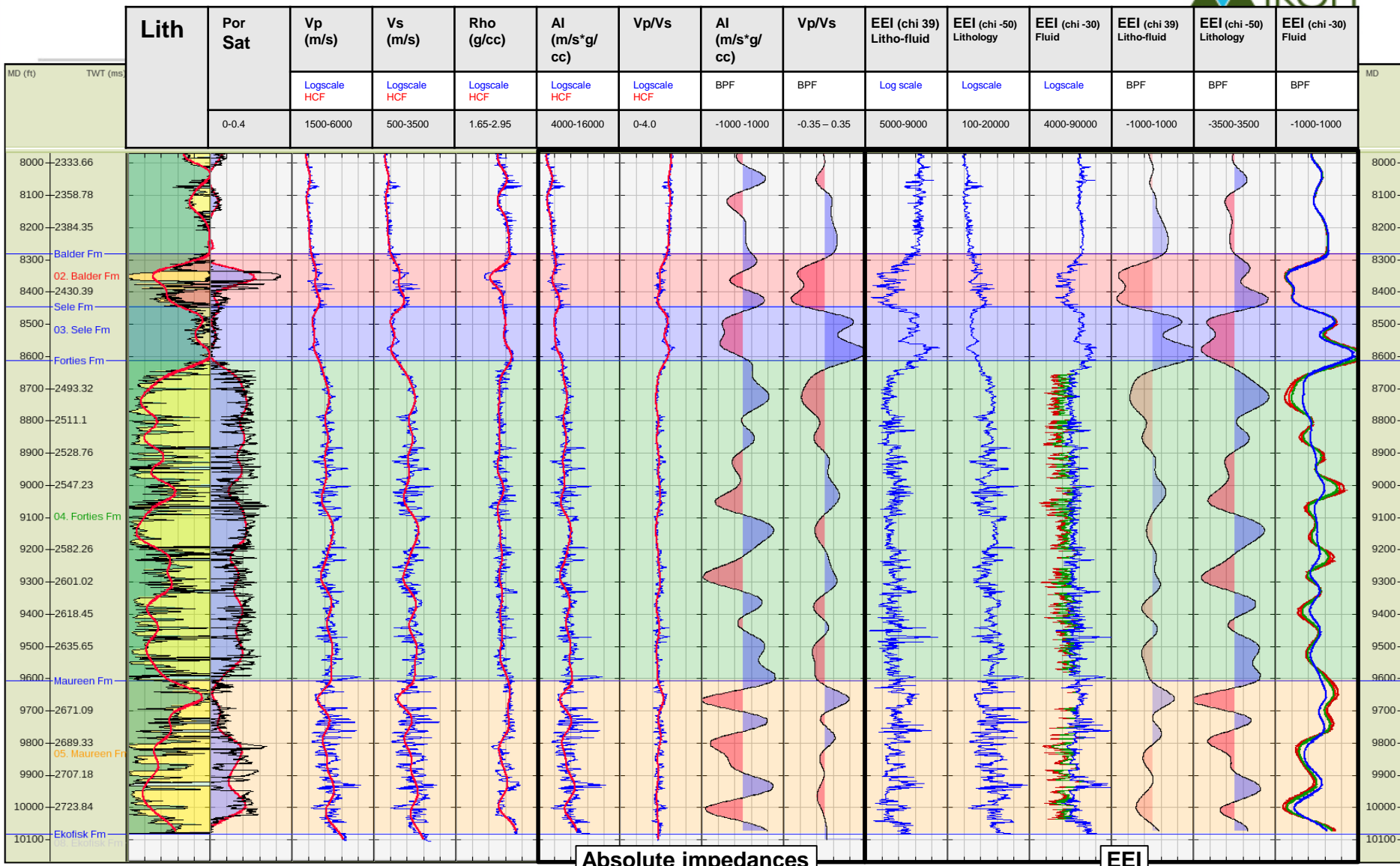


Absolute impedances that might be generated from a model based inversion are shown in the centre of the panel, EEI logs are shown on the right. The relative EEI profiles would normally be generated from the seismic.

As can be seen the sands are associated with higher AI and lower VpVs values than the sands. The sands show negative responses in the litho-fluid projection, and positive responses in the lithology projection. The fluid projection shows minimal sand/shale contrast in the brine case, with large fluid effects. Band-limited logs are generated using a band-pass filter (5-10-45-70Hz).

7.5 Well panel – 22/7-4

106

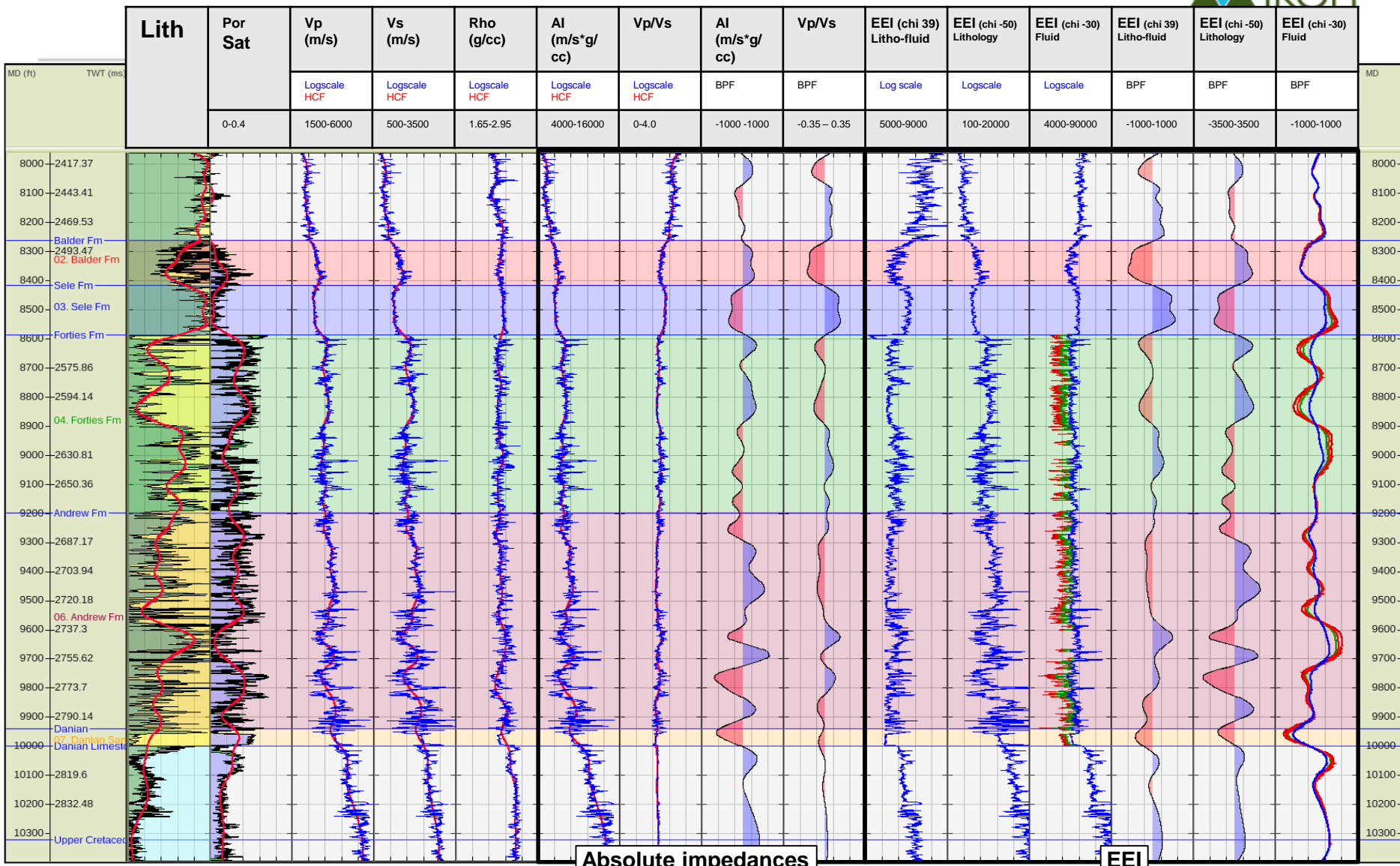


Absolute impedances that might be generated from a model based inversion are shown in the centre of the panel, EEI logs are shown on the right. The relative EEI profiles would normally be generated from the seismic.

As can be seen the sands are associated with higher AI and lower VpVs values than the sands. The sands show negative responses in the litho-fluid projection, and positive responses in the lithology projection. The fluid projection shows minimal sand/shale contrast in the brine case, with large fluid effects. Band-limited logs are generated using a band-pass filter (5-10-45-70Hz).

7.5 Well panel – 22/8A-2

107



Absolute impedances that might be generated from a model based inversion are shown in the centre of the panel, EEI logs are shown on the right. The relative EEI profiles would normally be generated from the seismic.

As can be seen the sands are associated with higher AI and lower VpVs values than the sands. The sands show negative responses in the litho-fluid projection, and positive responses in the lithology projection. The fluid projection shows minimal sand/shale contrast in the brine case, with large fluid effects. Band-limited logs are generated using a band-pass filter (5-10-45-70Hz).

Summary and Conclusions

Synthetic Gathers

- The brine sands in the study wells are always slightly harder than the overlying shales, due to the porosity of the sands (avg. porosity: 20%) and the level of cementation in the sands (avg. Vp 3628 m/s, indicating the presence of at least some level of contact cement). This generally produces a dim **Class I AVO response** for the shale/brine sand interface but some responses cross the zero axis at the far offsets (~30°), so are **Class IIp AVO responses**.
- Hydrocarbon saturation acoustically softens the sands and steepens the AVO gradient. The result is a dimmer response at zero offset and a phase reversal at near to mid off-sets, which is a stronger **Class IIp AVO response**. The oil and residual (10%) gas cases are always **Class IIp AVO responses** but the gas case (90%) sometime softens the sand to the point that it is acoustically softer than the overlying shale, which changes the polarity of the response, to become a **Class II AVO response**.
- The synthetic gathers are sometime difficult to interpret for a number of reasons.
 - Calcite stringers are present, sometimes at the top of a formation (e.g. Top Forties Fm in 22/3A-3, Top Maureen Fm in 22/7-4), but a clean shale/calcite interface will produce a bright **Class I AVO response**, so shouldn't be confused with a hydrocarbon response.
 - Thin layers and mixed lithologies are also often present, which makes it difficult to resolve a specific interface (e.g Andrew/Maureen Fm in all three wells). It also means that the low amplitude response associated with upscaled thin layers can suffer from interference from a bright response associated with a calcite stringer.

Summary and Conclusions

Well-based inversion feasibility

Absolute impedance profiles

The Palaeocene sands are generally acoustically harder than the overburden Sele and intra-formation shales, and the sands show lower VpVs responses than the shales. However the tuffaceous shale in the Balder exhibits a similar response in Al-VpVs. LambdaRho-MuRho shows similar separations to Al-VpVs. It is expected that these types of absolute impedance would be generated from the seismic angle stacks via the use of a simultaneous model based type inversion.

Extended Elastic Impedance (EEI) projections

Three EEI attributes have been identified by the analysis, these are a litho-fluid stack, and separate lithology and fluid stacks.

- The litho-fluid stack (at 39°X) separates sands and shales with a change in polarity of response. This attribute shows soft negative kicks where sands are present, and hard kicks where shales are present. Hydrocarbon in the sand pores results in a brightening of the soft-kick, the attribute is therefore termed a litho-fluid projection. The litho-fluid projection is insensitive to sandstone porosity, as the projection is made orthogonally to the porosity trend, so for a given pore fluid type both low and high porosity sands should have a similar response in this attribute. Sandstone packages can then be interpreted based on this attribute.
- The lithology stack (at -50°X) also separates sands from shales with a change in response polarity. In this attribute sands show hard positive kicks. The high angle lithology attribute cuts across the porosity trend, and is therefore sensitive to sandstone porosity. This can make the response highly variable throughout the sands, in addition higher porosity sands will show weaker responses than lower porosity sands (as the high porosity sands plot closer to the projection line). This high angle projection is also more dependant on the seismic gradient, and can therefore be more sensitive to noise in the seismic angle stack data. It is recommended that the lithology stack responses are examined once sand packages have been identified based on the litho-fluid stack.
- The fluid stack (at 30°X) highlights the effect of hydrocarbon saturation in the sands. Pay sands will show bright soft responses on the fluid stack, with brine sands showing minimal contrast with the encasing shales.

The EEI stack attributes are normally identified from seismic intercept/gradient products, and attributes are normally generated as relative attributes.

It is important to note is that the Balder tuffaceous shale can have a similar elastic response to the Forties sands.

Recommendations and Next Steps

Now that the expected AVO reflectivity and impedance responses have been determined for the formations encountered by the study wells, the following additional modelling work is recommended:

1. Modelling of reservoir sand properties outside of those encountered in the analogue wells. This includes modelling of porosities and NTG that are outside of the range of those encountered in the wells.
2. Investigation into the effects of tuning.

At this stage work is required to compare and attempt to match the modelled responses from the wells to the observed seismic AVO response at the prospect. This would rely not only on the responses modelled at the wells, but also those cases suggested above.

Alternatively, as the work on the analogue wells indicates reasonable separation of the different litho-facies in elastic impedance space, either an absolute or relative (EEI) inversion scheme could be used to further investigate the seismic responses at the prospect location.